A Power-Aware Routing Scheme for Ad Hoc Networks

Fahad Koujah

Dissertation submitted to the Faculty of the

Virginia Polytechnic Institute and State University

in partial fulfillment of the requirements for the degree of

Doctor of Philosophy

in

Computer Engineering

Scott F. Midkiff, Chair

Luiz A. DaSilva

C. Patrick Koelling

Thomas L. Martin

Amitabh Mishra

May 24, 2006

Blacksburg, Virginia

Keywords: MANET, power-aware, IEEE-802.11b, energy-efficient, WLAN, Routing

A Power-Aware Routing Scheme for Ad Hoc Networks

Fahad A. Koujah

(ABSTRACT)

Wireless network devices, especially in ad hoc networks, are typically battery-powered. The growing need for energy efficiency in wireless networks, in general, and in mobile ad hoc networks (MANETs), in particular, calls for power enhancement features. The goal of this dissertation is to extend network lifetime by improving energy utilization in MANET routing. We utilize the ability of wireless network interface cards to dynamically change their transmission power, as well as the ability of wireless devices to read the remaining battery energy of the device to create a table of what we term "reluctance values," which the device uses to determine how to route packets. Choosing routes with lower reluctance values, on average and with time, leads to better utilization of the energy resources of the devices in the network. Our power-aware scheme can be applied to both reactive and proactive MANET routing protocols. As examples and to evaluate performance, the technique has been applied to the Dynamic Source Routing (DSR) protocol, a reactive routing protocol, and the Optimized Link State Routing (OLSR) protocol, a proactive routing protocol. Simulations have been carried out on large static and mobile networks. Results show improvements in network lifetime in static and certain mobile scenarios. Results also show better distribution of residual node energies at the end of simulations, which means that the scheme is balancing energy load more evenly across network nodes than the unmodified versions of DSR

and OLSR. Average change in energy over time in the unmodified protocols show a steady increase with time, while the power-aware protocols show an increase in the beginning, then it levels for sometime before it starts to decrease. The power-aware scheme shows improvements in static and in coordinated mobility scenarios. In random mobility the power-aware protocols show no advantage over the unmodified protocols.

Acknowledgements

I would like to thank God for giving me the patience and the willingness to accomplish this task.

This research was accomplished with a lot of support from a number of individuals. I would like to thank my advisor, Professor Scott F. Midkiff, for his support, guidance, and encouragement throughout the course of my research. His support has helped me tremendously in my research, and has helped me gain the confidence and the persistence needed to graduate. I feel very fortunate to have had him as an advisor.

I would also like to extend my thanks to the committee members: Dr. Thomas Martin, Dr. Charles Patrick Koelling, Dr. Luiz DaSilva, and Dr. Amitabh Mishra for their helpful comments and suggestions.

I thank all my friends in the networking lab in particular, and in Blacksburg in general, for their help, valuable feedback, suggestions, and support.

I would like to extend my thanks to my colleagues at the Public Authority for Applied Education and Training in Kuwait for their help and support.

Furthermore, I would like to extend my thanks to Shoghig Sahakyan at the Kuwait Cultural Office in Washington D.C. for her help and support.

Finally, I would like to thank my parents, wife and kids for their patience and encouragements throughout my studies, and for always being there for me throughout this journey.

Contents

List of Figures

List of Tables

Chapter 1

Introduction

Mobile networks offer advantages for both the military and the civilian world. While they were originally meant for enhancing military communications in the battlefield or in areas hit by natural catastrophes, wireless networks have found their way into civilian life. Today people are using these networks in cafes, restaurants, malls, universities, and public gatherings, such as conferences.

While wireless networks have expanded and their technology has advanced considerably, there are still issues that need to be looked at more closely. These issues include throughput, delay, channel capacity, and power consumption. Regarding throughput and delay, the throughput and delay in wireless networks lag behind that of wired ones. There are many reasons for this. As an example, node mobility increases the likelihood that destination nodes become unreachable. Another factor limiting throughput is the long delay that net-

works incur due to channel interference. Frame losses in a wireless link could trigger the Transmission Control Protocol (TCP) to initiate congestion control between two communicating nodes, further degrading network performance [21]. Furthermore, wireless networks do not fully utilize channel capacity due to hidden and exposed node problems [32] [53] [42].

Power is also crucial in wireless networks, especially in mobile ad hoc networks, as it is the "fuel" that keeps the network alive. Thus, conserving power helps prolong network life. Moreover, energy conservation leads to smaller, more lightweight devices and helps reduce environmental hazards by minimizing discarded batteries [25].

The two most popular power sources for wireless networks are regular alternating current (AC) outlets and batteries. There are two main types of batteries, those that are perishable after one use and those that are rechargeable. Rechargeable batteries include Nickel Metal Hydride (NiMH), Nickel Cadmium (NiCd), and Lithium Ion (Li-Ion) [6]. Each of these battery technologies has a different charge/discharge rate and energy density. Energy density is the amount of energy a battery can provide in one volume unit (watt hour/Liter). It indicates how much energy the battery can store before a recharge [56].

There are two distinct types of wireless networks: infrastructure-based wireless networks and mobile ad hoc networks (MANETs). In infrastructure-based wireless networks, the mobile nodes rely on stationary nodes, usually called access points, with ample AC power to route their packets through the network. Usually, in this case, the access point coordinates and routes traffic between nodes. In MANETs, the mobile nodes rely on each other for packet delivery and traffic coordination. This type of coordination forms what is called multi-hop

connections. In ad hoc networks, the task of packet delivery and traffic coordination puts a lot of stress on the individual nodes' energy sources. As the nodes consume energy from their power sources, the network can become partitioned. This can hasten the "death", i.e. the point at which the network can no longer fulfill its intended functions, of the network.

An ad hoc wireless network is a collection of wireless mobile nodes that establish some kind of coordination among them to form a network. In ad hoc networks, all nodes share a single radio channel. Therefore, nodes that are within radio distance of other nodes can directly connect with each other at the link layer (layer 2), Figure 1.1 shows the structure of a typical ad hoc network. In this figure, three nodes form an ad hoc network. Node B can hear nodes A and C, while node A cannot hear node C. Mobility increases the difficulty of communications among nodes due to variable radio channels and multi-path fading [10].

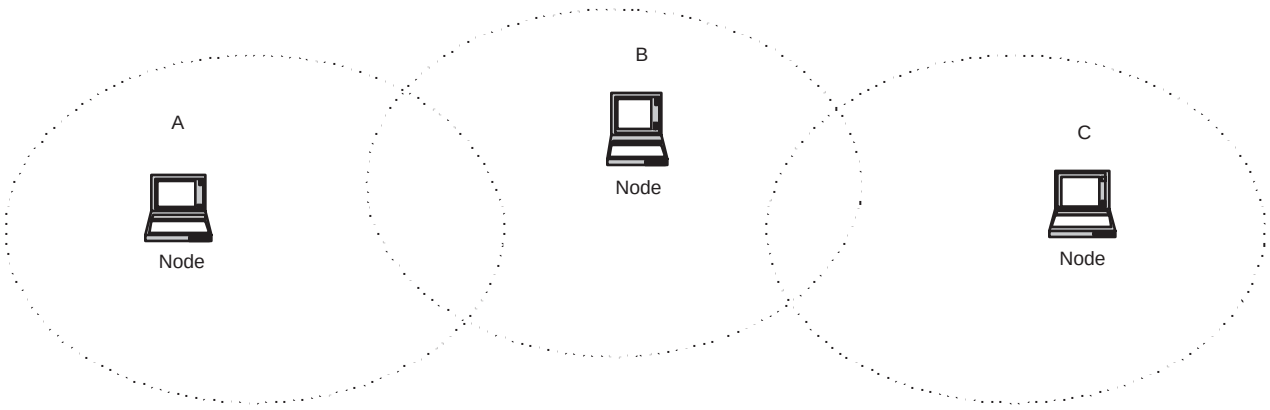

Figure 1.1: An ad hoc network of three mobile nodes.

Packet transmission consumes the majority of a mobile device's power. However, packet reception also consumes a sizeable amount of energy. Thus, concentrating on minimizing

the output power does not necessarily lead to minimum energy consumption [29]. Output power should be adaptive to channel conditions since reduction of transmitter output power results in a reduction of the instantaneous power needs, but a lower transmit power might result in a higher bit error rate (BER) in bad channel conditions. A high BER leads to retransmissions, which ultimately counteract the energy conservation process. Thus, to reduce power consumption, a simple power control mechanism and an appropriate transmit power level should be employed. After overcoming these challenges, determining the minimal operational power requirement for each node in the network increases the network's lifetime. This calls for an adaptive scheme that changes transmission power according to the channel conditions and the network load. Energy consumption also depends on the network load and number of mobile nodes in the network. As the number of nodes increases, the probability of the number of collisions increases, leading to higher energy consumption [29].

Evaluating the energy consumption of network protocols is a compromise between a precise estimate of the energy consumption and an insight into the protocol behavior [18]. Thus, analyzing energy expenditure in a network card requires the study of power usage in the transmit, send, idle, and sleep modes [18].

1.1 Thesis Motivation

Wireless network devices, especially in ad hoc networks, are typically battery-operated devices. The growing need for energy-efficient devices in wireless local area networks (WLANs),

in general, and in MANETs in particular, calls for a top-down approach toward developing power enhancement features. On the mobile device level, the hardware must be designed with energy-efficient components such as liquid crystal displays (LCDs), compact disk drives (CD-ROMs), integrated circuits, and so forth. On the communications level, physical, link, and network layers should all employ power management and enhancement features to minimize the energy expended during communication [8].

The advanced power management techniques employed in wireless devices on the operating system (OS) level give the OS direct control over the power management functionality of the wireless device. This allows the mobile nodes to take advantage of the power management features provided by the operating system and enhances the energy conservation process. Operating systems in mobile devices utilize new features found in the current generation of smart batteries. Smart batteries are generally batteries with electronic circuits that enable, over a two-wire bus, simple reading of battery status including remaining power, and remaining lifetime of the current charge [65]. A specification that defines the key components of a Smart Battery System (SBS) is put together by a group of companies with the aim of advancing the performance of portable devices [65].

The aim of this thesis is to extend the network lifetime by improving the power utilization of the routing mechanism in MANETs. We utilize the ability of wireless network cards to dynamically change the transmission power, as well as the ability of wireless devices to read the remaining battery energy to create a table of what we term "reluctance values", which the device uses to determine how to route packets. Reluctance values are assigned according

to the transmission power needed to reach the destination node, along with the battery status of the sending and intermediary nodes. Our hypothesis is that choosing routes with lower reluctance values on average, and with time, will lead to better utilization of the power sources of the communicating devices.

The literature presents ample papers about power-aware, and energy-minimizing routing schemes, as discussed in section 2.2. However, our approach is to extend existing routing schemes and make them power-aware. This avoids the need to create yet another MANET routing protocol.

1.2 Organization

This dissertation is divided into six chapters. Chapter 2 reviews the literature concerning power conservation in ad hoc networks. Chapter 3 states the problem of power awareness in ad hoc networks and, specifically, the problem addressed in this research. Chapter 4 presents simulation results, for a simple and static case, for our technique and describes the methodology used in obtaining these results. Chapter 5 presents results obtained for running the power-aware scheme with dynamic route discovery on large stationary and mobile networks for DSR and OLSR. Chapter 6 provides thesis summary, and describes future directions.

Chapter 2

Literature Review

The power conservation problem has been addressed extensively in the literature. This chapter reviews existing power saving methods and techniques developed for wireless LANs, in general, and mobile ad hoc networks, in particular.

2.1 Link Technologies for Ad Hoc Networks

This section discusses power management features employed in the IEEE 802.11 standard, HIPERLAN, and Bluetooth. There are several link technologies in existence today for mobile ad hoc networks (MANETs). Some of these technologies are geared toward small to medium size ad hoc networks, e.g. IEEE 802.11, Home RF and HIPERLAN. Others are geared toward personal area networks (PANs), e.g. Bluetooth and IEEE 802.15. These technologies share many similar characteristics, yet they differ in many ways, too. For example, all of these link

technologies support tether-less devices and provide low-power operation modes, while they differ in the number of nodes supported, the performance and throughput obtained, and the connectivity range.

2.1.1 Power Management in IEEE 802.11

IEEE 802.11 [27] takes advantage of switching off the transceiver as a means to conserve energy. It employs two power saving modes, "doze" (sleep) mode, and an "awake" (full power) mode. The standard describes two scenarios for power conservation.

The first scenario addresses mobile nodes connected in an infrastructure type of network. Nodes in this type of network connect directly with an access point (AP). Nodes that want to go into doze mode and conserve energy must inform the AP of their intention so that the AP can buffer data frames addressed to the dozing node. Dozing nodes have to periodically wake up and stay awake. During the wake up period, the AP sends a traffic indication map (TIM) with every beacon that contains a list of nodes for which it has buffered data frames. For the above communication to occur, IEEE 802.11 provides a timing synchronization function. This function helps the nodes, especially the dozed nodes, to wake up on time slightly before the beacon and the TIM arrive.

The second scenario addresses an ad hoc network where no AP is present. In this scenario, power management is more of a challenge. In ad hoc networks, nodes need to coordinate among themselves to buffer frames for dozing nodes. Either they designate a specific node

to buffer the frames or each node that has frames to send to a dozing node must buffer the frames until the next wake up period. Nodes that have buffered data frames announce the list of nodes for which they have buffered data in an ad hoc traffic indication map (ATIM) when all the power conserving nodes are awake during an ATIM window. In ad hoc networks, different nodes can generate a beacon. In this case all the nodes within the beacon's reception area wake up at the same time and stay awake for the ATIM period.

When IEEE 802.11 was standardized, saving power was not a major concern, even though limited power saving features were specified. Nodes in IEEE 802.11 always transmit at the highest power possible (unless manually configured to transmit at a specific lower power). This could result in delays, especially for nodes that are located at the edge of the transmission range of another ongoing communication and overhear the traffic exchanged. In this case the nodes at the edge of the transmission range have to wait for the channel to become idle before starting communication. Moreover, non-destination nodes that overhear a communication will end up depleting their energy resource from overhearing others. Woesner, *et al.* [22] have shown that the fixed size ATIM window degrades throughput and energy consumption. With a large ATIM window, nodes will be awake longer than necessary, while with a small ATIM window, fewer packets will be announced and transmitted.

2.1.2 Power Management in HIPERLAN

High Performance Radio Local Area Network (HIPERLAN) is a European Telecommunication Standards Committee Institute (ETSI) standard for wireless local area networks [17]. It offers services comparable to IEEE 802.11. It is mainly targeted toward small to medium size WLANS. HIPERLAN supports high-speed transfer rates (greater than 20 Mbps). Because HIPERLAN is based on a broadcast channel, transmitting at high bit rates unnecessarily wastes energy of non-destination nodes due to equalizer activation. Therefore, to save energy [22] and support interoperability at different data rates, HIPERLAN divides packets into two parts, a low bit rate portion and a high bit rate portion. The first 34 bits of a packet are sent at the low bit rate (1.47 Mbps) and the rest of the packet is sent at the high bit rate. This scheme allows non-intended receivers not to activate their equalizers [22] when they receive the low bit rate portion of the packet and decide they are not the intended destination. HIPERLAN devices can transmit at three different power levels, 1 W, 100 mW, and 10 mW [60].

HIPERLAN uses a distributed approach for power conservation. It is based on an agreement between a power supporting station (p-supporter) and a station that wants to save power (p-saver). P-supporters must be able to queue packets destined to p-savers. P-savers have wake-up intervals that the p-supporters know so that they send the queued packets for the p-savers. P-savers can have multiple p-supporters which all must be within radio range. This could lead to duplicate packets being forwarded to the p-saver, which will be detected by a HIPERLAN MAC entity (HM-entity). This could counteract the power conservation

process and waste bandwidth. Moreover, HIPERLAN allows each p-saver to define its own active period and the time between two active periods. This could lead to delays or packet loss since the p-supporter has to queue and delay the packets until the next active period of the p-saver.

2.1.3 Power Management in Bluetooth and IEEE 802.15

Bluetooth and IEEE 802.15 are short-range, peer-to-peer, radio technologies that make communications between portable devices feasible [16]. Both Bluetooth and IEEE 802.15 are considered wireless personal area networks (WPAN). Bluetooth is a specification put forward by an alliance of communication equipment vendors, while IEEE 802.15 is a standard set forth by the IEEE. IEEE 802.15 is backward compatible with Bluetooth and it supports data rates well above 20 Mbps, which is capable of handling multimedia content [61]. Devices communicating using the Bluetooth specification achieve data rates less than 1 Mbps. Both offer a short-range ad hoc wireless networking for personal digital assistants (PDAs), computers, printers, mobile phones, and so forth. They use the 2.4-GHz Industrial, Scientific and Medical (ISM) frequency band. They implement a frequency hopping spread spectrum (FHSS) scheme with binary frequency shift keying (BFSK) modulation. Devices that communicate using Bluetooth form what is termed a piconet. Piconets can connect up to eight different devices. Devices can be in more than one piconet. A group of piconets with connections between them is called a scatternet. Each piconet consists of a master and up to seven active slaves. The master unit characterizes the piconet channel by setting the

hop sequence. The master unit initiates a connection to a slave unit. Any unit in a piconet can become a master, thus the naming of master-slave convention refers only to the protocol on the channel [16].

Power management features in Bluetooth exist at two levels. At a low level, when handling packets, and at a high level, using low power operation modes [16].

Packet handling is minimized at both the transmit and the receive sides to minimize power consumption. At the transmit side, if only link control data is to be transmitted, power is minimized by sending only link control information using NULL packets. At the receive side, if the transceiver does not find a valid access code, a 72-bit code derived from the master identity which is unique for the channel, in the search window, then it goes to sleep. Otherwise the transceiver starts to process the packet header. Valid headers indicate if data follows and for how many slots [16]. Therefore, power minimization comes from the fact that no useless data has to be exchanged between the master and the slave to keep them synchronized. Moreover, the receiver can quickly decide whether a packet is present or not and, if not, the receiver goes to sleep [23].

At a high level, Bluetooth specifies two major states, the standby state and the connection state. The standby state is the default state. In this state the Bluetooth device is in low-power mode. Only a clock driven by a low-power oscillator, with relaxed accuracy, is active in this state. In the connection state, the connection has been established and packets can be sent back and forth. The Bluetooth device can be in one of four modes in the connection state: active, sniff, hold, or park. In active mode the device is awake and actively communicating

with other devices. Active mode supports regular transmissions to keep slaves synchronized to the channel. Active slaves listen in the master-to-slave slots for packets. If an active slave is not addressed, it may sleep until the master's next transmission. This is the most power consuming mode. In sniff mode the device is in reduced power consumption mode. The device listens for transmissions only at designated sniff time slots. To enter this mode, the master or slave device must issue a sniff command through the link management protocol (LMP). A slave in the sniff mode periodically wakes up to listen for transmissions from the master and to re-synchronize its clock offset. In hold mode the device is basically not actively communicating, yet it is still considered as an active member of the piconet. In hold mode the slave temporarily ceases support for asynchronous connectionless link (ACL) packets, while continuing support for synchronous connection-oriented (SCO) link packets. This mode uses less power than sniff mode. Park mode saves the most power. A device in park mode is not considered as part of the piconet. Even though the device is not part of the piconet, it still has to remain synchronized with the master's frequency hopping sequence. Therefore, like in the sniff mode, a slave in the park mode also periodically wakes up to listen for transmissions from the master and to re-synchronize its clock offset. These schemes help minimize power consumption in Bluetooth devices.

As mentioned earlier, in an effort to standardize WPANs, the IEEE formed a working group for such a task [26] [36]. This group is divided into four subgroups, each working on a different issue [26][36]. The first subgroup, 802.15.1, adopted the specifications (version 1.1) set forth by the Bluetooth Special Interest Group (SIG). Consequently, Bluetooth is

synonymous with 802.15.1. It is worth noting that the 802.15.3 subgroup is involved in developing a standard for higher data rate operation and low-power MAC and physical layers for applications such as multimedia and digital imaging. The 802.15.4 subgroup is working on ultra low-power, low-bandwidth specifications for applications such as sensors and automation demands. The industry acceptance of Bluetooth has given it an advantage over the IEEE 802.15 standard. Nonetheless, since both Bluetooth and IEEE 802.15 are similar in many ways, 802.15 could gain acceptance due to several factors. It is a set of standards proposed by a standards body, it supports higher data rates, several groups are working on the standards each with a specific task, and 802.15 is being developed to coexist with other wireless standards.

2.1.4 Summary

More than IEEE 802.11, HIPERLAN and Bluetooth were specified with power-saving in mind. Bluetooth has an extensive power-saving mechanism, however, it caters to a different segment of the market than that of IEEE 802.11 and HIPERLAN. Bluetooth is intended for wireless personal area networks, which are characterized by short distances between Bluetooth devices and lower data rates. IEEE 802.11 and HIPERLAN are intended for wireless local area networks. HIPERLAN does not distinguish between infrastructure and ad hoc networks. All networks are considered ad hoc, while IEEE 802.11 does make a distinction between the two types of networks and operates accordingly.

2.2 Routing Schemes

Network routing in MANETs can be classified into three classes, proactive, reactive, and hybrid. Routing schemes use control messages to learn the network topology. Most proactive routing schemes use link state or distance vector routing algorithms.

2.2.1 Reactive Routing Protocols

Reactive routing is an on-demand routing scheme. Nodes learn about the network topology on an as-needed basis. Two of the better known reactive ad hoc routing protocols are Dynamic Source Routing (DSR) [13] and Ad hoc On-demand Distance Vector (AODV) [9]. Reactive routing protocols are characterized by two phases, the route discovery phase and the route maintenance phase. In the route discovery phase, nodes build their routing tables on demand. The sending node sends a route request for a packet in its sending queue for which it has no route information to the destination or whenever a node receives a packet not destined to it for which it has no route information to the destination. Nodes send route inquiries to neighbors and add an entry to a list of previously discovered routes. For example, in AODV, nodes along the route store the route information, while in DSR the initiating node stores the source route returned to it from the route reply. The route maintenance phase uses route error packets and acknowledgments to maintain routes. Each node that sends a packet gets an acknowledgment back. Acknowledgments are either received at the link layer as defined by the MAC protocol of IEEE 802.11, or as passive acknowledgment

from the receiving node. If the receiving node fails to acknowledge the receipt of the packet, a route error is relayed back to the original sender which results in the removal of the broken link from its cache and use an alternative route if available or initiate a new route discovery. Route discovery and route maintenance do consume bandwidth, however. Sholander, *et al.* [48] state that reactive routing is preferable over proactive in situations where route concentration, route activity, and the number of active routes per node is low and mobility is high.

2.2.2 Proactive Routing Protocols

In proactive routing, nodes periodically monitor the network for changes in network topology. Therefore, every node in the network keeps an up-to-date copy of current network topology information by periodically broadcasting and receiving control packets. For instance, when a node receives a packet destined to another node, it knows how and where to forward the packet for final delivery of the packet. This relatively detailed information about the topology helps to improve the routing performance. However, this improvement in routing may come at a cost of increased overhead and a decrease in network capacity for data. Several proactive routing exist for MANETs. Two commonly referenced ones are Optimized Link State Routing (OLSR) [45] and Destination Sequenced Distance Vector Routing (DSDV) [50]. The way in which network topology information is gathered in proactive routing protocols is usually based on either of two algorithms, link state or distance vector.

Link State Protocols

In a link state protocol, each node keeps track of the changes that the network undergoes by keeping a map that reflects the state of all links in the network. Nodes use flooding, perhaps with some optimizations, to broadcast the link costs of their outgoing links to all neighboring nodes [50]. By exchanging link state, nodes learn the topology of the network. Each node creates a link-state packet that contains its identifier (ID), a list of its directly connected neighbors along with its cost to each one of them, a sequence number, and a time-to-live (TTL) value for the packet. These packets are broadcast whenever the TTL period expires or when the network topology changes. Link state routing is divided into two steps, flooding the network with link state information and the computation of routes based on link-state information using, typically, Dijkstra′s shortest path algorithm [50][57].

Distance Vector Protocols

Distance vector protocols are based on the assumption that each node knows the distance (cost) to its immediate neighbors [50][57]. Thus, in distance vector protocols, all nodes create a list of distances to their immediate neighbors and distribute this list to their immediate neighbors. Initially, each node assigns a cost of one to each of its immediate neighbors and a cost of infinity to other nodes. Afterwards, the nodes exchange these lists with all of their immediate neighbors and start to replace the large costs with lower ones based on the received lists. Distance vector protocols suffer from several problems. The count-to-

infinity problem occurs when a node fails and, as such, its neighbors keep increasing their cost to reach this node until they reach an infinite value [50]. Another problem with distance vector protocols is the slow convergence of routes throughout the network. By storing little information about links that are not directly connected to the node running the algorithm, distance vector protocols have lower complexity than link state protocols. In addition, the bandwidth requirement is also less [50].

2.2.3 Hybrid Routing Protocols

Hybrid routing protocols combine the use of reactive and proactive routing protocols to obtain a better balance between the dynamic nature of MANETs and the routing overhead and to reduce the average end-to-end delay [2]. These protocols usually introduce a hierarchical structure to the MANET to reduce the number of control packet retransmissions during route discovery [3]. In hybrid routing protocols, each node maintains a set of nearby neighbors with which it will use a proactive routing scheme and a set of more distant nodes with which it will use a reactive routing scheme. The use of different routing strategies at different times at different locations is used in routing protocols such as the Zone Routing Protocol (ZRP) [49] [2].

2.3 Power Conservation in Ad Hoc Networks

A number of power saving techniques have been proposed to minimize power consumption in WLANs. While there are some schemes proposed for ad hoc WLANs, the majority of the proposed schemes are meant for infrastructure-based WLANs. These schemes can be categorized into physical, link (MAC), network, transport and application layer approaches or a mix of these approaches. Some of these schemes are adaptive, others are non-adaptive. Some of the proposed energy conserving approaches include:

- turning off the network interface card (NIC) when the node is not actively engaged in communication [53];
- adjusting the power level according to the packet size [29];
- partitioning the network into different clusters and allowing each cluster to use a different spreading code [40];
- using transmission scheduling and slot reservation instead of contention-based schemes [8]; and
- using adaptive transmission strategies instead of persistent ones [52][29][46].

In multi-hop ad hoc networks, a large amount of energy may be wasted in listening by non-intended receivers. Since a lot of mobile devices are battery powered, this energy waste exacerbates the energy problem. Consequently, a lot of research has been conducted to

improve the energy capacity of batteries and to reduce power consumption. From a computer engineering standpoint, reducing energy consumption helps prolong the network life, which increases communications time as opposed to reducing interference and solving the near-far problem as in code-division multiple access (CDMA) based systems [20].

2.3.1 Techniques at the Physical Layer

Techniques used in energy minimization at the physical layer include miniaturizing circuit components, using efficient channel coding techniques, and improving amplifier characteristics of radio frequency (RF) circuits. Communication, in general, requires a lot of processing and processing consumes energy. Therefore, protocols designed to minimize energy must achieve a balance between the opposing goals of error-free communication and energy minimization. Lahriri, *et al.* [34] describe a new battery-driven system-level power management scheme, communication-based power management (CBPM), that aims to improve battery efficiency. CBPM regulates the execution of the various system components. System components are of two categories, bus masters and slaves. Bus masters are components that are capable of initiating a communication transaction such as central processing units and digital signal processors. Slaves, on the other hand, are components that respond to transactions initiated by masters such as memories. This scheme may delay the execution of some system components and adapt the current discharge of the system to suite the battery′s characteristics.

2.3.2 Techniques at the Medium Access Control(MAC)Layer

A comparison of power-saving techniques at the MAC layer in IEEE 802.11 and ETSI HIPERLAN is presented by Woesner, *et al.* [22]. In ad hoc networks, collisions and packet retransmissions deplete battery power unnecessarily. Therefore, it is highly recommended to avoid packet retransmissions as much as possible. Mobility is an inherent characteristic of ad hoc networks. As mobility increases, collisions increase and, hence, packet retransmissions increase. A transceiver going from the receive state to the transmit state consumes energy [8]. As a result, protocols that use slot assignments as a scheduling mechanism suffer a large overhead. Thus, to reduce the turnaround time, i.e., the time it takes to transition from a receive state to a transmit state and *vice versa*, and minimize energy, it is preferable to reserve several contiguous slots when transmitting or receiving [8]. Another solution in minimizing power consumption at the physical layer is to turn off the transmit/receive radio when the node does not anticipate any communication with other nodes. This technique is mentioned by Raghavendra and Singh [53]. Sivalingam, *et al.* [35] propose a reservation-based scheduling approach in which nodes broadcast their transmission time schedules so that they can go into standby mode and switch back to active mode when their transmit time comes. The Energy Conserving Medium Access Control (EC-MAC) protocol [35] [11] was developed with an energy conservation goal in mind. It was developed for an infrastructure-based wireless network where a single workstation serves mobile nodes within its coverage area. The authors argue that this protocol can be extended to an ad hoc network by allowing the mobiles to elect a coordinator to perform the base station functions. Others have

also devised new MAC protocols that take into account energy constraints [69]. Careful reservation and scheduling of packets help to enhance the performance of the protocol and reduce collisions. This avoids retransmissions and, hence, reduces power consumption [35]. El Gamal, *et al.* [1] use an algorithm, MoveRight, to solve a convex problem based on the idea that, in many channel coding schemes, lowering transmission power and increasing the duration of transmission leads to a significant reduction in transmission energy. The Power Aware Multi-Access (PAMAS) protocol modifies the Multiple Access with Collision Avoidance protocol (MACA) described by Karn [38]. PAMAS is based on the premise that by allowing separate channels for control and data packets, nodes know when and for how long to turn off their transceivers. Simulation results from the study show that a power savings of up to 70 percent can be achieved for a fully connected network [38].

2.3.3 Techniques at the Link layer

Avoiding and delaying transmissions when channel conditions are poor improve energy minimization. Rao, Zorzi and Ramesh [55] found that by improving currently used error control schemes to cater to limited energy devices produces favorable results. Therefore, persistence is not preferable when energy is a constraint. Due to the dynamic nature of wireless links, error rates due to fading, attenuation and interference are highly variable. As stated by Zorzi, *et al.* [55], error control schemes such as automatic repeat request (ARQ) and forward error correction (FEC) waste network bandwidth and consume energy. When using these techniques in wireless environments, care should be taken so that packet retransmission and

error correction do not overwhelm the wireless channel. Lettieri, *et al.* [47] describe an adaptive error control architecture that incorporates adaptive error control with forward error correction. This scheme changes the error control scheme according to the stream′s channel conditions over time. In wireless networks, channel conditions along with traffic characteristics dictate the type of error control scheme used. Agrawal, *et al.* [43] study the effect of dynamic power control and forward error correction on power consumption. In their study, each node determines the minimal power and forward error correction required that satisfy a quality of service (QOS) constraint. In their technique, the signal is encoded twice with different transmission powers acting as boundaries for the upper and lower bound of transmission power.

2.3.4 Techniques at the Network Layer

In wireless networks routing can be either through a base station or access point, as in the case of infrastructure wireless networks, or through the mobile nodes involved in the network, as in the case of ad hoc networks. Routing in wireless networks must take into account node mobility and route management and, when energy-efficient routing is required, routing through nodes with ample energy is preferable when extending network life is the goal. Several schemes have been devised to minimize power usage [59] [64] [58] [71]. Singh, *et al.* [59] use power-aware metrics for route discovery in addition to using PAMAS as a MAC protocol for their study. They report an energy improvement of 40 percent to 70 percent. The algorithm they use is based on lowest-cost, rather than shortest-hop, routing. Chang

and Tassiulas [64] propose a routing algorithm that maximizes the battery life leading to a maximization of the network lifetime. It maximizes the network lifetime by balancing routing and energy consumption among nodes according to the battery′s energy reserves. Another scheme is to use heuristics to adaptively adjust the transmit power whenever a topology change occurs, keeping in mind the connectivity of the network [54]. Banerjee and Misra [5] developed a transmission power adaptive algorithm that finds the minimum energy routing path. The authors also use analytical methods to find the optimum transmission energy on each individual path in a multi-hop wireless network.

In good channel conditions, more energy can be saved. Good channel conditions, generally, imply that packets reach their destinations error free. This leads to fewer retransmissions and ultimately, to increased network life. Spyropoulos and Raghavendra [62] propose an energy-efficient routing and scheduling algorithm for use in nodes equipped with directional antennas. The authors argue that using omni-directional antennas leads to a large waste in energy since power is broadcast in all directions. Directional antennas can direct power toward the intended node. Wieselthier, *et al.* [32] propose a similar approach, but for connection-oriented multicast traffic. The authors argue that the network life can be extended by incorporating the nodes′ residual energy into the cost function and equipping the nodes with directional antennas.

Feeney [18] has carried out simulations and experimental measurements of energy consumption on a per-packet basis for a Lucent WaveLan 2.4 GHz DSSS IEEE 802.11 wireless network interface card for two ad hoc routing protocols, DSR and AODV. The study mea-

sured the energy cost incurred at nodes that are in receiving range but are not destination nodes. The results indicate that the number of packets has a greater impact on energy consumption than packet size and that the power consumption cost of idle mode is high. Routing in wired networks relies on shortest paths and smallest delay. In wireless networks, the metrics differ since power limitation is a problem in mobile ad hoc networks. In this case routing through the closest node could hasten the death of that node. Therefore, other measures should be taken to alleviate this problem.

Singh, *et al.* [59] define five metrics for studying the performance of power-aware routing for unicast traffic: energy consumed per packet, time to network partition, maximum node cost, variance in power levels across nodes, and cost per packet. They study the effects of these metrics on end-to-end delay. Their results show that by using power-aware metrics instead of a shortest-hop metric, no extra delay is incurred.

Routing in MANETs requires the knowledge of node locations and the links between these nodes. This leads to higher communication overhead. Stojmenovic and Lin [71] propose a loop-free localized routing algorithm. In this localized cost and power-cost routing algorithm, additional nodes are placed between the source and destination to make the transmission power linear. Thus, transmission power is in terms of d instead of d^{α}, where d is the distance between source and destination nodes and α is the propagation constant, where $\alpha \geq 2$. In localized power routing, nodes make decisions based on location, determined with Global Positioning System (GPS) devices, and distance from source to destination. For broadcast traffic, where intermediate nodes are required to retransmit the packet, Singh,

et al. [30] show that channel allotment to nodes is important for power-efficient broadcast protocols. They also suggest that it is beneficial to spend some energy to gather topology information to determine the most energy-efficient broadcast tree. In another paper, Singh and Raghavendra [30] present a broadcast tree approach to share the cost of routing among all nodes in the system. In this case, a cost is associated with each node based on how much power the node has consumed. Priority in routing is given to nodes that have consumed lower amounts of power and nodes that have more neighbors. The study assumes that all nodes have only broadcast traffic. Packets from the same source may traverse different trees as the network topology changes. Wieselthier, *et al.* [31], combine routing decisions with transmission power levels. They describe an algorithm for determining a source-initiated minimum-energy tree for broadcast or multicast session requests. Their results show that the exploitation of routing and transmission power decisions provides greater energy savings than algorithms that are developed for link-based, wired networks.

Feeney [18] compared the Dynamic Source Routing (DSR) protocol and the Ad Hoc on Demand Distance Vector (AODV) routing protocol in terms of their energy consumption. The study takes into account the cost of sending and receiving packets, routing overhead and dropped packets. The study indicates that there is considerable energy being wasted on flooding the network with data packets and MAC control packets. In addition, receiving and discarding packets consumes a substantial amount of power. The study also indicates that the cost of source routing headers in DSR is not significant, but operating the radio in promiscuous mode for routing and caching of routes wastes energy. The study also indicates

that the generation of broadcast traffic in AODV results in high energy consumption.

2.3.5 Techniques at the Transport Layer

Several studies have been conducted to look at energy minimization at the transport layer. While TCP works well in wired networks, using the same version of TCP for wireless links can lead to inefficiencies in terms of performance and energy use. The characteristics of wireless links are inherently different than wired ones. Therefore, applying standard TCP to wireless links, without modification, may not provide good performance for wireless networks.

Several schemes have been proposed to reduce the effects of TCP retransmissions due to factors other than congestion [4], [51], [15]. These schemes have been classified by Jones, *et al.* [8] into three groups: split connection protocols, link-layer protocols, and end-to-end protocols. The studies of Bakre *et al.*[4] , Balakrishnan *et al.*[51], Gitlin *et al.*[15], show that these schemes provide better performance than standard TCP due to their adaptability to the dynamic nature of wireless links. Tsaoussidis, *et al.*[37] studied the energy versus throughput performance tradeoffs for different TCP variations. Their findings indicate that balancing energy consumption and throughput can be accomplished through the error control mechanism. Kravets and Krishnan [39] have designed and implemented a protocol that selectively chooses short periods of time to suspend communication and shut down the transceiver. The algorithm handles the queuing and management of packets during this period.

2.3.6 Techniques at the Middleware and Application Layers

In an energy efficient system design, it is crucial to have the operating system and the applications that run on top of the operating system support the underlying power management mechanisms. Recent operating systems have incorporated the Advanced Configuration Power Interface (ACPI) standard that can power down devices that have not been used for a certain period of time or even shut down the entire system after a certain period of inactivity [12]. Integrating power efficient features specific to wireless networks will certainly help increase the life of the network.

2.4 Other Approaches

Several approaches have been developed to reduce or help reduce power consumption. Here, we describe power-saving features in smart batteries that are intended mainly for mobile devices and the PRISM chipset′s power conserving features intended for wireless networks.

2.4.1 Smart Batteries

Smart batteries are battery cells that incorporate electronic monitoring circuitry. The monitoring circuitry is provided to prevent overcharging, undercharging, or short-circuiting of the battery cells [56]. In an effort to enhance rechargeable batteries, Duracell, Inc. and Intel Corp. have teamed up to develop a specification called the Smart Battery System (SBS).

The aim of this specification is to provide a monitoring device to read the remaining charge of the battery, the current, the voltage, and the temperature of the battery [6]. In addition, the specification intends to extend battery life and provide a set of standard signals to chargers. The hardware interface for smart batteries consists of an embedded controller with registers and a one- or two-wire bus that the device operating system or middleware accesses to read the state of the battery. Currently, nearly all newly manufactured notebook computers follow the SBS since power management is part of the ACPI specification required for compatibility purposes with modern operating systems [56]. ACPI allows the operating system to directly manage power information from users, applications, and the hardware by reducing power or shutting-down services or devices that are not used [66]. In our study, we make use of the information provided by smart batteries and apply it to the routing algorithm in making routing decisions. We use the remaining battery charge as a metric to help nodes select optimal routes.

2.4.2 PRISM II Chip Set

The PRISM II chip set is compliant with the IEEE 802.11b standard [7] [28]. PRISM II provides 100 mW of power at the antenna, which allows for data connectivity of up to 400 ft indoors and 1000 ft outdoors. IEEE 802.11b has one sleep mode with different sleep times. The PRISM II chipset takes advantage of this feature to set various doze modes with various sleep times. The MAC decides which PRISM II doze mode to use. The PRISM II radio has the ability to power off specific circuits of the radio depending on the doze mode.

Additionally, the baseband processor has the capability of turning off its clocks and portions of its circuitry giving additional doze modes. There are four power-saving (doze) modes. Each mode turns off a specific part of the radio circuit. The more circuits that are turned off means that more power is saved and that it takes longer to recover from the doze mode. Doze mode 4 is the maximum power saving mode with a recovery time of 5 ms, while mode 1 is the least power-saving mode with a recovery time of 1 us. An additional power saving mode is available by turning off all the circuits except the MAC. It is possible to slowly transition the PRISM II chip set from the last doze state to a fully awake state by performing stage awakening.

2.5 Evaluation Techniques and Methods

To test and evaluate the benefits and drawbacks of a scheme or an algorithm, an evaluation technique is needed. Evaluation techniques can be divided into three categories: simulation based, experimental, and analytical. Some combination of more than one technique may also be used. From the reviewed literature on power saving in wireless networks, three evaluation techniques are noted. A significant number of the performance evaluation studies are simulation based, followed by the mixed approach.

Singh, *et al.* [59] simulated a fixed network of 10 to 20 nodes and presented five power-aware metrics that are different from the usual routing metrics such as shortest-path and link quality. The new metrics outlined in their paper are energy consumed per packet, time

to network partition, variance in node power level, cost per packet, and maximum node cost. In their simulations, Singh, *et al.* studied the effects of these metrics on end-to-end packet delay. The performance of shortest-path routing was compared with that of least-cost routing. The simulations yielded significant reductions in energy cost by using shortest-cost routing as opposed to shortest-hop routing.

In Bergamo, *et al.* [44], the transmit power is used as the link cost function. Nodes need to store transmit power, P_{tx}, and estimate the receive power, P_{rx}, and estimate link attenuation by subtracting (in dB) the transmit power and received power. Bergamo, *et al.* [44] also simulate Dijkstra and link state algorithms using a simple ad hoc simulator (SAM) that integrates all traffic features, terminal mobility, channel behavior, medium access schemes, and routing protocols. Several simulation parameters were used in the study, including the minimum power necessary to correctly receive a packet before de-spreading. In addition, the parameter α is set to 2.5. The α parameter characterizes the path power loss, i.e. the further the signal travels the more the loss in signal power (d^{α}), where d is the distance the signal has traveled. Bergamo, *et al.* [44] found their distributed power control scheme achieves reduction in energy consumption while keeping the performance similar to that of the classic Dijkstra and Link State routing algorithms.

Banerjee and Misra [5] evaluated their energy conserving routing schemes, each with a different cost metric, using the NS-2 simulator [67]. They considered the routing effects on both Transmission Control Protocol (TCP) and User Datagram Protocol (UDP) traffic for different topologies. The topologies were divided into two types: (i) grid topologies in which

nodes are placed 100 units apart and each node′s transmission radius is limited to 150 units and, as such, each node has up to 8 neighbors; and (ii) random topologies in which nodes are uniformly distributed in a 1000×1000 square area. In the random topology, the experiments varied the transmission radii and the number of links were fixed to avoid unidirectional links. The authors studied two different metrics, normalized energy and effective reliable throughput. Normalized energy is the ratio of the average energy per data packet to the average energy per data packet required by the maximum energy experiment between all routing schemes among all the experiments. Effective reliable throughput is the number of packets reliably transmitted from source to destination over the simulated duration. Banerjee and Misra [5] found that their power adaptation scheme outpreforms existing techniques for a wide range of channel characteristics and across different modulation techniques. The power adaptation scheme is useful in static or slow moving multi-hop networks where parameters such as distance or attenuation coefficients do not change rapidly.

Doshi and Brown [14] also used NS-2 for their simulations. They used the power model that is included in NS-2. The NS-2 power model ignores the idle cost, which is the power expended by the node when it is idle, to simplify analysis. The authors added power information to the route request replies of DSR. Changes have been made also at the MAC level to include power control acknowledgments and data acknowledgments power sensing options. Further, the authors employed the exchange of two frames for the MAC level data transmission. The total energy was divided into three parts: energy expended in DSR routing packets, energy expended in MAC signaling packets, and energy expended in data packets. The last part was

further subdivided into three parts: energy consumed by the MAC header, energy consumed by the routing header, and energy consumed by the payload. Static and low-speed random waypoint scenarios were used to test the modifications. Doshi and Brown [14] found that as mobility increases the performance of the minimum energy routing protocol degrades yet reduction in energy is still achieved.

Feeney [18] models energy consumption in ad hoc networks by identifying four possible states for a NIC. These states, ordered in increasing energy consumption, are transmit, receive, idle, and sleep states. The cost function is a linear equation used to model the cost for a node to send and receive network packets. Utilizing the cost functions for different types of traffic, i.e. broadcast traffic, point-to-point traffic and traffic overheard by non-destination nodes (discarded traffic) for an IEEE 802.11 NIC, the authors show cost measurements for all four states of a WaveLan PC card using 2.4-GHz direct sequence spread spectrum with linear model power consumption. Simulations were carried out to test DSR and AODV with the new cost functions. Two versions of DSR were considered with and without promiscuous listening. The author found that there is a large energy cost in DSR due to promiscuous listening of source routes by all nodes in the network. The energy cost is significantly reduced in the non promiscuous version of DSR since only the forwarding nodes extracts the information form the source routes. This has resulted in DSR with out promiscuous listening being the most energy efficient among the three protocols studied. AODV also exhibited larger energy cost than that of DSR with out promiscuous listening at high mobility due to the need for AODV to initiate route discoveries more often, since nodes in AODV do not

maintain a network-wide topology information.

2.6 Summary

This chapter focused on previous work done in the area of power minimization in wireless networks, in general, and MANETs, in particular. We presented the techniques developed for the physical layer up to the application layer, with emphasis on the link and network layers.

Most of the research we reviewed focused on either new power-aware routing protocols or new strategies that can be applied to routing protocols. In our work we extend a well known MANET routing protocol, namely DSR, with power-aware features. We compare and contrast the performance of the power-aware DSR with the unmodified version in terms of power saved, end-to-end delay, network life, and percentage of packets delivered. We also extend a well known proactive MANET routing protocol, OLSR, and run the same tests with the power-aware version and the original version. We also study the effects of our proposed power-aware scheme on the reactive protocol and the proactive protocol on the power saved, network lifetime, delays, and overhead.

The next chapter deals with problem formulation and the approach we plan to carry out in our solution to the power saving problem in MANETs.

Chapter 3

Problem Statement and Approach

3.1 Motivation and Problem Statement

In wired networks the assumption is that nodes connected to the network have an unlimited amount of energy, hence minimizing energy is not a concern in protocol design. Unlike wired networks, mobile nodes in ad hoc wireless networks are typically powered by energy-limited devices, usually batteries. In this case minimizing energy consumption is of crucial importance to the feasibility and utility of the wireless network. Energy consumption is crucial to the life of the network. Network life is defined, for our purposes, as the time it takes a connected set of nodes to partition into two or more disjoint sets due to power exhaustion in one or more nodes [64][33]. Requirements for network life depend on the type of wireless network and its objectives. In networks where human life is endangered, such as

in battlefield or emergency response applications, the life of the network is likely of utmost importance. In contrast, in certain applications in sensor networks, the loss of few nodes due to power exhaustion might not be important as long as there exist redundant nodes that can take over tasks for the lost nodes. Therefore, relying on the fact that networks must be dense and redundant, the loss of a few nodes may not affect the survivability of the network. In some ad hoc networks, where the network is limited in functionality and duration, the life of the network might not be as critical as in the previous cases. In such networks, the life of the network and the task being accomplished are often short compared to the battery life, hence energy consumption is often not a priority.

In ad hoc networks nodes that are loosely coupled, i.e. nodes can join and depart the network at will and at any moment. Any node can function as a router. The task of routing or forwarding consumes precious energy resources. Nodes can cooperate with each other or they can be greedy in terms of using the resources available in the network without sharing their own resources. This type of behavior gives rise to two categories of ad hoc networks, cooperative and non-cooperative.

3.1.1 Cooperative Ad Hoc Networks

In cooperative ad hoc networks all nodes route and forward packets as if they are their own. The benefit to the network, versus the benefit to individual nodes, is relevant. An example of a cooperative ad hoc network is one where two nodes, multiple hops apart, engage in a

file transfer with all of the other nodes trying to help in forwarding and routing the packets from the source to the destination and *vice versa* without regard to the power expended due to packet forwarding even in cases where the nodes involved in forwarding have low energy. In this case, the cooperative nodes should ideally rely on the routing protocol to choose nodes with more reserve energy to forward packets and to distribute the load on different participating nodes so that longer network life is attained.

There are ample applications for cooperative networks. As an example, consider a team of scientists working in a remote area, e.g. a desert or jungle, where no network or electricity exists, studying the habitat of certain animals or group of animals. Sharing their findings among each other requires the cooperative use of resources available for maximum ad hoc network survivability.

3.1.2 Non-Cooperative Ad Hoc Networks

In non-cooperative ad hoc networks, each node can decide to not participate in packet routing and forwarding. Nodes are generally concerned only with their own benefit. In this case, communicating nodes must rely on other nodes within the ad hoc network to act as routers between the source and the destination. Non-cooperative nodes can be viewed as dormant or inert nodes when it comes to the overall activity of the ad hoc network even though they may be utilizing network resources and have ample battery energy.

A distinction can be drawn here between non-cooperative nodes and non-cooperative net-

works. In non-cooperative nodes, the particular resources of that node are off-limits to any node within the network. Since the broader sense of an ad hoc network is that any node can join and leave the network at will, there may exist a cooperative network with non-cooperative nodes joining and leaving utilizing the network resources. However, in non-cooperative networks, nodes within the network may be fully or partially cooperative, depending on the resources that each has to offer the other, while outside nodes can join the network with either limited or no services granted to them. Therefore, non-cooperative nodes render the network non-cooperative, while non-cooperative networks do not necessarily mean that all nodes in the network are non-cooperative. Examples of such nodes or networks can be countless depending on the specific application of the network or for security concerns, if not power. For example, file sharing ad hoc networks in public places such as cafes, dorms, etc. can follow the scenario where a few nodes can fully cooperate with each other, thus allowing each to utilize the other resources, while other nodes cannot use their resources. Also, not every one who is in a cafe is interested in file sharing, but may want to accomplish some work, therefore some nodes' resources are off limits to other nodes.

3.1.3 Approach

Prior research has found ways to minimize power consumption in wireless devices and measure the influence of routing protocols on energy consumption. The contention-based medium access control (MAC) protocol of IEEE 802.11 increases energy consumption which adversely affects the lifetime of a wireless network, especially in an ad hoc wireless network [11] [55]

[21]. Current implementations of IEEE 802.11b have some power saving mechanisms that try to reduce the total energy expended, for example using the schemes implemented in the PRISM II chipset as mentioned in Chapter 2. To fully reduce power expenditure, power reduction techniques must encompass all levels of the system [8]. On the hardware level, components must be designed to use minimum energy. On the software level, the software must utilize the hardware in the most energy efficient manner.

In this research, the focus is on energy reduction at both the network and the MAC layer. The enhancements are implemented mainly in the routing and MAC protocols, which we believe can aid in reducing energy consumption in nodes, in particular, and in a mobile ad hoc network, in general. The enhancements are based on adaptive power transmission, a feature found in many existing wireless network interface cards such as Cisco's Aironet 350 series [63] and the use of smart batteries in hand-held devices. Our scheme makes use of the dynamic transmission power employed in current wireless network cards, along with battery status, especially the remaining energy, provided by smart batteries powering hand-held and mobile devices. By using the appropriate transmission power, i.e., at a level just high enough to allow the transmitted packet to be received by the destination or intermediate node, we can reduce the overall expended power in the ad hoc network and, in addition, reduce interference between nodes. The routing algorithm can use remaining battery energy to balance the routing or forwarding of packets among nodes by choosing appropriate nodes as packet forwarders.

The power saving algorithm implements the following features. Each node keeps track of

the remaining energy of its battery and assigns a battery level to itself. The battery level is updated on a timely basis. Additional study is needed to determine appropriate intervals for updates. A routing table is built based on "cost" values instead of minimum hop values. In our scheme we use "reluctance" as our cost for routing a packet through a node. Each node stores a static table of all possible reluctance values. An assignment of a reluctance value is derived from the node's remaining energy and transmission power levels. A static table is used since reluctance assignments are not linear as will be explained below. The term reluctance was used by Singh, *et al.* [59] [70] to indicate the battery's remaining energy and, hence, the node's reluctance to forward packets. In our definition of reluctance we give it another dimension by including the transmission power required to reach the destination node. The larger the reluctance value of a node, the less likely it is that the node will route or forward packets for other nodes. If two nodes have equivalent remaining battery energy, a lower reluctance value is assigned to the node that can reach the destination node with lower transmit power. Also, a lower reluctance value is assigned to a node with higher remaining battery energy if the two nodes can reach the destination with equivalent transmit power. In an ad hoc network it is possible to have nodes with similar reluctance values. In such a situation it is unimportant, with respect to power, as to which route to choose and, hence, the least used route can be selected to deliver the packet. As time goes on, the battery energy gets depleted and the nodes move, so each node in the network must update its reluctance value, for the link over which it is communicating, in the table according to its remaining battery energy, assuming nodes move relative to each other and transmit power

stays the same. A node sends a packet to other nodes in the network with this information so they can update their routing tables accordingly. Reluctance updates should be generated at randomly chosen times, within a certain time limit, so that the nodes do not overwhelm the network with update packets. This is similar to the randomization procedure of route replies used in DSRs' NS-2 implementation, which is done to mitigate route reply storms [67]. The reluctance values are associated with a particular link and, hence, they are link dependent. This means that in non-cooperative ad hoc networks a node can ignore the reluctance values from the table and selectively choose a value for a link to another node with which it wants to cooperate or not cooperate. Our study is limited to cooperative ad hoc networks. Therefore, all nodes use the same reluctance table where the reluctance values are assigned to enhance network lifetime. Figure 3.1 shows route selection based on reluctance values. The figure shows node 1 communicating with node 4 and nodes 2 and 3 serving as intermediary nodes. After route discovery, at time T, node 1 finds that the route through node 3 has lower reluctance than the route through node 2, therefore it uses this route to forward its packets to node 4. After some time, at time $T+d$ after a route reluctance update, the route through node 2 returns a lower reluctance value, therefore, node 1 uses it to forward its packets to node 4.

Transmit power and remaining battery energy are quantized into several levels. The transmit power of typical IEEE 802.11 wireless network cards range from 0 dBm (1 mW) to 20 dBm (100 mW) [27]. We chose to segment the transmit power into six distinct levels separated by 4 dBm. A similar division can be applied to the remaining energy level. Battery

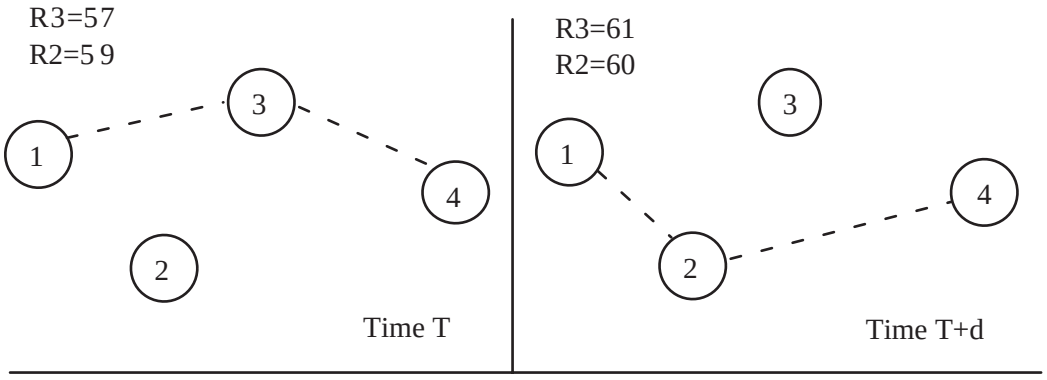

Figure 3.1: Example of reluctance-based route selection.

levels can be divided at 10 percent intervals, giving ten distinct levels. The levels are divided linearly for simplicity, however, future studies can examine non-linear power consumption to appropriately divide the battery levels to better match the non-linear behavior of batteries. Dividing transmit power or battery energy into discrete levels has the advantage of enabling the routing protocol to choose the appropriate node at the appropriate transmit power, alas, at the expense of increased processing.

Internet Protocol (IP) packets include the cost information, reluctance, battery and transmit power levels in an option field in the header so that receiving nodes can utilize this information to route and forward packets.

When using adaptive power transmission, different types of packets are sent at different power levels. For example, a broadcast packet should be sent at the highest power possible, while a non-broadcast packet can be sent according to its proximity to the destination. The term proximity here encompasses not only physical distance, but also channel interference

and any other impairment to the wireless link.

3.2 Network Model

An ad hoc network can be modeled as a weighted bi-directional graph **G = (N, L)**, where **N** is the set of all nodes, n, that comprise the network and **L** is the set of edges or links, l, between connected nodes. A node can have more than one route from source s to destination d. Hence, **K** is a set of routes k_x, where $x = \{1, 2, 3...\}$, **K**=$\{k_1, k_2, k_3, ...k_x\}$. Each route is composed of a set of edges or links l_x, where $x = \{1, 2, 3...\}$. Therefore a route k from the source node s to the destination node d is denoted by k_x=$\{l_s, l_{s+1}, ..., l_{d-1}, l_d\}$, where l_s is the starting link from the source node, l_{s+1} is the next hop in the route from the source, l_{d-1} is the hop prior to last from the destination and l_d is the last hop leading to the destination. Figure 3.2 shows a depiction of a route.

Figure 3.2: A route from source s to the destination d.

The weight function maps the links to a positive integer domain **I**, (**L** $\longrightarrow$ **I**). We assume that each node calculates the weight, also known as reluctance value r, of each of its edges by using a pair of measurements, measurement P_{tx} is the transmission power needed to transmit

a packet successfully along link l_x and e_i is the node remaining battery energy. The weight, or the reluctance value for node i along link l_x is r_{ix}. The weight of route k_x from a source node s to a destination node d, $W(k_x)$, is the sum of all the reluctance values r_{ix} for each link along route k_x starting from the source node s and ending at the destination node d. $W(k_x)= \{r_s + r_{s+1} + ... + r_{d-1} + r_d\} = \sum_{x=s}^{d} r_{ix}$ where, $x \in \mathbf{L}$, and $i \in \mathbf{N}$ for route k_x.

The problem now is reduced to finding a minimum cost route in a weighted graph, where the cost is related to energy. This implies that if a node has more than one way to reach a destination, the route k with the minimum sum is chosen, $W(k)= \min\ (W(k_x))$, where $x \in K$.

3.3 Cost Function and Metrics

To implement our energy-aware routing scheme, we consider a hierarchy of two categories, one category for remaining battery energy, the *e-cat*, and another category for transmit power required, the *p-cat*. The e-cat and p-cat are divided into three different levels, high, medium, and low. Each level within a category is assigned a range of reluctance values from a set of integers. A node sets the reluctance value for a link, depending on the quantized values for the remaining battery energy and transmit power the node needs to send a packet on the link. To incorporate such a scheme, we introduce three variables in the cost function.

- P_x: power level of transmitting node along link l_x

- B_i: battery energy level of node i
- r_{ix}: reluctance of node i along link l_x

Our goal is to reduce the power consumed to transmit the packet to the destination. Reluctance is the node's unwillingness to route packets for other nodes, possibly due to selfishness or a low battery level. Using a least-cost algorithm, we can find a route with the minimum cumulative reluctance value, which means a route using nodes that provide relatively high available energy and low required transmit power. As mentioned earlier, reluctance values are assigned to ordered pairs of (transmit_power_level, remaining_battery_level), or, using the variables defined above, (P_x, B_i). These values are stored in a static table that encompasses all the different combinations of power and remaining battery levels. During the neighbor discovery procedure, neighbors send their reluctance values back to the route discovery initiator based on their value of B_i and the transmit power associated with the route request, P_{tx}. This assumes that links are bi-directional and nodes are capable of measuring the received signal power, so that they can calculate the power level P_x. Neighboring nodes assign their own reluctance to a specific link based on (P_x, B_i) and send it back to the route request initiator in the route reply message so that the initiator can calculate all links reluctance values and find the route with least total reluctance. The research initially looked at static nodes, therefore, the transmit power is known *apriori*. The second part of the research looked at discovering routes by gradually increasing the transmit power starting from a low power state.

We measure reluctance by assigning a node with high battery level and low transmit power level a low reluctance value and a node with low battery and high transmit power a high reluctance value. For instance, we might specify that (6, 4) has a higher reluctance value than (5, 4) since the power is higher in the first pair. The same is true for (3, 4) and (3, 5) since the battery level is lower in the first pair. Table 3.1 shows the reluctance values and their division according to battery level and transmission power. From Table 3.1 the following corresponds to transmission power.

- P_x1 corresponds to transmission power ($P_x<$ 10 dBm)
- P_x2 corresponds to transmission power (10 dBm $\leq P_x <$ 13 dBm)
- P_x3 corresponds to transmission power (13 dBm $\leq P_x <$ 17 dBm)
- P_x4 corresponds to transmission power (17 dBm $\leq P_x <$ 21 dBm)
- P_x5 corresponds to transmission power (21 dBm $\leq P_x <$ 23 dBm)
- P_x6 corresponds to transmission power ($P_x>$ 23)

Table 3.1: Reluctance Values Division According to Battery Level

	P_x1	P_x2	P_x3	P_x4	P_x5	P_x6
Low Battery Level	61	62	63	64	65	66
$(0 \leq B_i < 4)$	51	52	53	54	55	56
Medium Battery Level	41	42	43	44	45	46
$(4 \leq B_i < 7)$	31	32	33	34	35	36
High Battery Level	21	22	23	24	25	26
$(7 \leq B_i \leq 9)$	11	12	13	14	15	16

In the routing procedure, the reluctance values are partitioned into three levels. A range of integer values is assigned for high battery level (7-9), a second range is assigned for medium battery level (4-6), and a third range is assigned for low battery levels (0-3). Therefore, the routing cost function can be computed and used as follows.

IF *battery_level is "high" ($7 \leq B_i \leq 9$)*

IF *a direct link from S to D exists* **THEN**

set reluctance value to lowest value from the range of high-level values

send packet directly to D

ELSE

set reluctance value according to (P_x,B_i)

send the packet through lowest cost route (min $W(k)$)

IF *battery_level is "medium" (4 ≤ B_i < 7)*

IF *a direct link from S to D exists* **AND** *(B_i ≥ 6)* **THEN**

set reluctance value to lowest from the range of the medium-level values

send packet directly to D

ELSE

set reluctance value according to (P_x,B_i)

send the packet through lowest cost route (min $W(k)$)

IF *battery_level is "low" (0 ≤ B_i < 4)*

IF *a direct path from S to D exists* **AND** *P_x is low* **THEN**

set reluctance value to lowest value from the range of the low-level values

ELSE

set reluctance value according to (P_x,B_i)

send the packet through lowest cost route (min $W(k)$)

In mission critical applications, it is advantageous to have a cooperative ad hoc network where all nodes cooperate with each other during the life of the network. At the same time it is also possible to have an ad hoc network where not all the nodes are truly cooperative. In such scenarios, which can be categorized as a form of greedy ad hoc networks, nodes start with a credit value for routing others' packets. Once the credit limit is reached, the node

will cease routing packets for others.

The number of packets to forward can be used as a credit value, for example a node sets a limit on the number of packets that it will forward for others, beyond this limit it will not forward for them. Also, a node can specify that it will forward for others as long as the remaining battery energy is above a certain threshold. When the battery level falls below this threshold it will cease routing for others.

When the ad hoc network is cooperative, reluctance values should be chosen on the basis of transmit power and battery level to best take advantage of power minimization and network survivability. But, in a greedy ad hoc network, reluctance values can be skewed such that nodes generating traffic bear the cost of their traffic in terms of energy, i.e. the reluctance values are set in a way that routes are more likely to go through nodes that generate more traffic. It is worth mentioning that reluctance information is local in reactive routing protocols, while in proactive routing protocols, reluctance information is global.

3.4 Evaluation Methodology

To evaluate and study the enhancement for energy conservation, a series of simulations and measurements are carried out using modified and unmodified versions of two existing MANET routing protocols. We test the enhancements with a reactive protocol, DSR, and a proactive routing protocol, OLSR. We study the effects of the enhancement primarily on the network lifetime under different mobility scenarios and network topologies. We also

study the side effects of the enhancement on network performance metrics such as delay and percentage of packets delivered to the application. The testing performed on single-hop and multiple-hop ad hoc networks. Moreover, we implement the same scheme on a proactive routing protocol and compare and contrast the relative performance under stationary and mobile scenarios.

Initial experiments were conducted on sparse and dense static ad hoc networks. We ran the experiments until the communicating nodes stopped communicating due to battery power exhaustion in the intermediate nodes, then gathered the information needed for the metrics under study. Each experiment was repeated five times with different seeds to determine any effects of randomness. Later, experiments were performed on large network scenarios under static and mobile conditions. Table 3.2 lists the static parameters used in all experiments. Note that 'CBR' stands for constant bit rate.

Table 3.2: Static Parameters for Experiments

Static Parameter	value
Data Rate	2 Mbps
Traffic Type	CBR
Frequency	914 MHz
Antenna Height	1.5 m
Initial Battery Energy (intermediate nodes)	10 J
Initial Battery Energy (sending nodes)	15 J

We ran these simulations for power-aware and the non-power-aware versions of a reactive and a proactive protocol under stationary and mobile scenarios. Table 3.3 shows the simulation parameters, or factors, that were varied in the simulation experiments.

Table 3.3: Factors for Experiments

Factor	Values
Routing Protocol	U-DSR, PA-DSR, U-OLSR, PA-OLSR
Node Density	Sparse, Dense
Mobility	Static, Mobile
Number of Nodes	5, 16
Number of Flows	1, 3
Packet Size (bytes)	512, 1000
Traffic Rate (packets/second)	27.7, 33.3, 50
Battery Model	Linear, Non-Linear

The simulations were carried out in NS-2. NS-2 is a freely available network simulator for wireless and wired networks. The main reason for choosing NS-2 over other simulation tools is because of the extensive wireless protocol models that are available for NS-2, especially a MANET library that includes different routing protocols including DSR and OLSR [68].

The power model used, summarized below, is similar to that outlined by Feeney [18]. Researchers have used different equations to calculate the cost of energy. A simple power consumption equation that models the power consumed mainly a function of packet size and

the cost of transmission is shown in 3.1.

$$Cost = (l_{pkt} \times C_{tr}) + C_{ca} \tag{3.1}$$

Here, l_{pkt} is packet size, C_{tr} is the cost of transmission, and C_{ca} is the channel acquisition cost. As a first order approximation a fixed channel access cost is assumed. The transmission cost depends on the transmit power. In Equation 3.1, there is no distinction between broadcast and point-to-point traffic. Also, reception costs are ignored.

A more advanced power model takes into account the cost of transmitting, receiving, and discarding both data and control packets. Moreover, the more advanced model takes into account whether the traffic is broadcast or point-to-point.

For broadcast traffic, the cost is given by Equation 3.2. The broadcast cost is the sum of the cost of sending the broadcast message, the cost to acquire the channel, and the cost incurred at all the receivers of the message.

$$Cost_{brdcst} = (l_{tr} \times C_{tr}) + C_{ca(tr)} + \sum_{n \in S} (l_{recv} \times C_{recv} + C_{ca(recv)}) \tag{3.2}$$

Here, l_{tr} and l_{recv} are the length of the transmitted and received packets, respectively. Normally, l_{tr} is equal to l_{recv}. C_{tr} is the cost to transmit. $C_{ca(recv)}$ and $C_{ca(tr)}$ are the cost to access the channel in receive and transmit modes, respectively. S is the set of of receiving nodes n.

For point-to-point traffic, the cost is divided into transmitter and receiver costs. The cost

at the transmitter is given by Equation 3.3.

$$Cost_{p-to-p(tr)} = C_{tr(RTS)} + C_{recv(CTS)} + (l_{tr} \times C_{tr}) + C_{ca(tr)} + C_{recv(Ack)} \tag{3.3}$$

Where $C_{tr(RTS)}$ is the cost of transmitting a request-to-send message, $C_{recv(CTS)}$ is the cost of receiving a clear-to-send, and $C_{recv(Ack)}$ is the cost of receiving an acknowledgment from the receiver. The cost at the receiver is given by Equation 3.4.

$$Cost_{p-to-p(recv)} = C_{recv(RTS)} + C_{tr(CTS)} + (l_{recv} \times C_{recv}) + C_{ca(recv)} + C_{tr(Ack)} \tag{3.4}$$

Where $C_{recv(RTS)}$ is the cost of receiving a request to send message, $C_{tr(CTS)}$ is the cost of transmitting a clear to send message, and $C_{tr(Ack)}$ is the cost of transmitting an acknowledgment to the sender.

Nodes within wireless range of the transmitter and nodes within wireless range of the receiver that are not the destination must discard received packets. The cost of discarding traffic depends on the MAC implementation [18]. For The 802.11 MAC, nodes that overhear the transmitter hear the RTS message, while nodes in the destination range hear a CTS message and an ACK message. Therefore, the cost of discarding traffic is as follows in Equation 3.5.

$$\begin{aligned}\text{Cost}_{discard} = & \sum_{n\in S} C_{discd(RTS)} + \sum_{n\in D} C_{discd(CTS)} + \\ & \sum_{n\in S}([l_{discd} \times C_{discd}] + C_{ca(recv)}) + \\ & \sum_{n\in D}([l_{discddiscd}] + C_{ca(recv)}) + \\ & \sum_{n\in D} C_{discd(Ack)} + \sum_{n} C_{discd(Ack)} \end{aligned} \tag{3.5}$$

Here, S is the set of nodes that are within the wireless range of the source node and D is the set of nodes that are within the wireless range of the destination node. $C_{discd(RTS)}$ is the cost of discarding a request to send message received by nodes within wireless range of the transmitter. $C_{discd(CTS)}$ is the cost of discarding a clear to send message received by nodes within wireless range of the destination node. $C_{discd(Ack)}$ is the cost of discarding acknowledgment messages heard by nodes within wireless range of the destination node. C_{discd} is the cost of discarding data messages overheard by nodes within wireless range of the sender.

The cost of discarding occurs, in the worst case, when the nodes receive the data packets then discard them [18]. This implies that the maximum discard cost occurs when C_{discd} is equal to C_{recv}. In our study we use a cost function that is takes into account transmit, receive, discard and idle costs.

3.5 Summary

In this chapter, we described the power problem in MANETs and the schemes we use to reduce power consumption. We also presented the notion of cooperative and non-cooperative

ad hoc networks and gave examples of each. A description of the network model, cost functions, metrics under study, and an evaluation methodology including the design of simulation experiments were also presented. In the next chapter, we present results for our power reduction technique applied to a reactive routing protocol in a static network scenario. In Chapter 5 we present simulation results for a large network under static and mobile cases for reactive and proactive protocols. We also study energy variation, average energy expended over time, and residual energies of nodes in the network.

Chapter 4

Initial Power-aware Protocol Assessment Results

4.1 Objectives

The objective of the simulation experiments described in this chapter is to assess the relative performance of the proposed power-aware scheme for a reactive protocol, DSR, in sparse and dense static network scenarios. A description of the simulation environment is presented in the next section followed by metrics used for the assessment followed by the presentation of the results.

4.2 Simulation Environment

We used NS-2 [67] as a platform for our simulations. Our initial assessment simulation scenarios consist of mobile nodes, albeit stationary for initial simulations, confined to a 1000×1000-square unit area. Node locations are randomly placed. However, because we have not implemented the dynamic power discovery procedure, node positions are altered somewhat to allow us to study specific scenarios. In our initial study we consider two topologies.

The first topology consists of five mobile nodes with one node designated as the sender and one node designated as the receiver. The other three nodes lie between the sender and the receiver and act as intermediate nodes. The intermediate nodes forward packets between the sender and the receiver.

In this topology only one traffic flow exists in the network. Constant bit rate (CBR) traffic is generated at a rate of 50 packets per second. Each packet is 1000 bytes in length, resulting in a data rate of 0.4 Mbps.

In the second topology, sixteen nodes are placed on a grid and there are three simultaneous CBR traffic flows in the network. One flow generates 50 packets per second. Each packet is 1000 bytes, resulting in a data rate of 0.4 Mbps. The second flow flows generates 33.33 packets per second,each packet is 512 bytes, resulting in a data rate of 0.136533 Mbps. The third flow generates 27.77 packets per second and each packet is 512 bytes, resulting in a data rate of 0.11377 Mbps.

NS-2 supports three radio propagation models, free space, two-ray ground, and shadowing models. The free space model assumes ideal propagation conditions. It also assumes one line-of-sight path with no obstacles between the transmitter and receiver [68]. The two-ray ground reflection model is similar to the free space model with consideration given to a direct path and a ground reflection path instead of one direct path [68]. The shadowing model consists of two parts, a path loss model and a shadowing model. The path loss model predicts the mean received power at a distance, while the shadowing model reflects the variation of the received power at a certain distance [68]. Both the free space and two-ray ground models predict the received power as a deterministic function of distance and represent the communication range as an ideal circle [68]. In our simulations we use the two-ray ground model because it predicts the received power as a deterministic function of distance [68] and simplifies the design of the node layout and analysis of the network. The wireless interface parameters are those for an early Lucent WaveLan wireless interface card with a carrier sense threshold of -78 dBm, receive threshold of -64 dBm, and a frequency of 914 MHz [67]. To make the simulations run faster and the analysis of the results easier, we set the link capacity for the simulations to 2 Mbps. While these values do not represent current wireless interface card parameters, they form a suitable wireless card interface representation for our initial studies. Each node is equipped with a default antenna at an altitude of 1.5 meters above the ground.

NS-2 provides a linear battery model, where a fixed "cost" is subtracted from the battery every time a packet is sent or received. Therefore, nodes expend the same amount of energy

from the battery whether they are sending to nearby nodes or to far away nodes [24] [42]. In the normal battery model in NS-2, energy consumption does not depend on the location of the sending node with respect to the receiving node. We introduce a slight modification to the way energy is consumed from the energy source to allow for dynamic energy consumption based on the output power of the transmitter. This modification assumes a major part of the energy consumed is used by the transmitter and that 70% of this energy consumed is consumed by the receiver. The receive power is set to 70% to indicate that the receiver also consumes a considerable amount of energy, contrary to early studies that tend to marginalize the receiver energy consumption in MANETs [14] [5]. Processing power by the mobile node is ignored for both sending and receiving nodes. This assumption could easily be compensated for by adding a fixed cost for processing, however, we can assume that, on average, all nodes are similar and they perform similar processing, therefore, on average, the nodes expend the same amount of processing power.

The main metric in our simulations is network life (see Section 4.2), therefore, we let the simulations run until communications stop in the network due to battery exhaustion in all possible intermediate nodes. We give the sending nodes more battery energy than the intermediate nodes since we want to study the effect of our scheme on forwarding by intermediate nodes to maximize network life time. We did not want to limit the network life due to energy exhaustion at the sending nodes.

4.3 Simulation Factors

The simulation experiments study a number of factors. The number of flows, network density (an aspect of topology), mobility, and routing protocol are all factors considered. The study considers a single flow and three flows simultaneously flowing in the network. It also considers sparse and dense networks. A dense network is a network with nodes located close to each other allowing communicating nodes to transmit at lower transmit powers than the maximum, while a sparse network is a network with nodes located far away from each other, thus, a transmitting node needs to transmit at or closer to full power to be able to reach its neighbor(s). Linear battery model is also considered in the study since we are concerned with MANETs in which nodes are predominantly battery powered. The study also considers static and mobile nodes and both reactive and proactive routing protocols.

The initial experiments consider a reactive routing protocol, DSR, with static nodes, a linear battery model, variable network density, and a variable number of flows.

4.4 Performance Metrics

To evaluate the performance of our proposed power-aware DSR (PA-DSR) algorithm, we conducted a simulation study to investigate performance under the different factors mentioned above. Since our aim is to conserve energy and extend network life, one of the performance metrics we study is the relative network life using unmodified DSR (U-DSR) compared to

using our new PA-DSR routing scheme under various network mobility and packet size factors. We also study the relative percentage of packets delivered to the application, number of packets delivered during the lifetime of the network, and end-to-end delay between the two protocols. Definitions of the metrics follow. Network lifetime was defined in Chapter 3 as the time it takes the network to partition. While in general this definition holds for both dense and sparse networks, it is important to clarify that in multiple-flow networks the definition of network life is the time until none of the flows can communicate with its destination due to one or more failures in the intermediate nodes, i.e. the network cannot establish a route from any sender to its associated receiver. End-to-end delay is the average time a packet takes in going from the application in the sending node to the application in the receiving node. The percentage of packets delivered is the ratio of the number of packets received by the application to the total number of application packets sent by source nodes.

4.5 Simulation Results

We simulated our proposed power-aware scheme by carrying out four experiments for each of the two topologies, and compared the results to those for DSR. These are listed below.

1. Single flow experiment in a dense scenario network

2. Single flow experiment in a sparse scenario network

3. multiple flow experiment in a dense scenario network

4. multiple flow experiment in a sparse scenario network

4.5.1 Single Flow Experiments

This section describes experiments comparing PA-DSR with U-DSR with one flow running in the network in dense and sparse network topologies.

4.5.1.1 Dense Network Scenario

In this experiment, nodes were placed in a way that the sender and the receiver cannot establish direct communication. All communication must be established through the intermediate nodes. The transmit power between the sender and the intermediate nodes and between the receiver and the intermediate nodes was adjusted to be large enough to establish a two-way wireless communication link. Figure 4.1 shows the topology for this experiment. In this topology, direct communication can be established between the sender and nodes 1, 3 and 4. However, the receiver transmit power is high enough to only establish a communication link between the receiver and nodes 3 and 4. Therefore, only nodes 3 and 4 are considered intermediate nodes and traffic between the sender and the receiver will pass through these nodes. Node 1 will hear traffic sent to or generated by the sender, but cannot route packets to the receiver. The experiment was repeated five times with different initial seeds. We collected the results and compared them against the "unmodified" NS-2 implementation of DSR. We observed that by utilizing a controlled transmission power feature we were able to

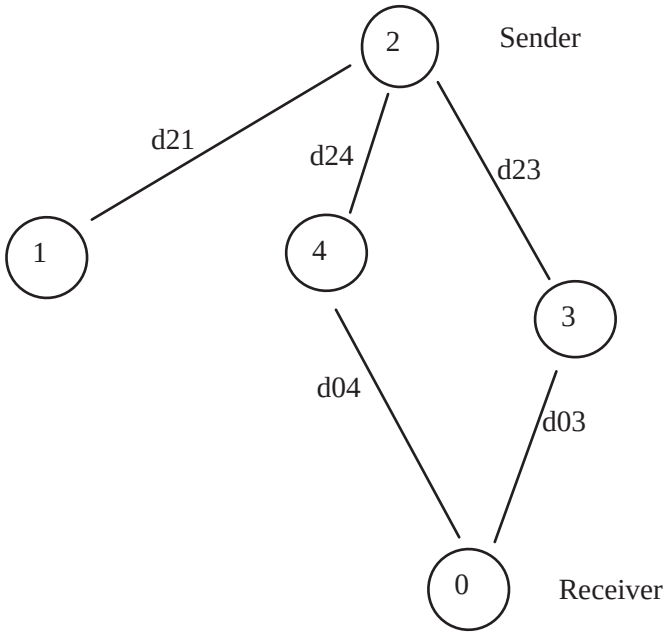

Figure 4.1: Network topology for the dense network scenario.

extend the life time of the network by more than twice the time, 103.2 seconds for PA-DSR with a 95% confidence interval of (102.32, 104.13) as opposed to 41.68 seconds for U-DSR with a confidence interval of (41.67, 41.7). The confidence intervals show that the results are tight for a small number of sample runs. Figure 4.2 shows a graph of the network runs against the network life time of U-DSR for five runs each. Table 4.1 summarizes the results for the dense network single flow scenario.

Also, by alternating routes according to their energy reserves, we observed that the energy variation between intermediate nodes can be minimized. This is crucial to the survivability of the network. Instead of completely draining the energy resources of nodes along the route one-by-one, PA-DSR distributes the load and shares the resources available in the network to

Table 4.1: Summary of Results for Single Flow Dense Network

	U-DSR	PA-DSR
Average lifetime (s)	41.68	103.22
95 % confidence interval (s)	(41.66, 41.7)	(102.32, 104.13)
Average number of packets delivered	2056	5068.6
Average percentage of packets delivered	99.81	97.48
Average end-to-end delay (s)	0.05	0.50

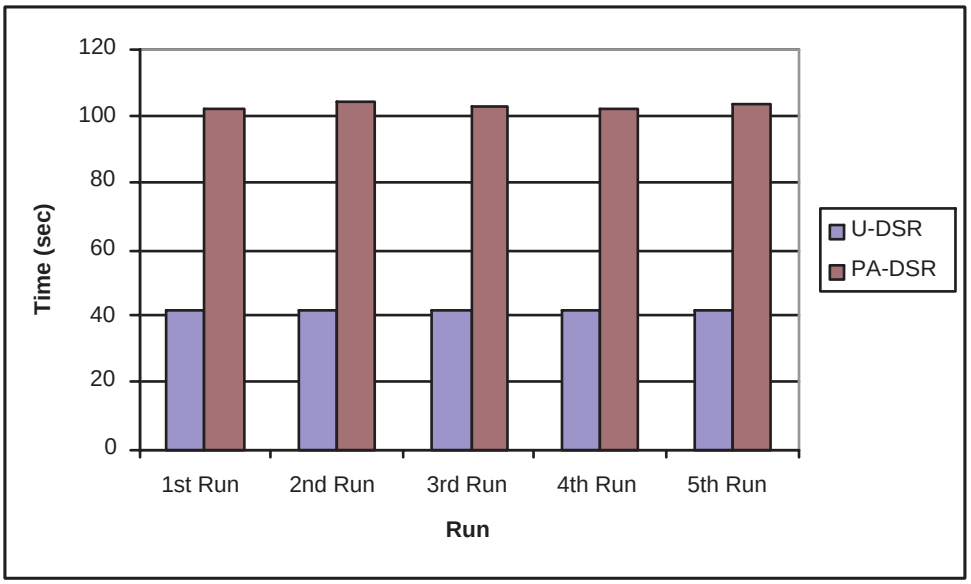

Figure 4.2: Comparison of network life for the dense network scenario.

do routing. Figure 4.3 shows the node energy variation with time for the intermediate nodes using PA-DSR as compared to using U-DSR. The graph shows that the remaining energy of the intermediate nodes are close together for PA-DSR, which shows that the residual energy of the intermediate nodes gets expended at equal rates. To clarify, we consider Figure 4.4 which illustrates a hypothetical outcome for energy variation over time. This figure shows a network with three intermediate nodes where the sender exhausts the energy resources of the intermediate nodes in succession, i.e. the sender uses intermediate node 1 first until it depletes its battery, then it uses intermediate node 2 until it depletes its battery and so on for intermediate node 3. Such behavior is unfair to the intermediate nodes. More over, it hastens network failure in cases where more than one sending node requires a particular intermediate node to forward packets.

In Figure 4.5, we see an improvement in the number of packets delivered by PA-DSR compared to the number of packets delivered by U-DSR. The enhancement is a direct result of the network life time extension. The average value for the number of packets delivered for PA-DSR and U-DSR are 5068.6 and 2056, respectively. The 95% confidence interval is (5066.36, 5070.83) for PA-DSR. The number of packets was the same for all five runs for U-DSR, and therefore, the standard deviation is zero and no confidence interval can be calculated.

Since the number of packets delivered might not show, in this case, the relative performance of the routing protocols, further, since more packets are sent using PA-DSR than using U-DSR due to longer network lifetime, and since the extra packets might be dropped, the

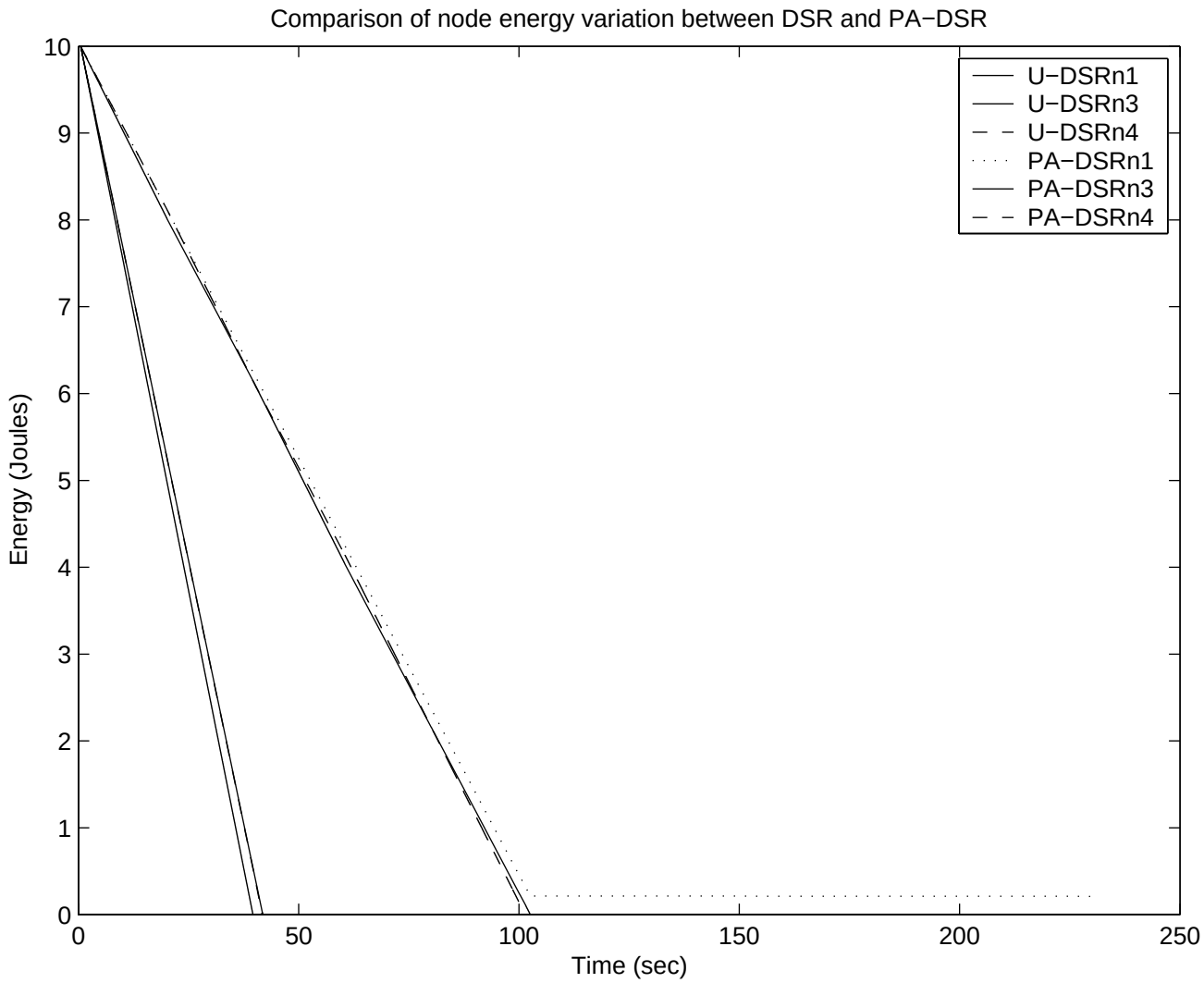

Figure 4.3: Node energy variation with time for the dense network scenario.

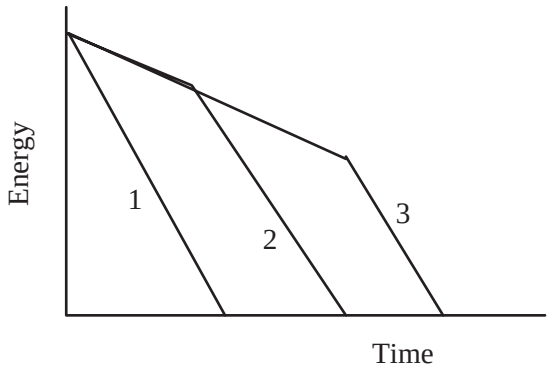

Figure 4.4: Hypothetical outcome for a non-distributive energy depletion over time.

percentage of packets delivered from source to destination, as shown in Figure 4.6, is chosen to show the relative performance of the two protocols. For both U-DSR and PA-DSR, we see the percentage of packets delivered to the application to be above 97%. U-DSR does provide slightly better performance for this metric because it has less overhead, i.e. route discovery is done only once during the simulation lifetime for U-DSR, while PA-DSR does several route updates to potentially choose new routes with lower reluctance values.

PA-DSR exhibited much higher end-to-end delay when compared to U-DSR. This is mainly due to the way DSR prevents route reply storms. PA-DSR periodically uses route discovery whenever an update for routes with lower reluctance values, i.e. routes with high energy reserves, is due. Therefore, when a node generates a route request, nodes that have a route to the destination must wait a random amount of time depending on the number of hops specified in the route reply. This time is the sum of twice the wireless link delay plus a random number between 0 and 1 before a node can send a route reply [13]. Since PA-DSR

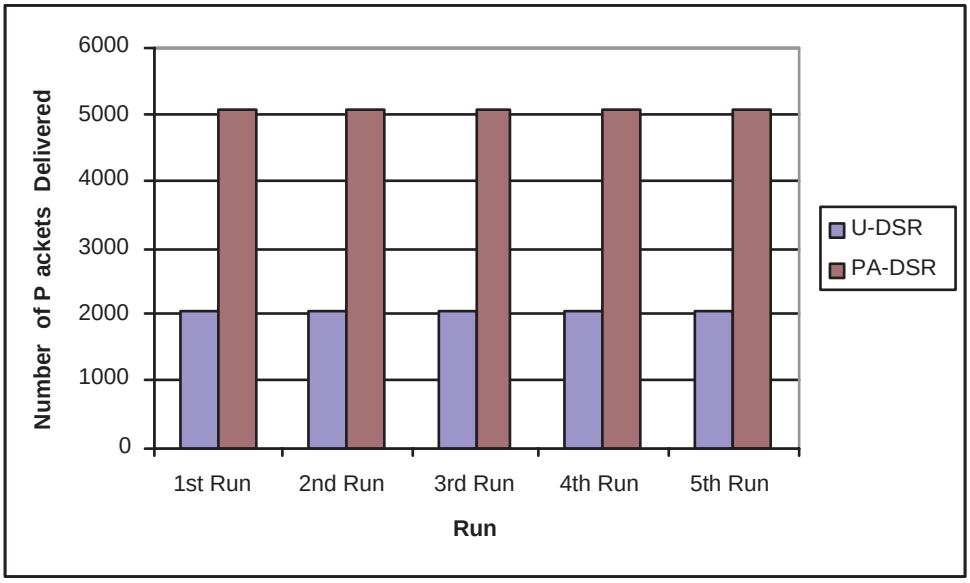

Figure 4.5: Number of packets delivered in the dense network scenario.

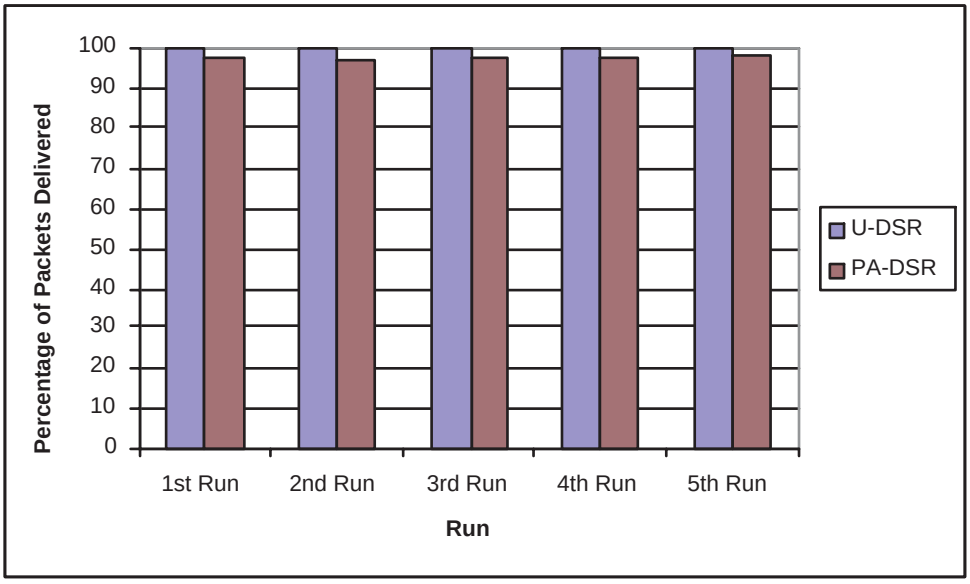

Figure 4.6: Percentage of packets delivered in the dense network scenario.

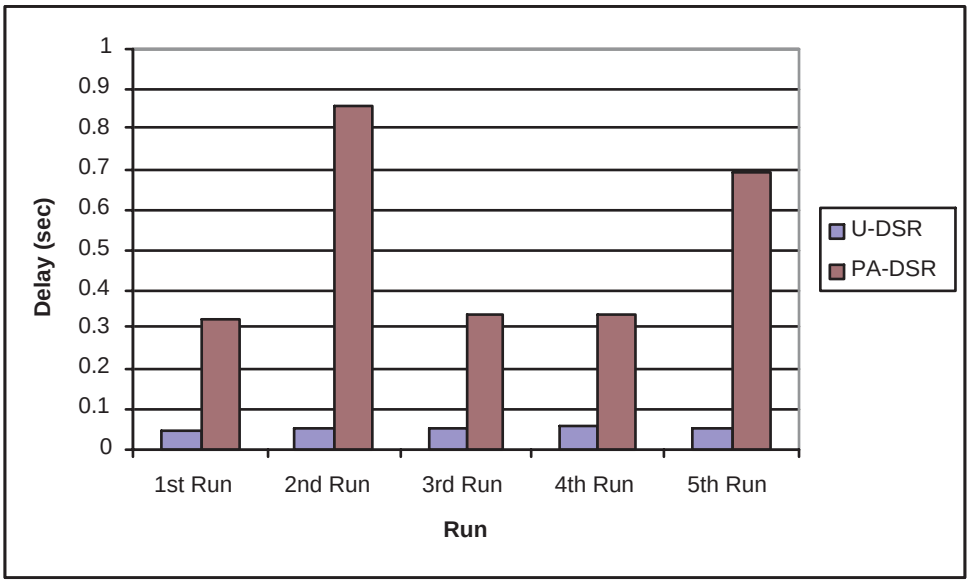

Figure 4.7: End-to-end delay in the dense network scenario.

utilizes the route discovery mechanism several times during the network lifetime, we believe that this explains the increased end-to-end delay observed in the graph of Figure 4.7.

4.5.1.2 Sparse Network Scenario

This scenario represents the worst case for our proposed PA-DSR protocol. In this scenario all nodes transmit at the maximum power of 0.2808 Watts specified by the IEEE 802.11b standard [27]. We repeated the simulation five times using both PA-DSR and U-DSR. Our observations from this set of experiments showed no noticeable improvements in terms of network life; both protocols exhibited the same network life of around 40 seconds. However, some improvements were noticed in node energy variation for PA-DSR over U-DSR due to the periodic route changes implemented by PA-DSR.

Figures 4.8 and 4.9 compare the network life and node energy variation with time, respectively. The number of packets delivered by U-DSR is slightly more than that for PA-DSR.

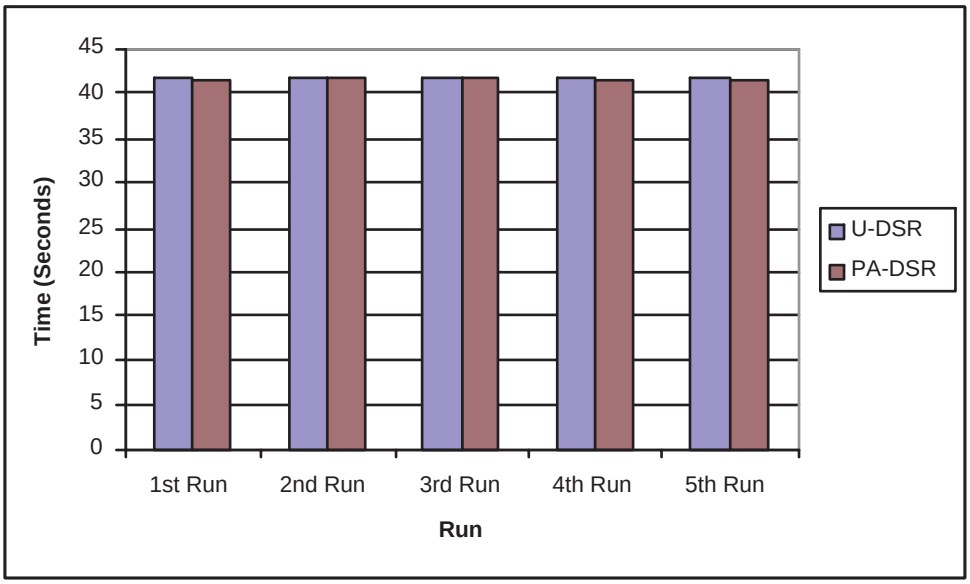

Figure 4.8: Network life time for the sparse network scenario.

This could be attributed to the time spent by PA-DSR doing route discovery instead of sending packets. Also, end-to-end delay for PA-DSR is slightly higher than for U-DSR.

Figures 4.10 and 4.11 compare the number of packets delivered and end-to-end delay, respectively. From 4.10 it is apparent that on average both U-DSR and PA-DSR deliver the same number of packets even though it is slightly lower for PA-DSR since it spends time doing route discoveries. This also negatively impacts the end-to-end delay for PA-DSR.

Figure 4.12 shows the percentage of packets delivered for both protocols. The figure shows that for a single flow there is a slight reduction in the percentage of packets delivered by

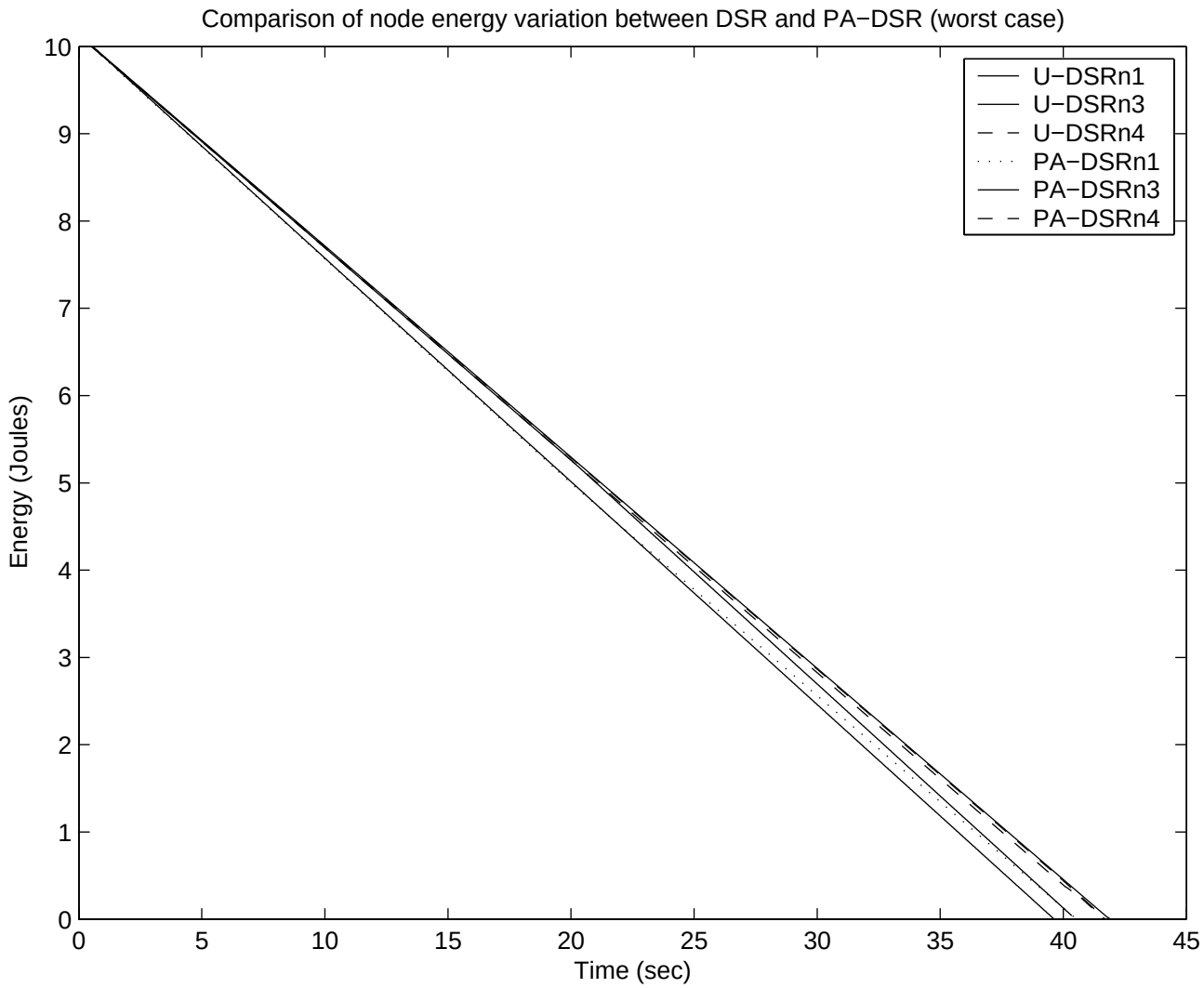

Figure 4.9: Node energy variation for the sparse network scenario.

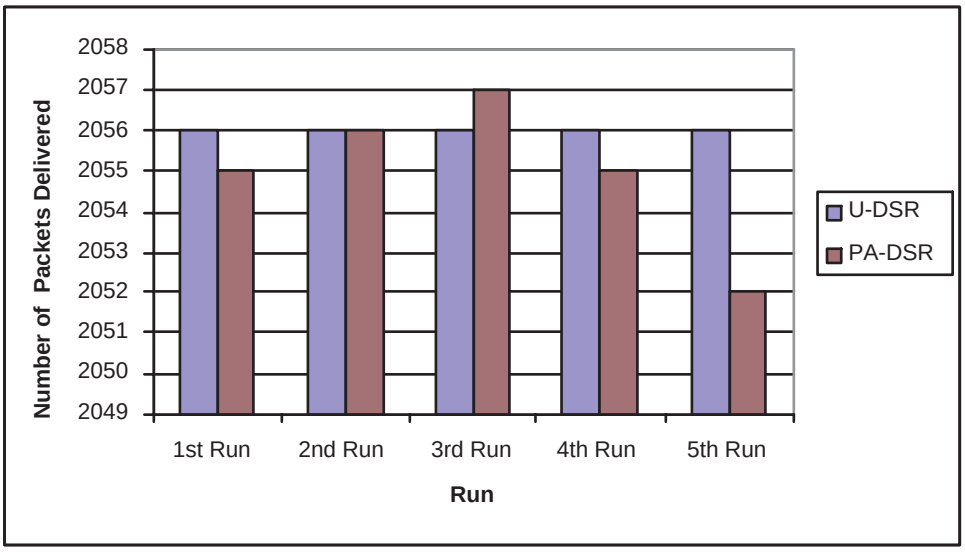

Figure 4.10: Number of packets delivered for the sparse network scenario.

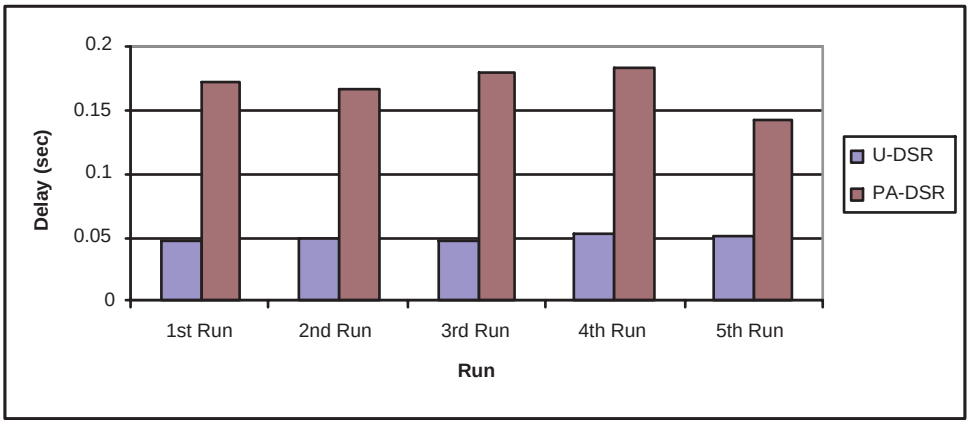

Figure 4.11: End-to-end delay for the sparse network scenario.

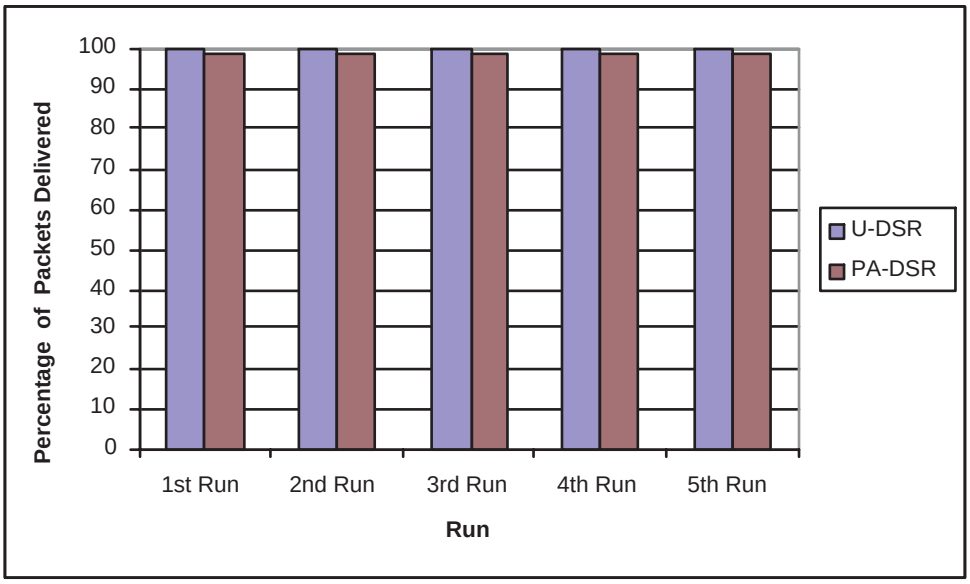

Figure 4.12: Percentage of packets delivered for the sparse network scenario.

PA-DSR. Table 4.2 shows a summary of the average results obtained for the single flow sparse network simulations.

4.5.2 Experiments with Multiple Traffic Flows

In this set of experiments we use three traffic flows to simultaneously flow in a network of sixteen static nodes positioned on a grid, separated by d units apart, where d=150 units. The experiments are run for both dense and sparse network scenarios.

Table 4.2: Summary of Results for Single Flow Sparse Network

	U-DSR	PA-DSR
Average lifetime (s)	41.68	41.48
95 % confidence interval (s)	(41.66, 41.7)	(41.395, 41.57)
Average number of packets delivered	2056	2055
Average percentage of packets delivered	99.81	99.1
Average end-to-end delay (s)	0.05	0.16

4.5.2.1 Dense Network Scenario

As mentioned above, the topology for the multiple flow experiments is a grid. Figure 4.13 shows the topology of this network. In this scenario, there are three traffic flows in the network. Nodes transmit and receive at reduced power based on their distance from neighbors. However, since the nodes are separated by equal distance, all the nodes send using a constant power of 111 mW and receive using 77.7 mW. Since the sending nodes are sending at a substantially reduced power from the maximum power specified the IEEE 802.11b specification [27] of 280.8 mW, this qualifies this topology as a dense one. The three flows are established between nodes 12 and 3, 11 and 0, and 4 and 15, where nodes 12, 11 and 4 are senders, and nodes 3, 0, and 15 are receivers. In this scenario, all nodes are potential forwarders.

Again, we obtained substantial network lifetime improvement in PA-DSR over U-DSR, specifically 115.86 seconds for PA-DSR versus 41.16 seconds for U-DSR. The 95% confidence

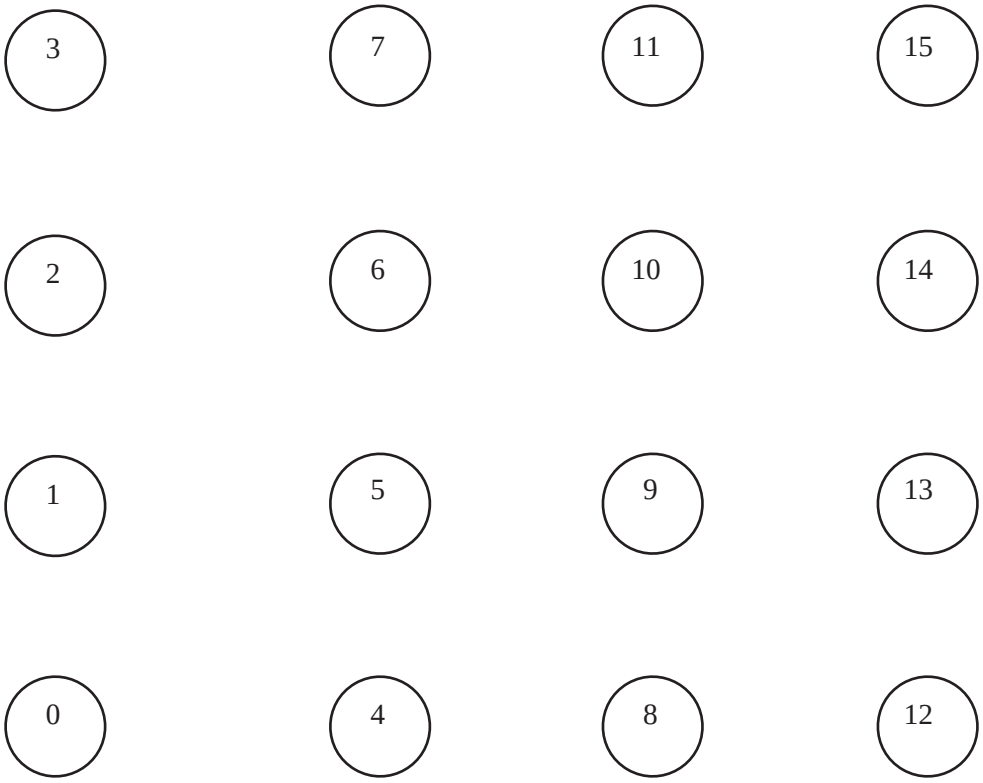

Figure 4.13: Grid topology used in Multiple flow experiments.

for the five runs is tight for both cases ±0.198 for U-DSR and ±0.951 for PA-DSR. Since we have more than one flow in this scenario and, according to the lifetime definition stated in Section 4.3, the network lifetime for multiple flow networks reflects the time until none of the flow sources can communicate with its destination. Figure 4.14 compares the network lifetime for PA-DSR versus U-DSR.

In addition, the node energy variation over time for PA-DSR differs from U-DSR as seen in Figure 4.15. The increase in network lifetime translates into a higher number of pack-

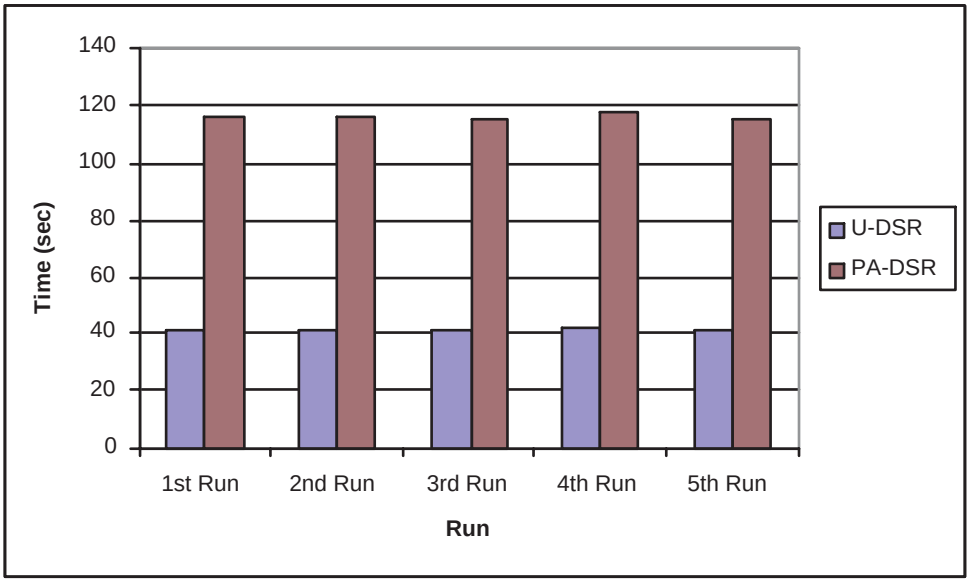

Figure 4.14: Network life for multiple flow dense network scenario.

ets delivered from application to application for PA-DSR. The average number of packets delivered using PA-DSR for the five runs is 2414.2, while the average for U-DSR is 1893.8 packets. As expected, having more than one flow results in increases in the back-off time for route replies, the number of dropped packets, and the number of collisions in the network.

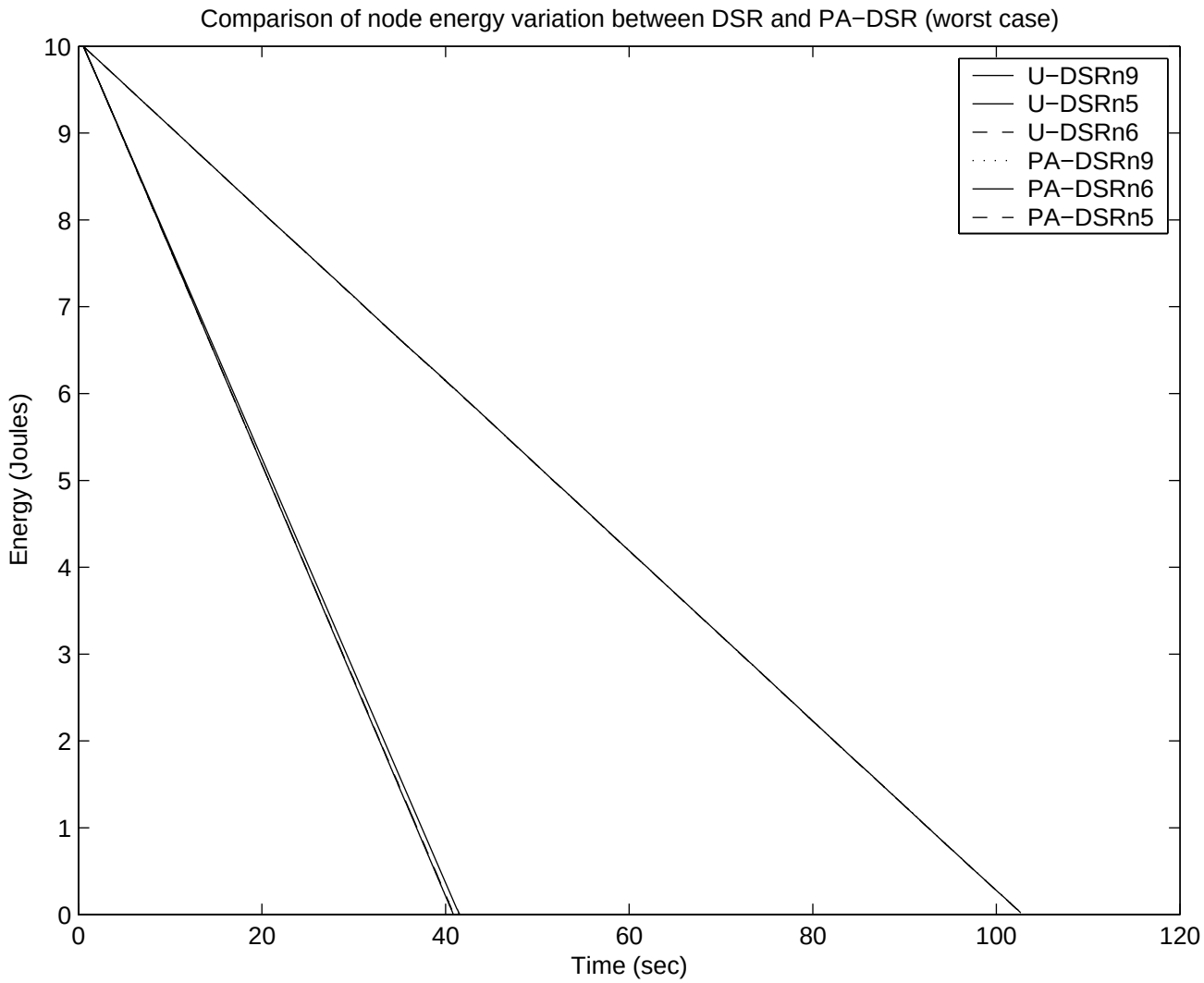

Figure 4.15: Node energy variation with time for the multiple flow dense network scenario.

This negatively impacts the end-to-end delay for PA-DSR. Figures 4.16 and 4.18 show the number of packets delivered to the application and end-to-end delay, respectively, for the multiple flow dense network scenario.

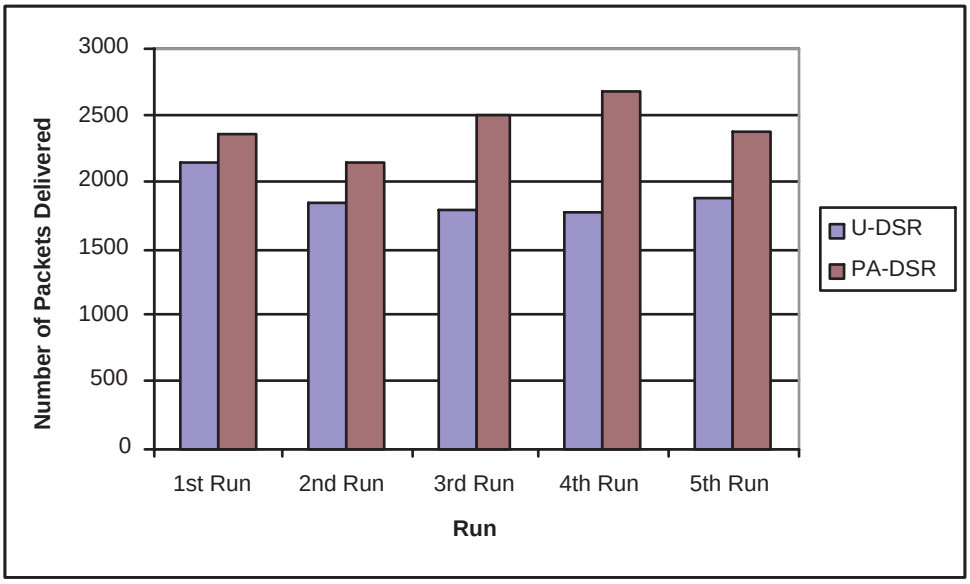

Figure 4.16: Number of packets delivered for the multiple flow dense network scenario.

The percentage of packets delivered to the application declined considerably from that of the single flow scenario due to more dropped packets and collisions, which are mainly a result of channel contention. U-DSR delivered a slightly higher percentage of packets to the application than PA-DSR, which can be attributed to route updates seeking lower reluctance routes. In both instances, we observe that the percentage of packets delivered varies per run. This can be attributed to the number of alternative routes available for each flow. Figure 4.17 shows the percentage of packets delivered for the multiple-flow dense network scenario.

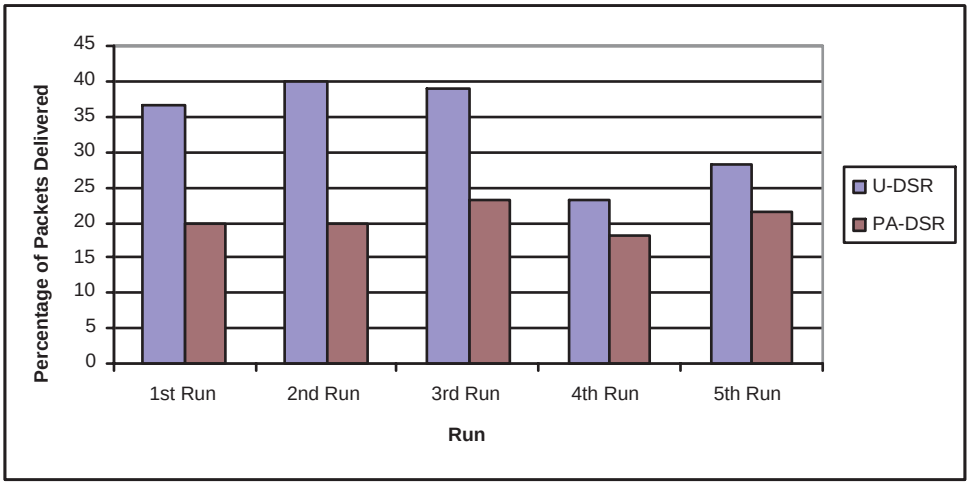

Figure 4.17: Percentage of packets delivered for the multiple-flow dense network scenario.

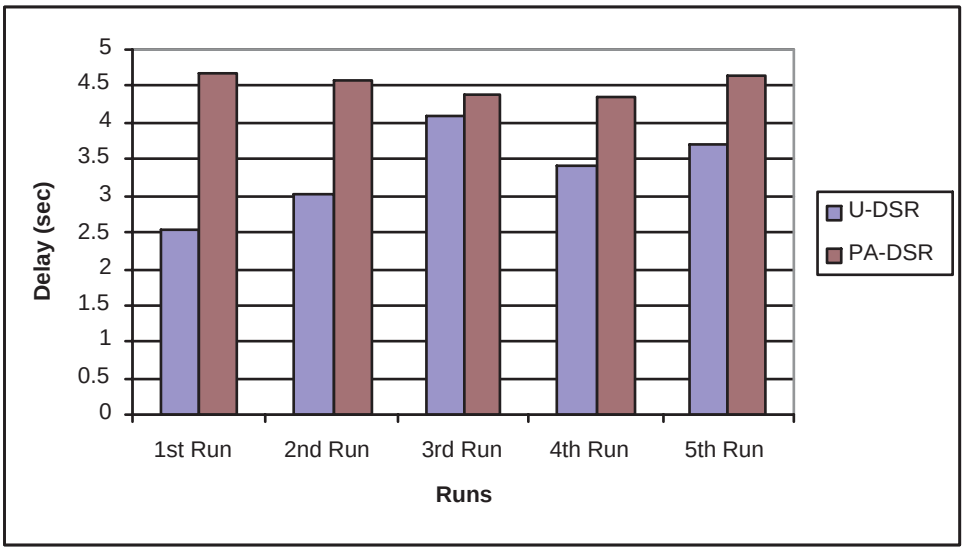

Figure 4.18: End-to-end delay for the multiple-flow dense network scenario.

Table 4.3 summarizes the simulation results obtained for the multiple traffic flow dense network scenario.

Table 4.3: Summary of Results for Multiple Flow Dense Network

	U-DSR	PA-DSR
Average lifetime (s)	41.16	115.86
95 % confidence interval (s)	(40.96, 41.36)	(114.91, 116.81)
Average number of packets delivered	1893.8	2414.2
Average percentage of packets delivered	33.38	20.51
Average end-to-end delay (s)	3.36	4.52

4.5.2.2 Sparse Network Scenario

In the sparse network scenario, nodes transmit at 280.8 mW as specified by IEEE 802.11b standard [27]. Simulation results show no considerable improvements to network lifetime in PA-DSR as can be seen in Figure 4.19. However, node energy variation with time for intermediate nodes is reduced. Energy expended in intermediate nodes is similar over time. Figure 4.20 shows energy variation with time for PA-DSR and U-DSR.

End-to-end delay increases for PA-DSR due to an increased number of dropped packets, collisions, and route discoveries. Figure 4.21 shows end-to-end delay. The number of packets delivered to the application for both PA-DSR and DSR is relatively low, however, results are similar with an average of 1687 packets for PA-DSR and 1893 packets for U-DSR. Figure

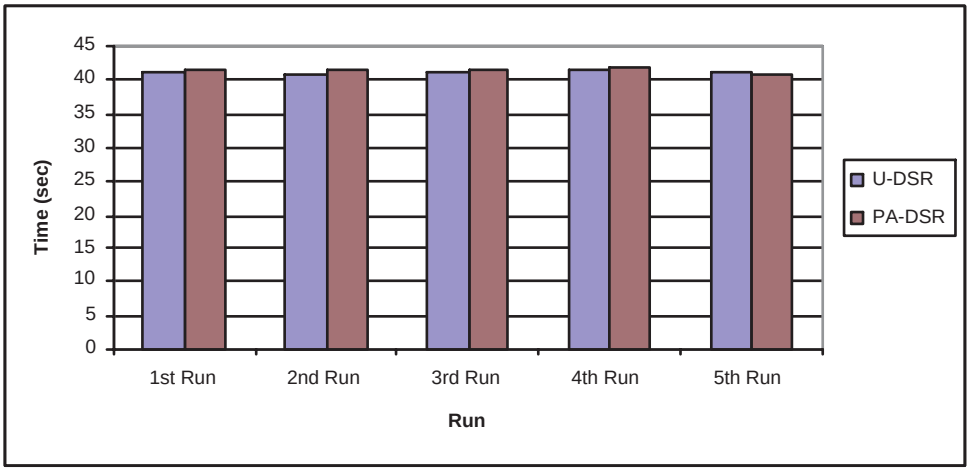

Figure 4.19: Network life for the multiple flow sparse network scenario.

4.22 shows the number of packets delivered for both protocols.

Figure 4.23 shows the percentage of packets delivered for DSR and PA-DSR. Although results vary more for PA-DSR, average results are similar for the two schemes.

Table 4.4 summarizes the simulation results obtained for the multiple traffic flow sparse network scenario.

4.6 Discussion of Results

The results demonstrate that PA-DSR extends the network life in sufficiently dense networks, while maintaining comparable network life times in sparse networks when compared to U-DSR. In both dense and sparse networks, PA-DSR maintains similar energy levels over time at intermediate nodes, thus utilizing network energy resources in an evenly distributed

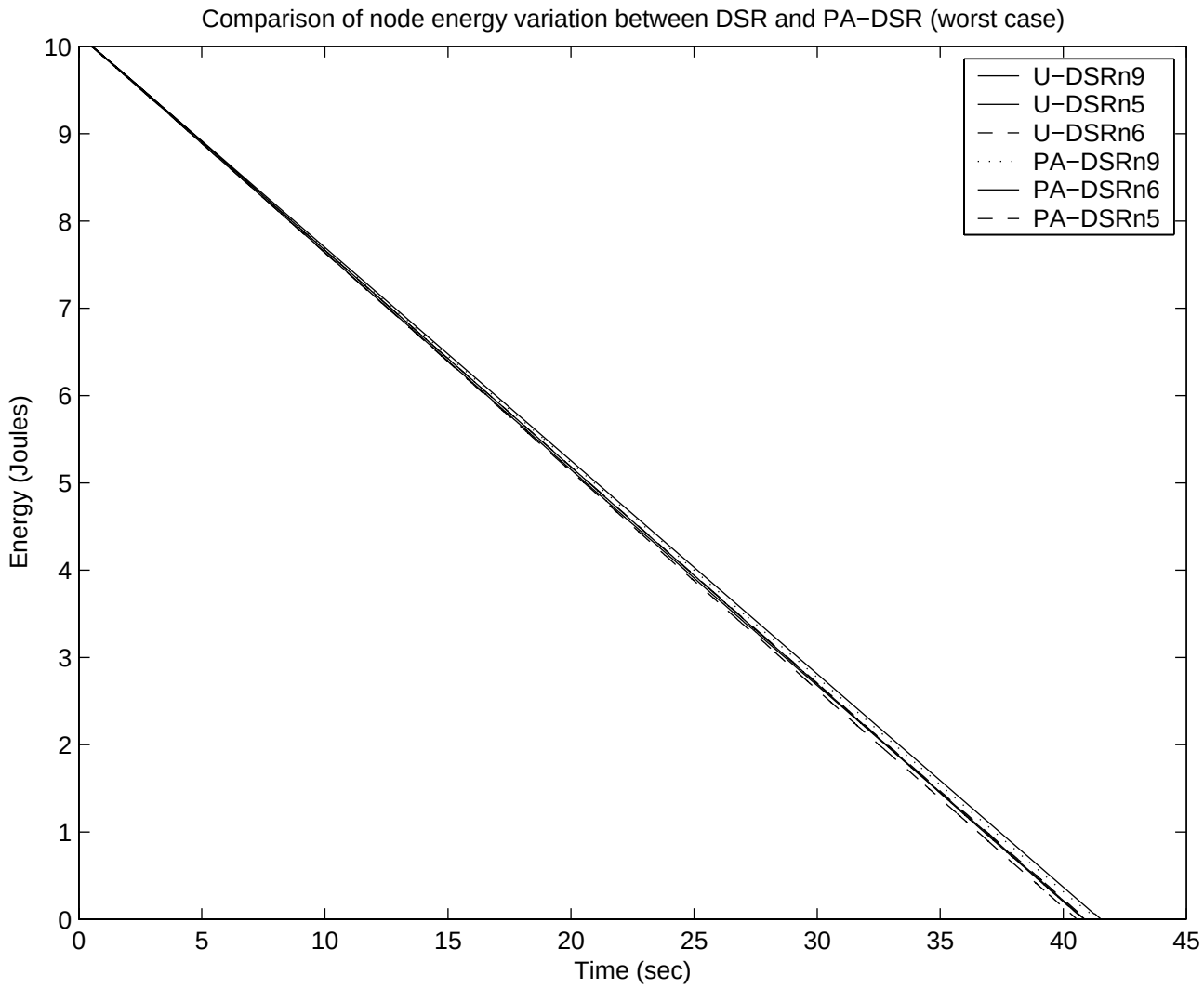

Figure 4.20: Node energy variation for the multiple flow sparse network scenario.

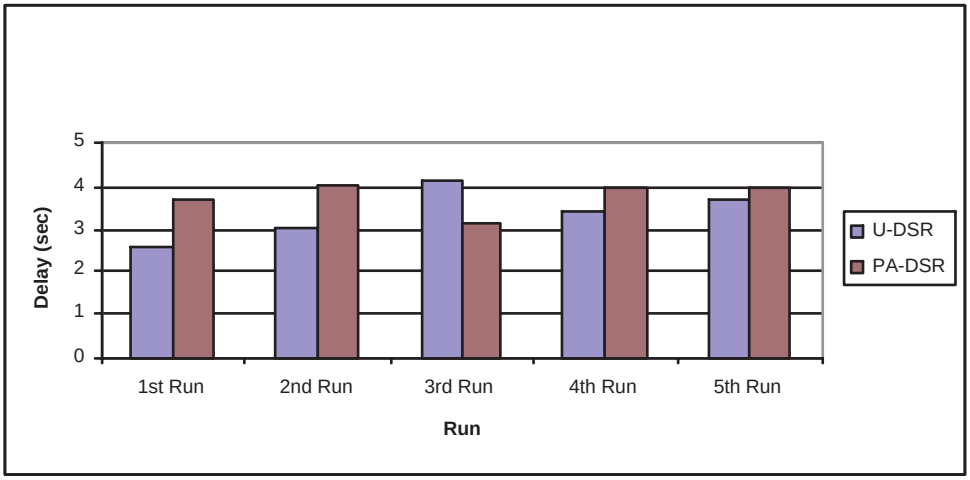

Figure 4.21: End-to-end delay for the multiple flow sparse network scenario.

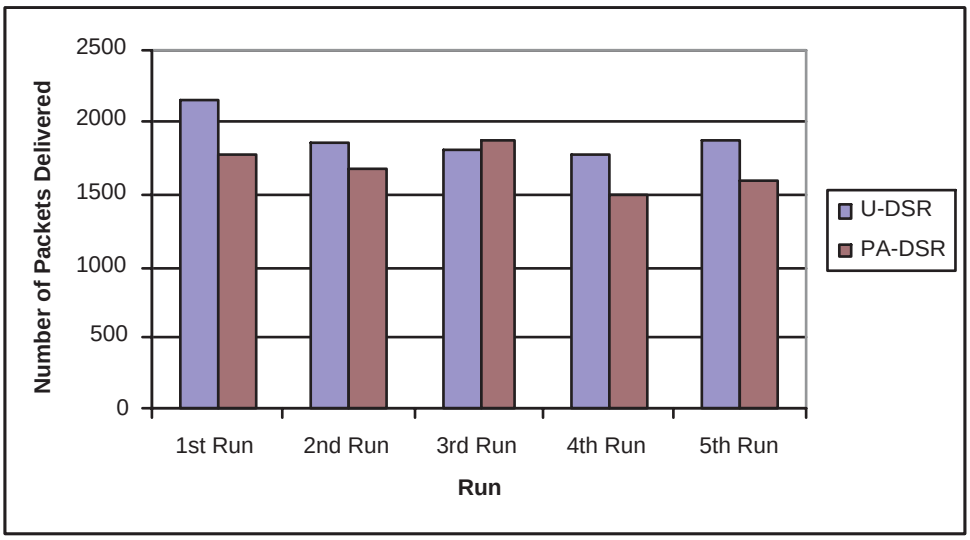

Figure 4.22: Number of packets delivered for the multiple flow sparse network scenario.

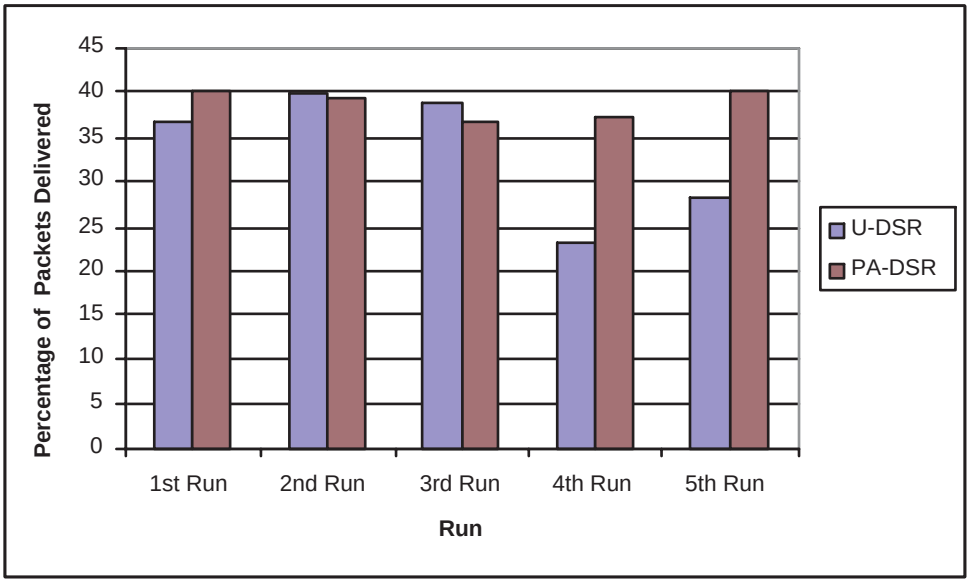

Figure 4.23: Percentage of packets delivered for the multiple flow sparse network scenario.

Table 4.4: Summary of Results for Multiple Flow Dense Network

	U-DSR	PA-DSR
Average lifetime (s)	41.16	41.39
95 % confidence interval (s)	(40.96, 41.36)	(41.08, 41.71)
Average number of packets delivered	1893.8	1687.4
Average percentage of packets delivered	33.38	38.75
Average end-to-end delay (s)	3.36	3.77

manner. It is also apparent from the results that there is a tradeoff between power-awareness and delay. By choosing routes with least reluctance values, PA-DSR might use longer routes to deliver packets to the destination. This increases the delay in the network and makes power-aware protocols more suitable for applications that are not delay sensitive. In addition, route discovery used by PA-DSR to find routes with lower reluctance values adds overhead that contributes to the delay and energy exhaustion of the nodes' batteries.

We also observe that more packets are delivered to the application when the network is dense and that the number of packets delivered by PA-DSR declines compared to U-DSR when the network is sparse. The decline in the number of packets delivered and the increase in end-to-end delay contribute negatively to the percentage of packets delivered to the application layer. An interesting observation is that the percentage of packets delivered by PA-DSR in the sparse network case is higher than in the dense network case. Due to the improved network lifetime in the dense scenario, more packets are dropped and more collisions occur during the lifetime of the network, thus lowering the percentage of packets delivered. Therefore, our proposed scheme improves the lifetime of the network and the distribution of network energy resources at the expense of longer delays.

4.7 Summary

We presented proof of concept results to our proposed PA-DSR protocol and compared them to results to U-DSR. The results were based on static networks. The study examined results

in both dense and sparse networks. It is clear that PA-DSR increases network lifetime and reduces node energy variation by distributing energy resource use in the network. However, the improvement of network lifetime comes at the expense of delay. Next chapter presents results that reflect an implementation of dynamic route discovery for DSR, and an implementation of our proposed power-aware scheme to a proactive protocol, OLSR. The study, also considers large stationary and mobile scenarios under different network offered loads and node speeds.

Chapter 5

Simulation Results and Analysis for Large Static and Mobile Ad Hoc Networks

5.1 Introduction

This chapter presents results and analysis of the proposed power-aware extensions for static and mobile scenarios made to Optimized Link State Routing (OLSR) and Dynamic Source Routing (DSR) protocols. In our preliminary analysis (see chapter 4) we showed preliminary results for our power-aware scheme in small and static network scenarios. In this chapter, we present and analyze results collected from simulation experiments of large static and mobile

ad hoc network scenarios. This chapter starts with Section 5.1 by presenting an overview of the simulation scenarios considered. Section 5.2 presents simulation results gathered from the different simulation scenarios. Section 5.3 discusses the results obtained. Section 5.4 investigates high percentage packet drop rate observed in the low contention scenario. Section 5.5 compares our proposed power-aware protocol with protocols that either use transmit power or residual battery energy to conserve power, followed by a summary of the chapter in Section 5.6.

5.2 Simulation Scenarios and Workloads

Our aim for these simulations is to test our proposed power-aware scheme in large ad hoc networks under mobile conditions. However, to establish a base for the results we have also included simulation results gathered from large stationary networks. Therefore, we have divided the study into two cases, a stationary nodes case and a mobile nodes case. In the stationary nodes case, we study the effects of our proposed power-aware scheme in a network of 30 nodes on a rectangular grid with an area of 2500×1000 under two traffic contention scenarios, high and low contention. We should note that our use of the word contention actually refers to the network offered load. Each scenario has 6 simultaneous active flows that stay active until the energies of the sending nodes are exhausted. In the low-contention scenario, the flows are chosen such that interference between flows is minimized, while in the high-contention scenario flows are chosen such that interference between active flows is

maximized. Each case is studied in situations of limited and unlimited energy per node. In all unlimited-energy situations, we assume that each node is supplied with a fully charged battery of 140,000 Joules. Therefore, in this case, simulations do not stop due to depletion of battery energy. In the limited-energy situation, each node is assumed to have a limited battery energy of 2000 Joules. In the mobile nodes case, we consider two movement scenarios, coordinated and random. In the coordinated movement scenarios, source and destination nodes move in tandem at a certain speed, while in the random movement scenario, source and destination nodes move at random speed and direction. We used random waypoint model to generate movement scenarios. Random waypoint is a statistical model used for ad hoc network simulations to model mobility [68]. In random waypoint nodes move in a non uniform manner with certain speed and direction with an optional pause time [68].We study each movement scenario under three different speeds. low-, medium-, and high-speed. In the low-speed case, nodes move at speeds not faster than 2 m/s (7.2 km/hr). This speed is analogous to walking or brisk walking speed. In the medium-speed, nodes move at a speed not faster than 10 m/s (36 km/hr). This speed is resembles driving in a neighborhood. In the high-speed case, nodes move at speeds not faster than 20 m/s (72 km/hr), which is like driving on a major road. In both stationary and mobile cases, transmit, receive, and idle costs are measured values of the WaveLAN 802.11b interface adapter as reported by Feeney and Nilsson [19]. The measured cost for transmit is 1.35 W, for receive is 901 mW, and for idle is 739 mW. Even though a big factor of the cost for transmit and receive is due to interface card overhead, by reducing the transmit/receive power when doing transmits and

receives helps extend the lifetime of the network over time and minimizes interference among nodes in the network during data sends and receives. Traffic flows were at a rate of 50 UDP packets per second of size 512 bytes. Simulation experiments were repeated 5 times with different initial seeds.

5.3 Simulation Results

As stated earlier, our aim for these experiments is to study the behavior of our proposed power-aware scheme on large and mobile ad hoc networks for both proactive and reactive routing protocols assuming measured values of transmit, receive, idle powers and battery energy. Unfortunately, due to hardware and software limitations we were not able to simulate larger networks for larger periods of time. Therefore, simulations were carried on networks of 30 nodes having 6 simultaneously active flows, and node battery energy of 2000 Joules. We present our results for the stationary node case followed by the mobile node case.

5.3.1 Stationary Node Experiments

This section presents results from experiments carried out for the stationary nodes case. This case, as described above, consists of 30 stationary nodes situated on a rectangular grid of an area of 2500×1000, with 6 simultaneously active flows. The flows are categorized as causing low- and high-contention according to the positions of the sending and receiving nodes. We consider two initial battery energy scenarios, unlimited energy, which assumes each node's

battery has 140,000 Joules and a limited energy scenario where each node's battery starts with 2000 Joules.

5.3.1.1 Low-contention, Unlimited Energy

In this section we look at simulation results obtained for power-aware DSR (PA-DSR) and compare it with results obtained for the unmodified version of DSR (U-DSR). We also look at simulation results obtained for power-aware OLSR (PA-OLSR) and compare it with the unmodified version of OLSR (U-OLSR). Looking at the first 3000 seconds of simulation time, we observe a slight improvement in the percentage of packets delivered to the destination for both PA-DSR and PA-OLSR. A modest improvement of about 2% is obtained in PA-DSR, while an improvement of about 1% for PA-OLSR. This translates into 35,232 more data packets delivered to the application by PA-DSR and 29,825 more delivered to the application by PA-OLSR. Figure 5.3 shows the average percentage of packets delivered for DSR and OLSR in the low-contention, unlimited-energy scenario. Figure 5.2 shows the average end-to-end delay gathered for the protocols in the same scenario. From the graph we observe a slight increase in delay (0.13 seconds) for PA-DSR over U-DSR. The increase in the end-to-end delay is attributed to route discoveries and choosing longer routes over shortest paths to save energy in PA-DSR. Delay is slightly decreased for PA-OLSR (0.5s) versus that for U-OLSR (0.64s). The 0.14 seconds decrease in delay is counter intuitive in PA-OLSR since the protocol favors longer routes with high energy nodes over short routes with low energy nodes. One possible explanation to this behavior is that frequent changes of

the routes in OLSR reduce the contention on certain forwarding nodes, which brings about the reduction in the average end-to-end delay. Table 5.1 summarizes the results for the low-contention, unlimited-energy scenario.

Table 5.1: Summary of Results for Low-contention, Unlimited-energy Scenario

	U-DSR	PA-DSR	U-OLSR	PA-OLSR
Average number of packets sent	929741.4 (±762.12)	965013.4 (±2488.56)	964238.40 (±2124.5)	986160.20 (±2826.30)
Average number of packets delivered	413162 (±772.44)	448394.4 (±2475.69)	412211.74 (±2933.4)	442036.78 (±2329.88)
Average percentage packets delivered	44.44 (±0.046)	46.46 (±0.305)	42.75 (±0.372)	44.82 (±0.947)
Average end-to-end delay	0.57 (±0.10)	0.67 (±0.04)	0.63 (±0.1)	0.50 (±0.08)

5.3.1.2 Low-contention, Limited Energy

In the low-contention limited-energy scenario, we see a decrease of 14.21% in the percentage of packets delivered for PA-DSR. However, the increase in the network lifetime results in an increase in the number of packets delivered to the application. An increase of 37,816 extra data packets are delivered to the application by PA-DSR. For PA-OLSR, 27,821 more packets delivered to the application. An increase of 0.43% over U-OLSR. Figure 5.4 shows

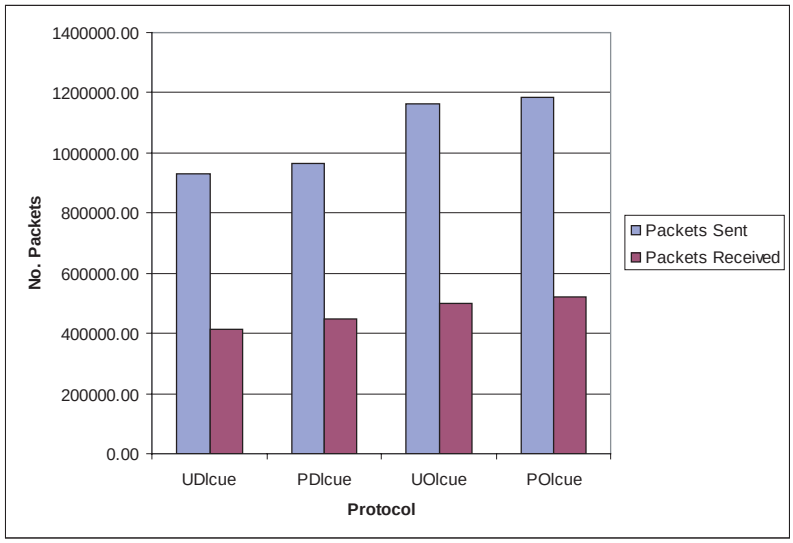

Figure 5.1: Average number of packets sent and delivered in the low-contention, unlimited-energy scenario.

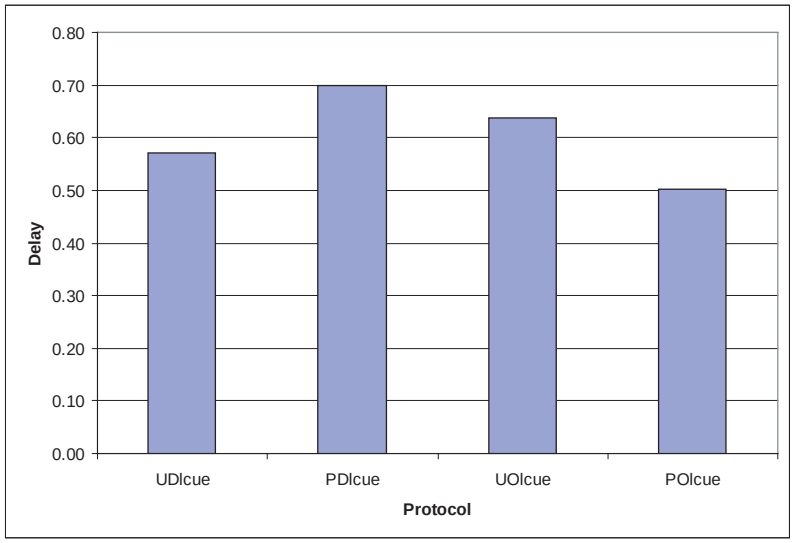

Figure 5.2: Average end-to-end delay in the low-contention, unlimited-energy scenario.

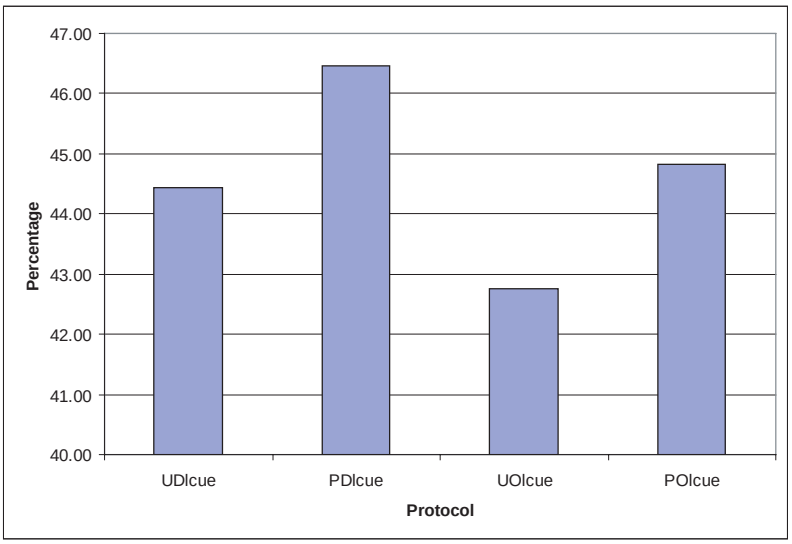

Figure 5.3: Average percentage of packets delivered in the low-contention, unlimited-energy scenario.

the number of packets sent and delivered in the low-contention, limited-energy scenario and Figure 5.6 shows the percentage of packets delivered to the application. We also see improvements in network lifetime in the power-aware versions of the protocols. In PA-DSR we see an average improvement of 9.15% in network lifetime, while an average improvement of 9.69% is seen with PA-OLSR. Figure 5.7 shows the network lifetime for both protocols. Average end-to-end delay is slightly higher for PA-DSR than for U-DSR by 0.47 seconds. Average delay is statistically the same for PA-OLSR and U-OLSR. Figure 5.5 shows end-to-end delay for low-contention limited-energy scenario. Table 5.2 summarizes the results for the low-contention, limited-energy scenario.

Table 5.2: Summary of Results for Low-contention Limited-energy Scenario

	U-DSR	PA-DSR	U-OLSR	PA-OLSR
Average number of packets sent	561582.0 (±1061.38)	827216.4 (±2582.23)	488759.2 (±1345.31)	548945.4 (±2185.16)
Average number of packets delivered	328560.0 (±982.32)	366376.6 (±2135.85)	206194.2 (±1335.09)	234015.2 (±2526.66)
Average percentage packets delivered	58.50 (±0.131)	44.29 (±0.276)	42.19 (±0.158)	42.63 (±0.789)
Average end-to-end delay	0.52 (±0.0196)	0.99 (±0.1004)	0.54 (±0.0158)	0.58 (±0.1529)
Average network lifetime	2068.30 (±3.77)	2254.77 (±18.386)	1875.42 (±2.30)	2057.20 (±12.51)

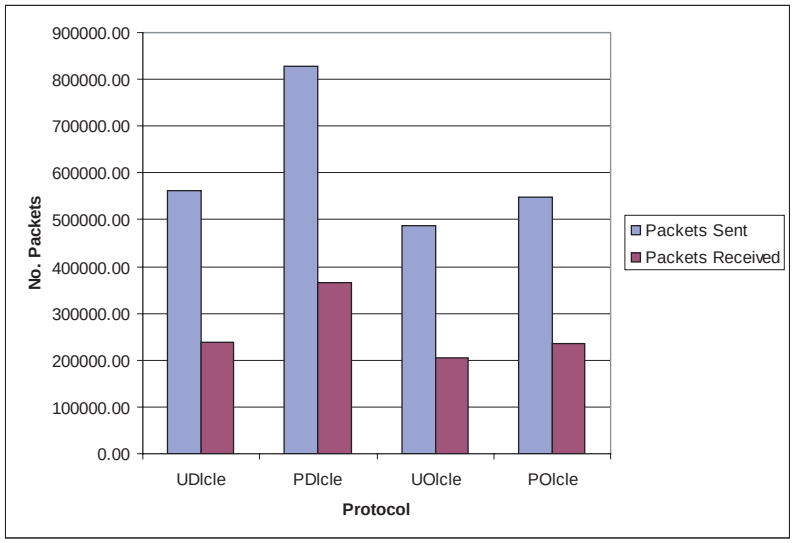

Figure 5.4: Average number of packets sent and delivered in the low-contention, limited-energy scenario.

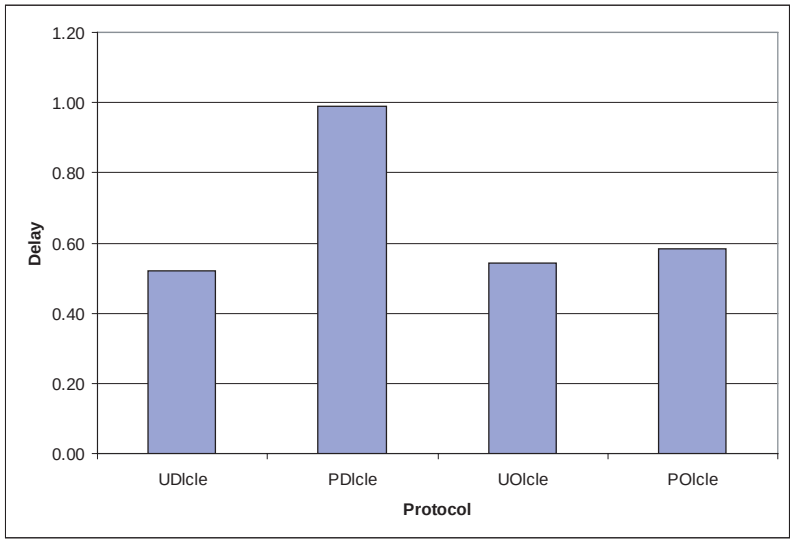

Figure 5.5: Average end-to-end delay in the low-contention, limited-energy scenario.

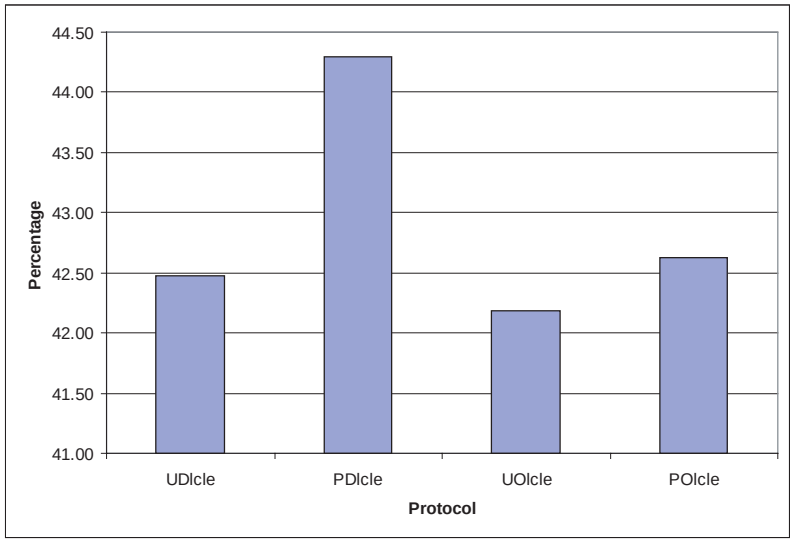

Figure 5.6: Average percentage of packets delivered in the low-contention, limited-energy scenario.

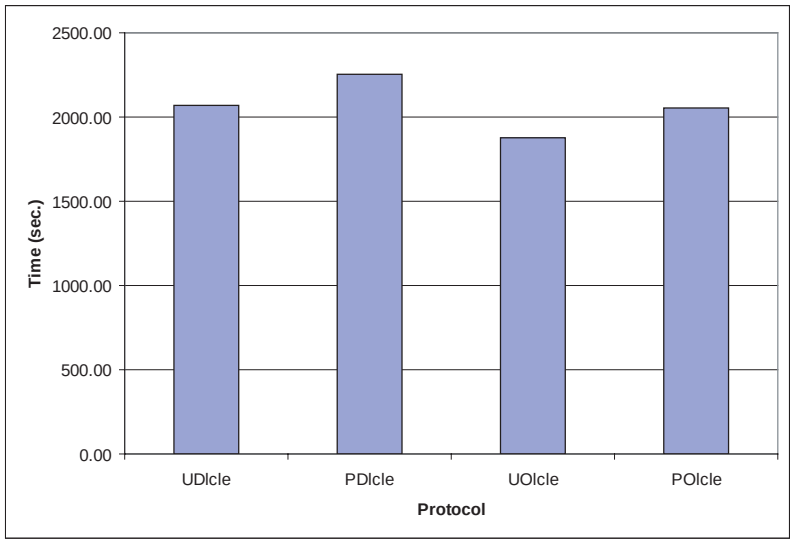

Figure 5.7: Average network lifetime in the low-contention, limited-energy scenario.

5.3.1.3 High-contention, Unlimited Energy

In this scenario, our proposed power-aware scheme showed a slight improvement over the unmodified versions of DSR and OLSR. We observed a slight increase in the percentage of packets delivered to the application of 2.21% in PA-DSR. This is equivalent to 22,258 extra data packets delivered to the application. Also observed was an increase of 1.73% of data packets delivered to the application, resulting in 33,757.8 extra data packets, in PA-OLSR. Figure 5.8 shows the average number of packets sent and delivered to the application for both DSR and OLSR, and Figure 5.9 shows the average percentage of packets delivered to the application. We believe that this slight increase in the percentage of packets delivered to the application in the high-contention scenario is not always sustainable as the overhead of our protocol might negatively impact the outcome. We think the increase in the percentage of packets in this case is scenario-dependent. In a high-contention scenario, choosing high-energy routes can negatively impact the number of packets delivered to the application, hence a drop in the percentage in the number of packets delivered to the application might occur. choosing high-energy routes over shorter ones has increased end-to-end delay for DSR. An increase of 3.91 seconds is seen in PA-DSR. However, a decrease in average end-to-end delay of 1.33 seconds is observed in PA-OLSR. Even though the average delay is lower for the PA-OLSR, when we factor in the confidence interval, we see the average end-to-end delay for U-OLSR and PA-OLSR overlap which can be considered statistically identical. The decrease in average end-to-end delay in PA-OLSR could be due to the proactive nature of OLSR. In proactive routing protocols, routes are constantly being discovered and, as was mentioned

earlier, periodic changes of the routes, can help reduce the contention on certain forwarding nodes, therefore, reducing the end-to-end delay. Figure 5.10 shows end-to-end delay for the high-contention unlimited-energy scenario and Table 5.3 summarizes the results for the high-contention, unlimited-energy scenario.

Table 5.3: Summary of Results for High-contention Unlimited-energy Scenario

	U-DSR	PA-DSR	U-OLSR	PA-OLSR
Average number of packets sent	786132.40 (±1898.92)	828389.80 (±1847.83)	714327.60 (±2408.81)	819797.80 (±2078.66)
Average number of packets delivered	72930.40 (±1451.21)	95188.80 (±1038.19)	132579.2 (±2352.34)	166337 (±2243.33)
Average percentage packets delivered	9.28 (±0.521)	11.49 (±0.961)	18.56 (±0.321)	20.29 (±0.720)
Average end-to-end delay	8.57 (±0.69)	12.48 (±1.50)	4.15 (±0.06)	2.82 (±1.41)

5.3.1.4 High-contention, Limited Energy

This scenario shows similar results as the high-contention, unlimited-energy scenario. An increase of 2.17% in the percentage of packets delivered to the application is observed in PA-DSR, resulting in 9,567 more data packets. The increase in the percentage of packets delivered in PA-OLSR is 0.86% and 20,677 more data packets are delivered to the application.

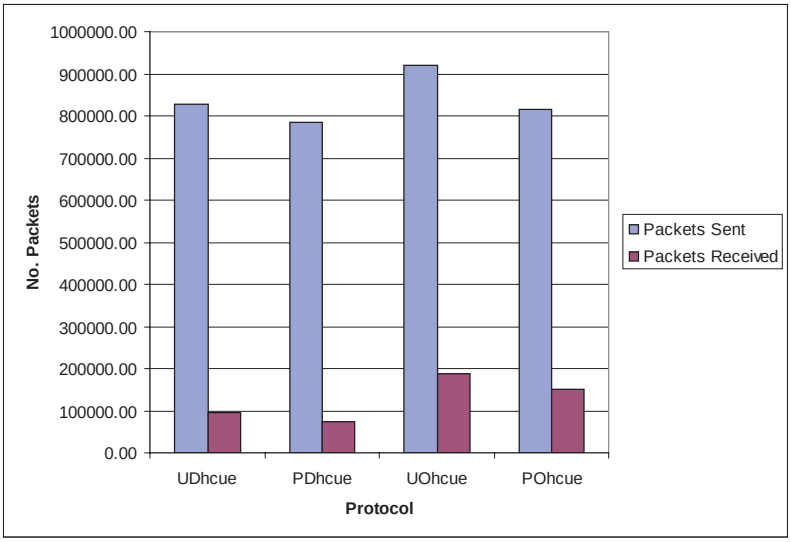

Figure 5.8: Average number of packets sent and delivered in the high-contention, unlimited-energy scenario.

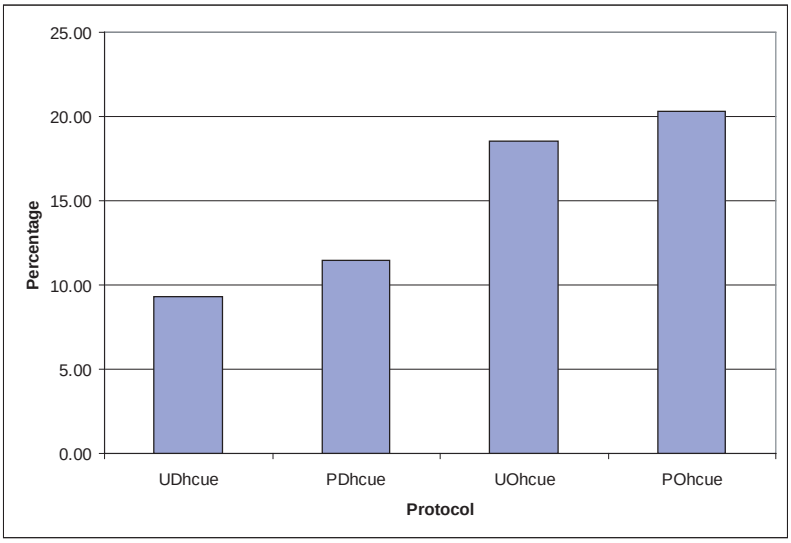

Figure 5.9: Average percentage of packets delivered in the high-contention, unlimited-energy scenario.

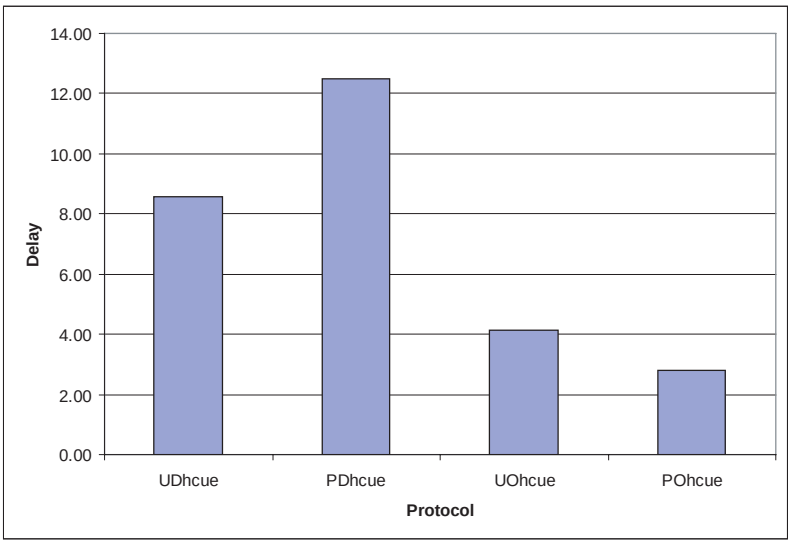

Figure 5.10: Average end-to-end delay in the high-contention, unlimited-energy scenario.

Figure 5.11 shows the number of packets sent and delivered to the the application, Figure 5.13 shows the percentage of packets delivered to the application. Again, we observe an increase in end-to-end delay in PA-DSR of about 6.15 seconds due to protocol overhead, collisions, and traffic contention. A slight decrease in the average end-to-end delay (0.76 seconds) is observed in PA-OLSR. However, factoring in the confidence interval the average end-to-end delay for U-OLSR and PA-OLSR become statistically identical. Figure 5.12 shows average end-to-end delay for the high-contention, limited-energy scenario. The average network lifetimes are also slightly improved in the power-aware protocols. An increase of 122.41 seconds is observed in PA-DSR, while an increase of 117.51 seconds is observed in PA-OLSR. Figure 5.14 shows network lifetime for the high-contention, limited-energy scenario. Table 5.4 summarizes the average results for the high-contention, limited-energy scenario.

Table 5.4: Summary of Results for High-contention Limited-energy Scenario

	U-DSR	PA-DSR	U-OLSR	PA-OLSR
Average number of packets sent	382745.40 (±1426.40)	391246.60 (±1615.27)	406245.00 (±1279.5)	486022.40 (±2262.78)
Average number of packets delivered	48493.60 (±1245.09)	58061.00 (±982.69)	84011.40 (±1784.04)	104689.00 (±2051.81)
Average percentage packets delivered	12.67 (±0.516)	14.84 (±0.624)	20.68 (±0.484)	21.54 (±1.81)
Average end-to-end delay	7.37 (±0.4717)	13.52 (±0.1679)	4.06 (±0.0731)	3.30 (±2.14)
Average network lifetime	1753.01 (±1.82)	1875.42 (±3.58)	1539.78 (±3.69)	1657.29 (±14.77)

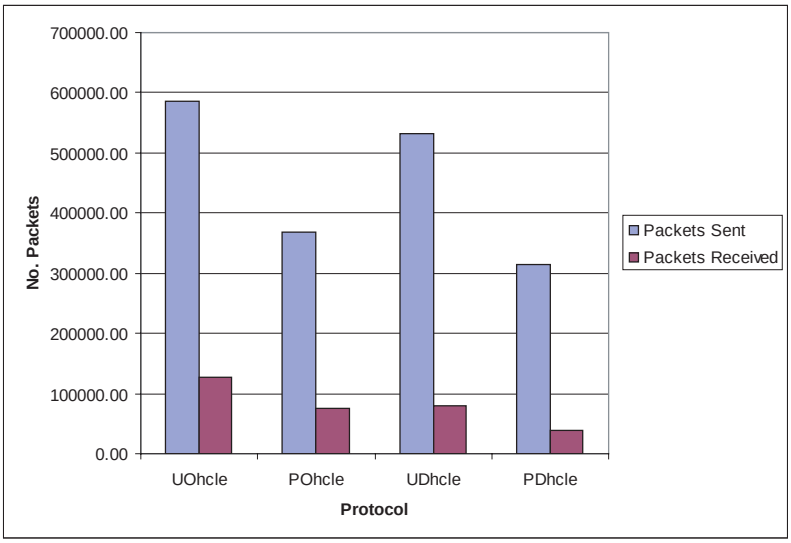

Figure 5.11: Average number of packets sent and delivered in the high-contention, limited-energy scenario.

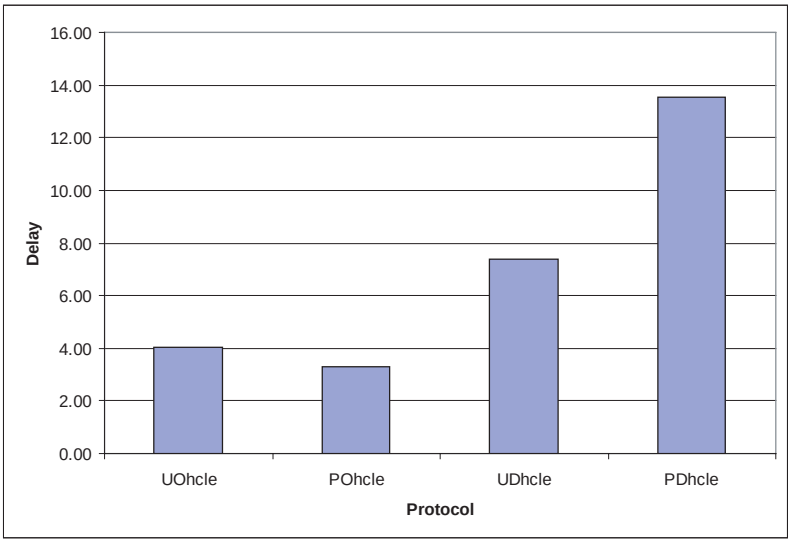

Figure 5.12: Average end-to-end delay in the high-contention, limited-energy scenario.

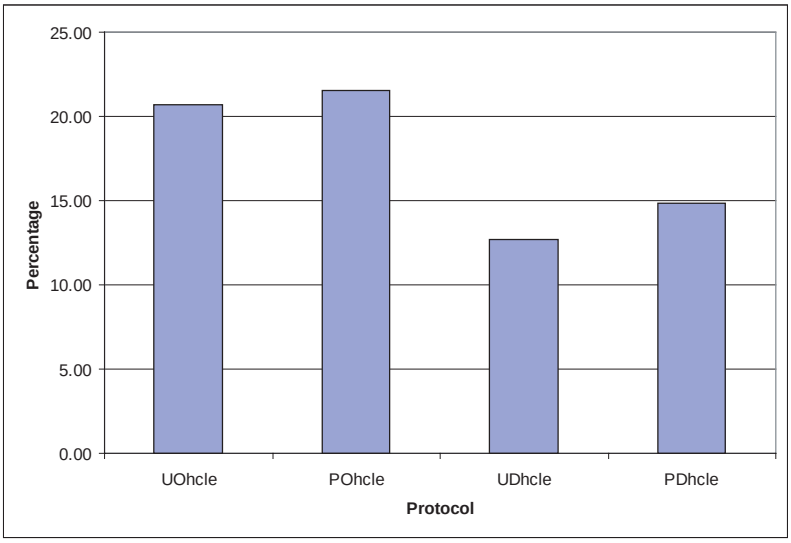

Figure 5.13: Average percentage of packets delivered in the high-contention, limited-energy scenario.

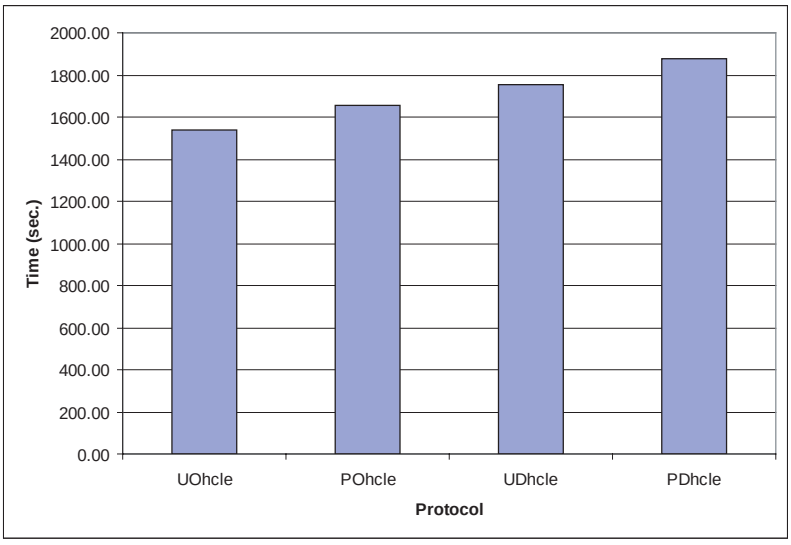

Figure 5.14: Average network lifetime in the high-contention, limited-energy scenario.

5.3.2 Mobile Nodes Experiments

In this section we present results for mobility experiments. Each experiment consists of 30 mobile nodes that are constantly moving at a certain speed. Three different speeds are considered. These speeds can be categorized as slow, medium, and fast. Node movement is split into two modes, random and coordinated. Simulations are carried on a rectangular area of 2500×1000, with 6 simultaneously active flows.

5.3.2.1 Coordinated Movement Experiments

In the coordinated movement mode, senders and receivers move in a coordinated fashion in terms of speed and direction. Sender and receiver pairs are kept within reachable distance of each other.

5.3.2.1.1 Low Speed At low speeds, we see improvements in the power-aware protocols for DSR and OLSR over the unmodified versions. In terms of number of packets we see an increase in the number of packets delivered to the application in PA-DSR versus U-DSR and similarly for PA-OLSR over U-OLSR. There are 55,012 extra packets delivered to the application for PA-DSR and 24,076 extra packets delivered for PA-OLSR. Figure 5.15 shows the number of packets sent and delivered to the application in DSR and PA-DSR. Figure 5.19 shows the number of packets sent and delivered to the application in OLSR and PA-OLSR. The increase in the number of packets delivered to the application is reflected in the percentage of packets delivered to the application. An increase of 5.34% is observed in

the PA-DSR and 1.3% for PA-OLSR. Figures 5.17 and 5.21 show the percentage of packets delivered to the application for DSR and OLSR, respectively. End-to-end delay results are comparatively similar for both the power-aware and unmodified versions of the protocols. Figures 5.16 and 5.20 show end-to-end delay for both DSR and OLSR. An increase in network lifetime of 280.34 seconds and of 251.76 seconds is observed for PA-DSR and PA-OLSR over U-DSR and U-OLSR, respectively. Table 5.5 summarizes the results for the low-speed, mobile scenario.

Table 5.5: Summary of Results for Low-speed, Coordinated Movement Scenario

	U-DSR	PA-DSR	U-OLSR	PA-OLSR
Average number of packets sent	465531.08 (±993.0)	546879.00 (±1382.61)	466816.92 (±1043.20)	509072.00 (±3056.49)
Average number of packets delivered	147558.46 (±1054.14)	202570.00 (±1573.68)	193122.20 (±1260.14)	217198.80 (±2575.24)
Average percentage packets delivered	31.70 (±0.466)	37.04 (±0.418)	41.37 (±0.054)	42.67 (±0.085)
Average end-to-end delay	0.07 (±0.0219)	0.09 (±0.0072)	0.02 (±0.0072)	0.02 (±0.00175)
Average network lifetime	1631.65 (±2.82)	1911.99 (±3.74)	1682.54 (±2.35)	1934.30 (±11.59)

5.3.2.1.2 Medium-speed At medium speeds, we see a decrease in the number of packets delivered to the application from the previous low-speeds scenario. However, we still see the effect of using the power-aware scheme versus the unmodified versions of the protocols. The increase in the number of packets delivered to the application is 18,073 packets for PA-DSR and 23,314 packets for PA-OLSR. Figures 5.15 and 5.19 show the average number of packets sent and delivered to the application for DSR and OLSR, respectively. Figures 5.17 and 5.21 show the percentage of packets delivered to the application for both DSR and OLSR. End-to-end delay is slightly increased for PA-DSR, while it is essentially the same for PA-OLSR and OLSR. Figures 5.16 and 5.20 show end-to-end delay for both DSR and OLSR protocols, respectively. Figures 5.18 and 5.22 show the network lifetime for both DSR and OLSR. From these graphs we see a slight improvement in network lifetime of 135.46 seconds for PA-DSR and 268.89 seconds for PA-OLSR. Table 5.6 summarizes the results for the mobile nodes traveling at medium-speeds.

5.3.2.1.3 High-speed At high-speeds we see similar results as before, specifically a slight improvement for the power-aware versions of the protocols over the unmodified versions. An improvement in the number of packets delivered to the application is noticed for PA-DSR and PA-OLSR, an increase of 10,260.76 packets for PA-DSR and 217.84 packets for PA-OLSR. This is reflected in the percentage of packets delivered to the application for both protocols. Figures 5.15 and 5.19 show the average number of packets sent and delivered to the application, while Figures 5.17 and 5.21 show the average percentage of packets

Table 5.6: Summary of Results for Medium-speed, Coordinated Movement Scenario

	U-DSR	PA-DSR	U-OLSR	PA-OLSR
Average number of packets sent	414515.64 (±2349.37)	450036.40 (±3135.32)	441851.62 (±1557.41)	482097.40 (±3761.78)
Average number of packets delivered	72250.66 (±2545.07)	90323.20 (±2121.82)	151687.66 (±1543.2)	175002.00 (±2878.69)
Average percentage packets delivered	17.43 (±0.68)	20.07 (±0.57)	34.33 (±0.043)	36.30 (±0.231)
Average end-to-end delay	0.11 (±0.0211)	0.19 (±0.0288)	0.04 (±0.00163)	0.01 (±0.0062)
Average network lifetime	1618.04 (±6.26)	1753.50 (±28.33)	1660.93 (±2.04)	1929.82 (±17.48)

delivered to the application for DSR and OLSR. End-to-end delay is slightly increased by 0.43 seconds in the case of PA-DSR, while it is slightly decreased in OLSR. Figures 5.16 and 5.20 show the average end-to-end delay for DSR and OLSR. Figures 5.18 and 5.22 show the network lifetime for DSR and OLSR. A slight improvement in the network lifetime in the power-aware versions of the protocol over the unmodified versions can be noticed from these graphs. Table 5.7 summarizes the results for the high-speed, mobile scenario. We note that the improvement in the lifetime in this scenario is due to the fact that a lot of packets are dropped which triggers the back-off scheme of IEEE802.11 and nodes stay inactive for some period of time.

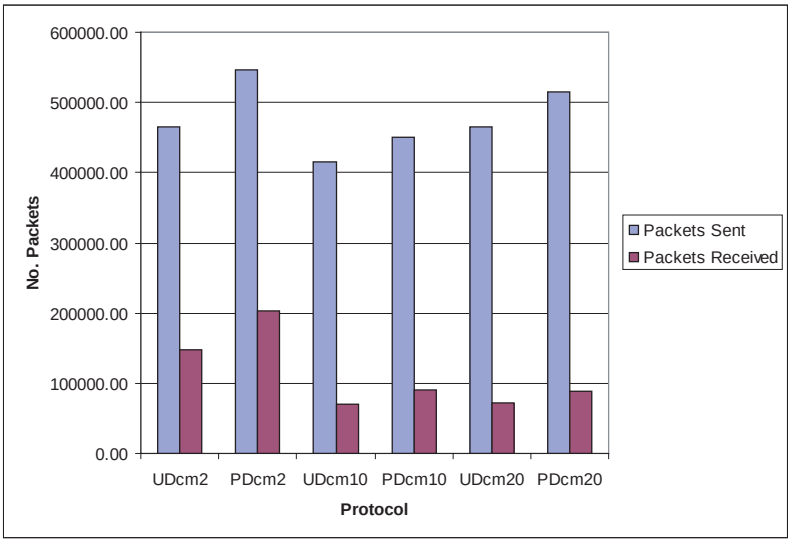

Figure 5.15: Average number of packets sent and delivered in DSR for the coordinated movement scenario.

Table 5.7: Summary of Results for High-speed, Coordinated Movement Scenario

	U-DSR	PA-DSR	U-OLSR	PA-OLSR
Average number of packets sent	465228.96 (±3529.67)	485938.40 (±3599.31)	437434.32 (±2416.88)	457649.80 (±3761.45)
Average number of packets delivered	70083.44 (±3518.14)	80344.20 (±3932.58)	75344.76 (±2201.01)	77515.60 (±3466.03)
Average percentage packets delivered	15.06 (±0.793)	17.32 (±0.39)	16.53 (±0.086)	16.94 (±0.217)
Average end-to-end delay	0.14 (±0.0457)	0.57 (±0.0341)	0.25 (±0.0011)	0.04 (±0.0158)
Average network lifetime	1668.30 (±1.47)	1782.93 (±6.67)	1879.33 (±3.62)	2208.75 (±15.67)

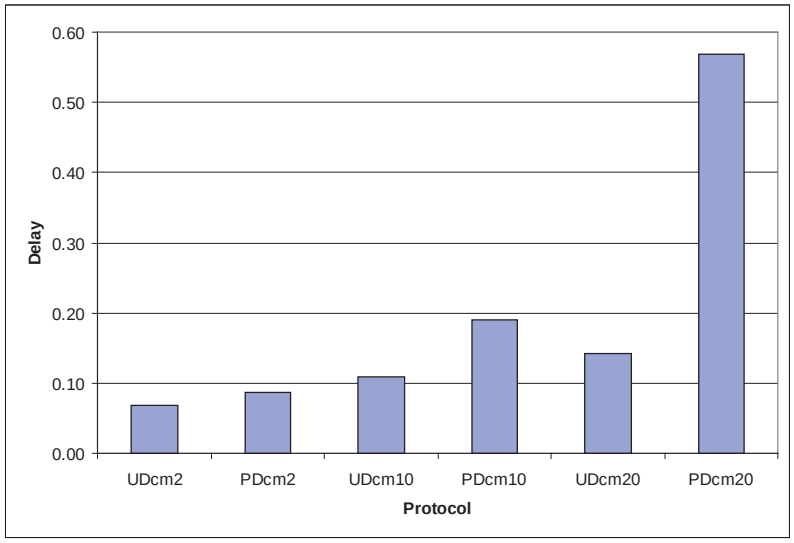

Figure 5.16: Average end-to-end delay of DSR for the coordinated movement scenario.

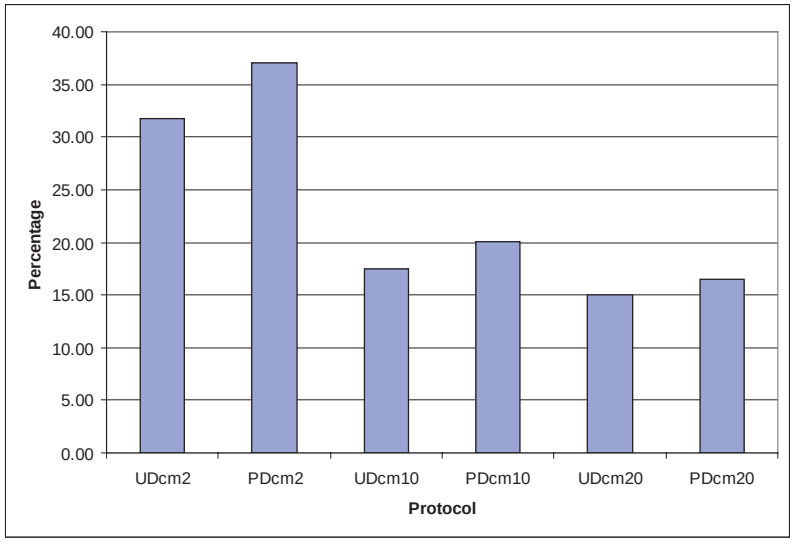

Figure 5.17: Average percentage of packets delivered in DSR for the coordinated movement scenario.

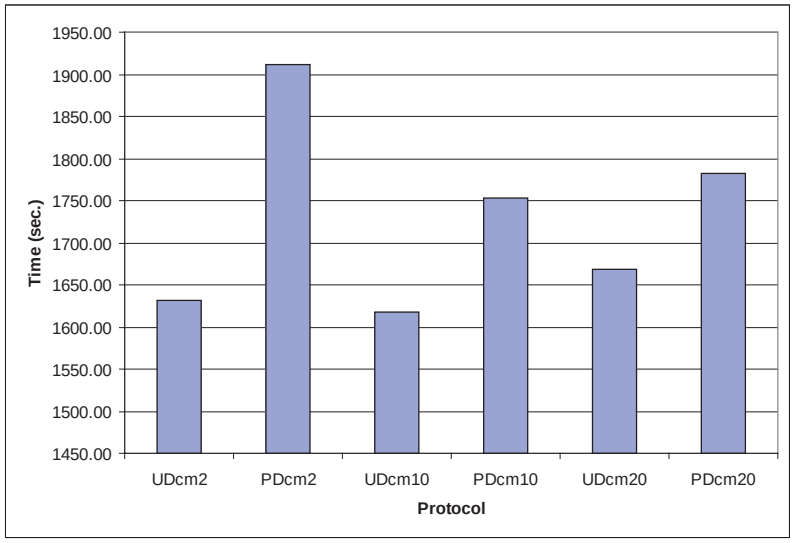

Figure 5.18: Average network lifetime of DSR for the coordinated movement scenario.

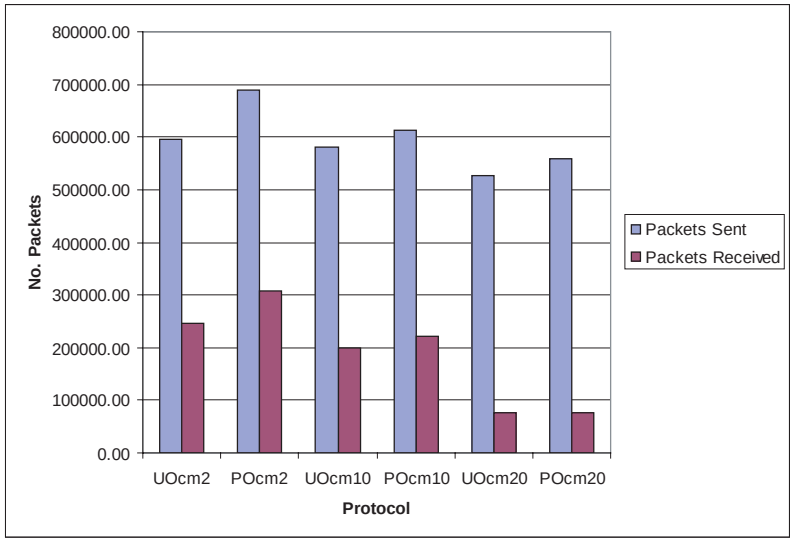

Figure 5.19: Average number of packets sent and delivered in OLSR for the coordinated movement scenario.

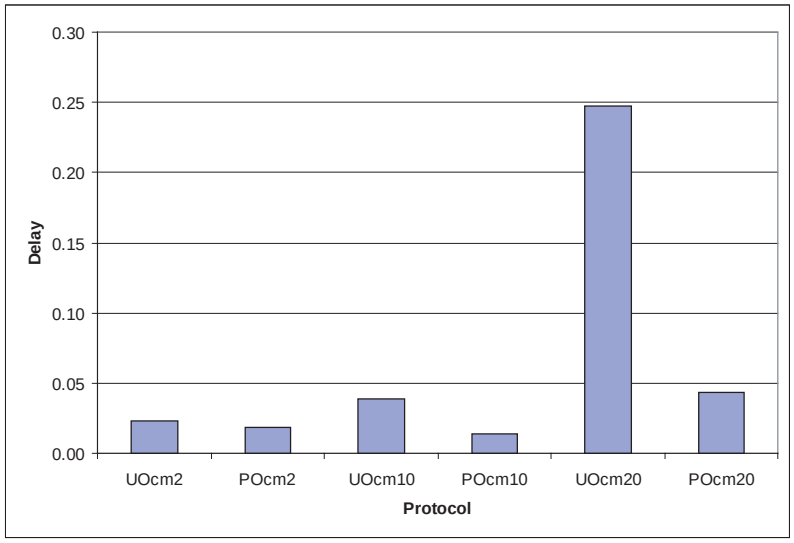

Figure 5.20: Average end-to-end delay of OLSR for the coordinated movement scenario.

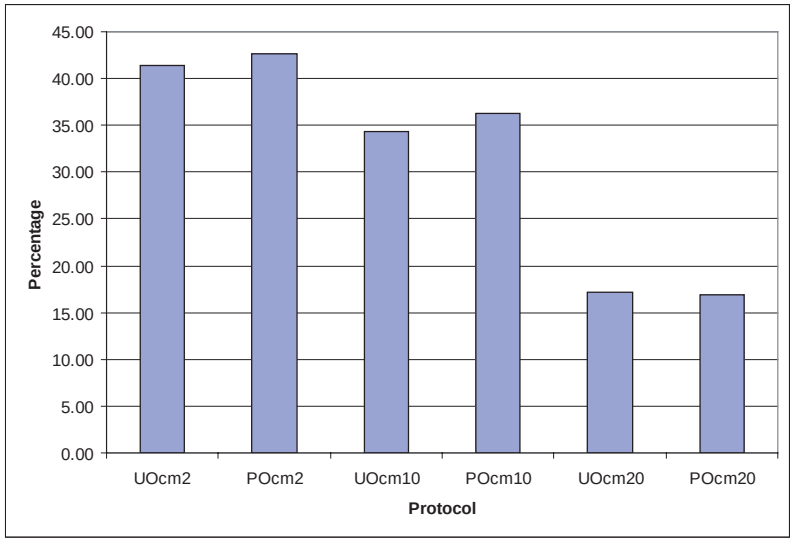

Figure 5.21: Average percentage of packets delivered in OLSR for the coordinated movement scenario.

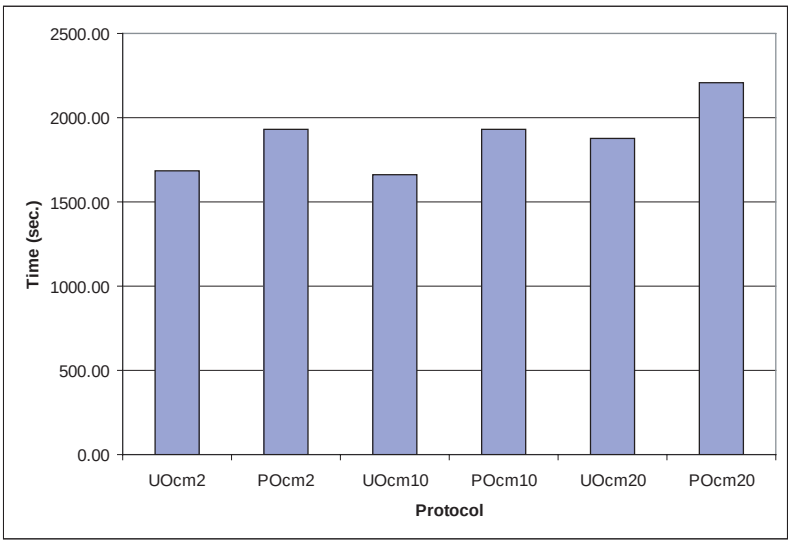

Figure 5.22: Average network lifetime of OLSR for the coordinated movement scenario.

5.3.2.2 Random Movement Experiments

In this set of experiments all nodes in the experiments move at random speeds and directions, including sending and receiving nodes. Three speeds are chosen for these experiments, low, medium, and high.

5.3.2.2.1 Low Speed At low speeds, we observe poor performance in terms of sending and receiving packets. The average percentage of packets delivered to the application is slightly higher for U-DSR than for PA-DSR. PA-DSR delivered 830 packets more than that of U-DSR. This is because the average network lifetime for PA-DSR is slightly longer than that of U-DSR, specifically 147.21 seconds longer. End-to-end delay is 0.38 seconds for PA-DSR, while it is 0.78 seconds for U-DSR. The decrease in the average end-to-end delay in PA-DSR

can be attributed to the fact that the random movement of the nodes contributed to the establishment of routes favored by PA-DSR that consist of nodes that are in close proximity and have lower aggregate reluctance values. Also, the inability to establish routes most of the time helps in keeping end-to-end delay low. PA-OLSR showed an almost 4% decrease in the percentage of packets delivered to the application. While the network survived longer in PA-OLSR, fewer packets were delivered to the application. Delay is lower for PA-OLSR at 0.07 seconds, and 0.42 seconds for U-OLSR. Figures 5.23 and 5.27 show the average number of packets sent and delivered for DSR and OLSR, respectively. Also, Figures 5.25 and 5.29 show the average percentage of packets delivered to the application for DSR and OLSR, respectively. Average network lifetime is shown in Figures 5.26 and 5.30 . Figures 5.24 and 5.28 show average end-to-end delay experienced by DSR and OLSR respectively.

Table 5.8 summarizes the results for the low-speed, random movement scenario.

5.3.2.2.2 Medium Speed At medium speed, we observe a sharp decrease in the number of packets received and in the percentage of packets received in the power-aware and unmodified versions of DSR and OLSR. This is due to the fact that all nodes are randomly moving at speeds such that the sending and receiving nodes cannot establish a connection for an extended period of time. Results show slightly higher performance for PA-DSR and lower performance for PA-OLSR. Figures 5.23 and 5.27 show the average number of packets sent and received by the application in DSR and OLSR, respectively. Figures 5.25 and 5.29 show the average percentage of packets delivered to the application in DSR and OLSR, re-

Table 5.8: Summary of Results for Low-speed, Random Movement Scenario

	U-DSR	PA-DSR	U-OLSR	PA-OLSR
Average number of packets sent	475816.60 (±1237.81)	497904.60 (±2763.66)	458065.16 (±1039.52)	428693.80 (±2734.45)
Average number of packets delivered	57106.94 (±1886.16)	57937.00 (±2919.14)	92328.88 (±1393.29)	69707.00 (±2707.82)
Average percentage packets delivered	12.00 (±3.49)	11.64 (±3.88)	20.16 (±3.43)	16.26 (±4.17)
Average end-to-end delay	0.78 (±0.2260)	0.38 (±0.2306)	0.42 (±0.1637)	0.07 (±0.0626)
Average network lifetime	1533.05 (±19.77)	1680.21 (±9.51)	1526.68 (±14.50)	1860.28 (±18.1)

spectively. End-to-end delay observed is low because it only reflects delay for the established routes. In random node movement, all nodes travel at medium speed and we expect high end-to-end delays. This means that any established route must be one-hop away. Moreover, routes cannot be maintained for an extended period of time, leading to small delays. Figures 5.24 and 5.28 show the average end-to-end delay for DSR and OLSR. Network lifetime values are comparable to other scenarios where the percentage of packets delivered to the application is higher than the values we observe in this scenario. The network lifetime values can be misleading since in this scenario sending nodes spend most of their time trying to establish a connection with the receiving nodes, which causes a slow drain in battery energy. Figures 5.26 and 5.30 show the average network lifetime for a random motion at medium speed for DSR and OLSR, respectively.

Table 5.9 summarizes the results for the medium-speed, random movement scenario.

5.3.2.2.3 High Speed At high-speeds we observe similar results as the medium-speed scenario. The percentage of packets delivered to the application is quite low for both protocols. Figures 5.23 and 5.27 show the average number of packets sent and received by the application in DSR and OLSR. Figures 5.25 and 5.29 show the average percentage of packets delivered for DSR and OLSR, respectively. End-to-end delay is low due to similar reasons pointed earlier in the medium-speed section. Figures 5.24 and 5.28 show the average end-to-end delay observed for DSR and OLSR. Network lifetime follows similar patterns as in the previous section due to similar reasons. Therefore, network lifetimes are not indicative

Table 5.9: Summary of Results for Medium-speed, Random Movement Scenario

	U-DSR	PA-DSR	U-OLSR	PA-OLSR
Average number of packets sent	451156.02 (±2866.74)	460846.00 (±3851.82)	434106.96 (±2246.05)	457306.80 (±2287.95)
Average number of packets delivered	13184.08 (±2773.04)	19171.40 (±3928.72)	49363.72 (±1934.9)	43672.60 (±2676.94)
Average percentage packets delivered	2.92 (±0.817)	4.16 (±1.605)	11.37 (±2.85)	9.55 (±2.18)
Average end-to-end delay	0.74 (±0.2898)	0.79 (±0.4635)	0.35 (±0.0875)	0.05 (±0.053)
Average network lifetime	1607.79 (±8.19)	2044.87 (±13.07)	1688.13 (±5.01)	2057.64 (±5.22)

of any advantages in either protocol. Figures 5.26 and 5.30 show average network lifetime for DSR and OLSR, respectively.

Table 5.10 summarizes the results for the high-speed, random movement scenario.

Table 5.10: Summary of Results for High-speed, Random Movement Scenario

	U-DSR	PA-DSR	U-OLSR	PA-OLSR
Average number of packets sent	437315.62 (±5802.84)	481212.20 (±6696.32)	440447.98 (±4190.56)	561328.00 (±2311.54)
Average number of delivered	12828.76 (±5747.15)	23621.00 (±6359.46)	30263.56 (±4422.37)	37708.20 (±2533.47)
Average percentage packets delivered	2.93 (±1.235)	4.91 (±1.916)	6.87 (±2.53)	6.72 (±3.71)
Average end-to-end delay	0.92 (±0.3158)	0.37 (±0.1996)	0.30 (±0.1446)	0.04 (±0.01664)
Average network lifetime	1625.44 (±13.08)	2196.83 (±19.22)	1720.09 (±15.13)	2229.54 (±20.13)

5.3.3 Node Energy Variation (NEV) Analysis

In this section we study the effects of our proposed power-aware protocol on node energy variation. As has been pointed in chapter 4, in U-DSR and U-OLSR, routes are used on the basis of shortest paths. In reactive protocols in general, and in DSR in particular, once a

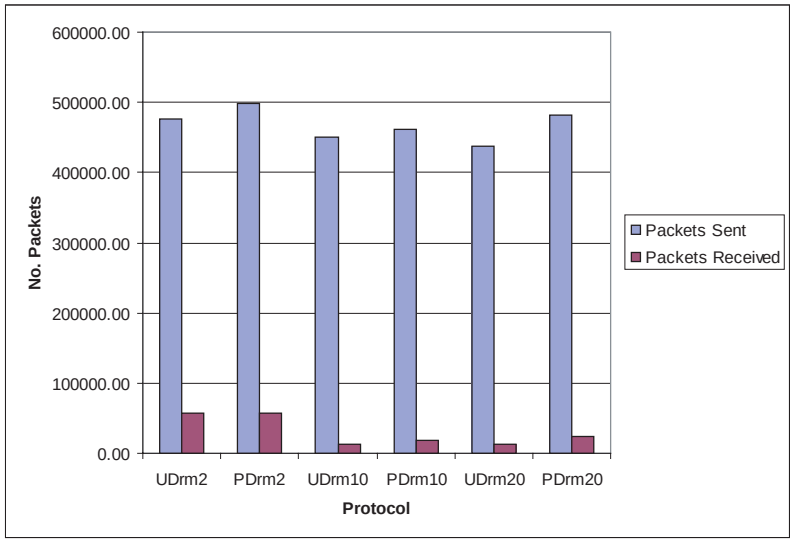

Figure 5.23: Average number of packets sent and delivered in DSR for the random movement scenario.

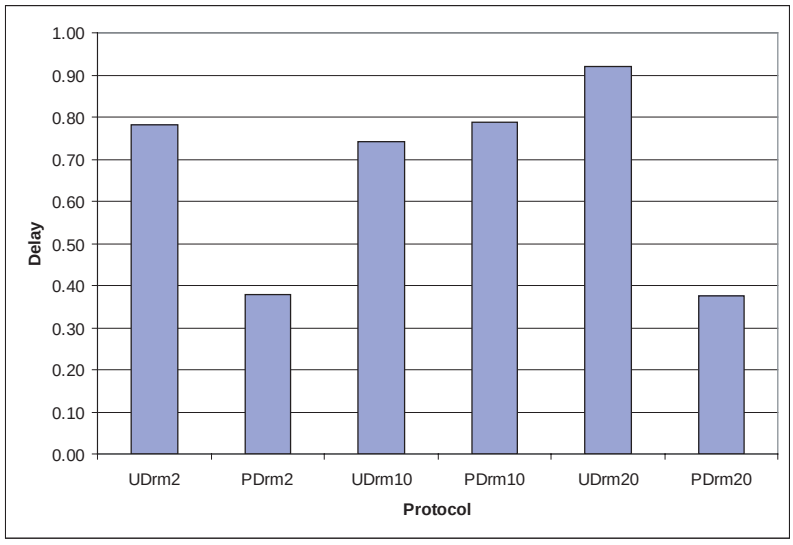

Figure 5.24: Average end-to-end delay of DSR for the random movement scenario.

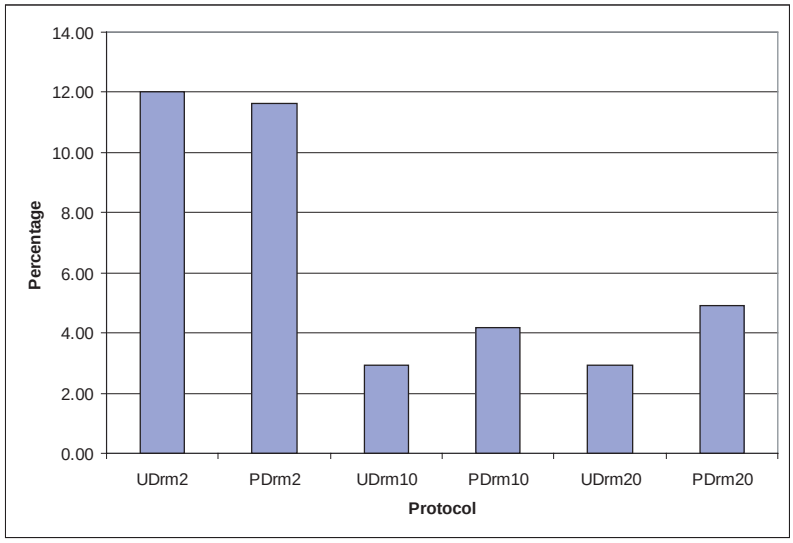

Figure 5.25: Average percentage of packets delivered in DSR for the random movement scenario.

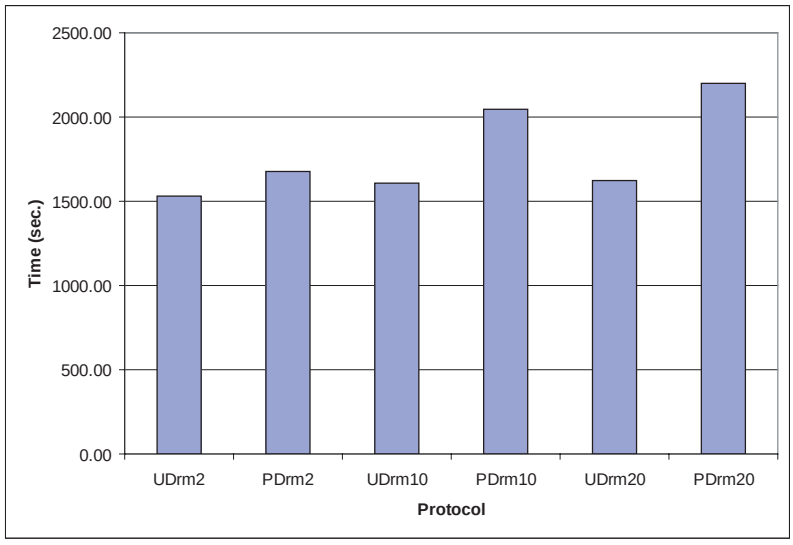

Figure 5.26: Average network lifetime of DSR for the random movement scenario.

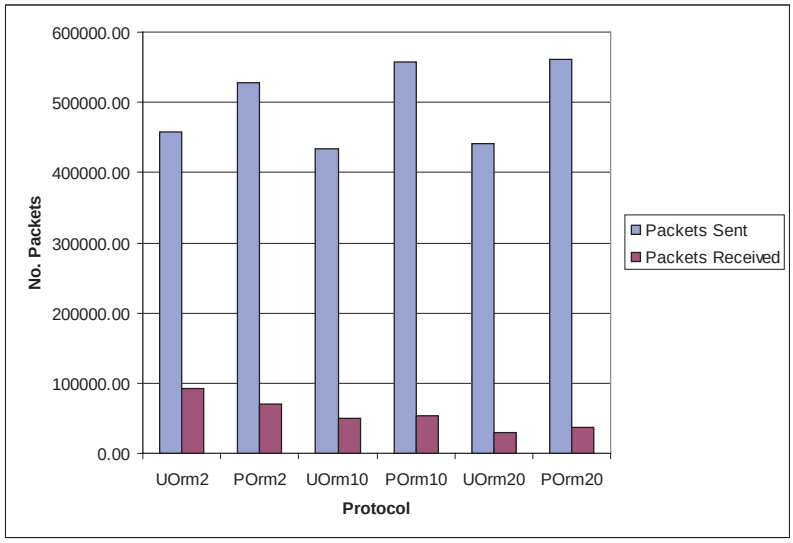

Figure 5.27: Average number of packets sent and delivered in OLSR for the random movement scenario.

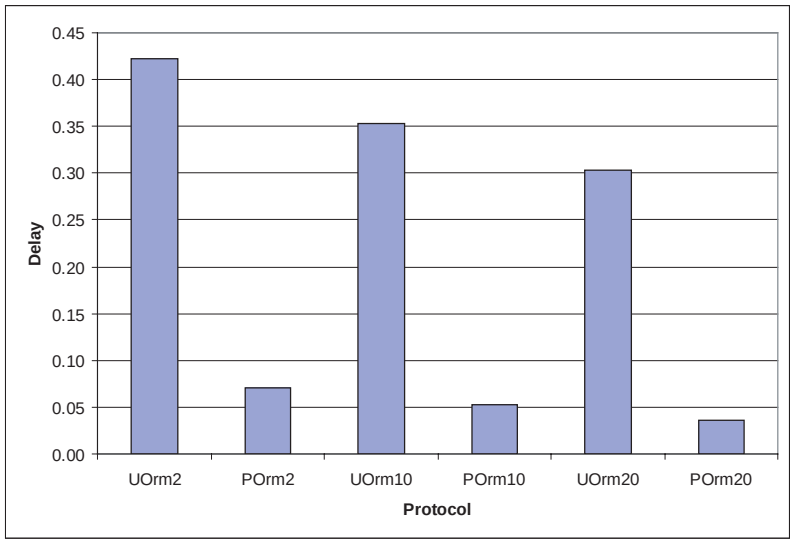

Figure 5.28: Average end-to-end delay of OLSR for the random movement scenario.

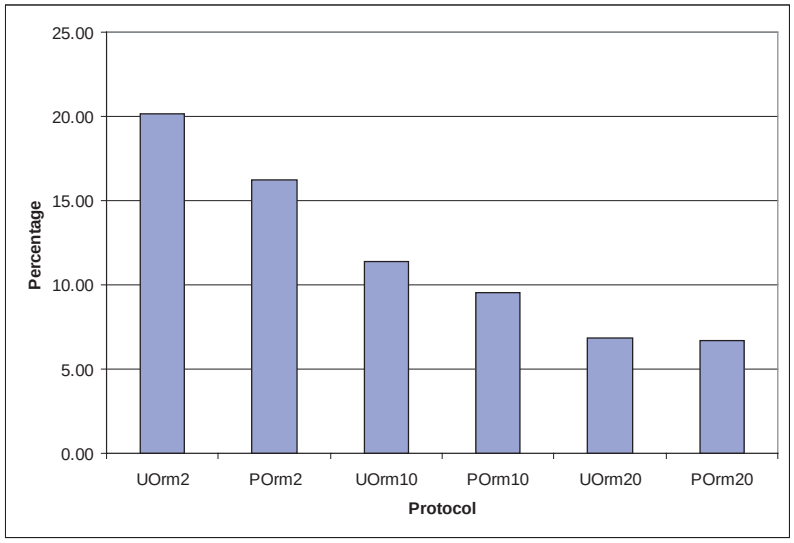

Figure 5.29: Average percentage of packets delivered in OLSR for the random movement scenario.

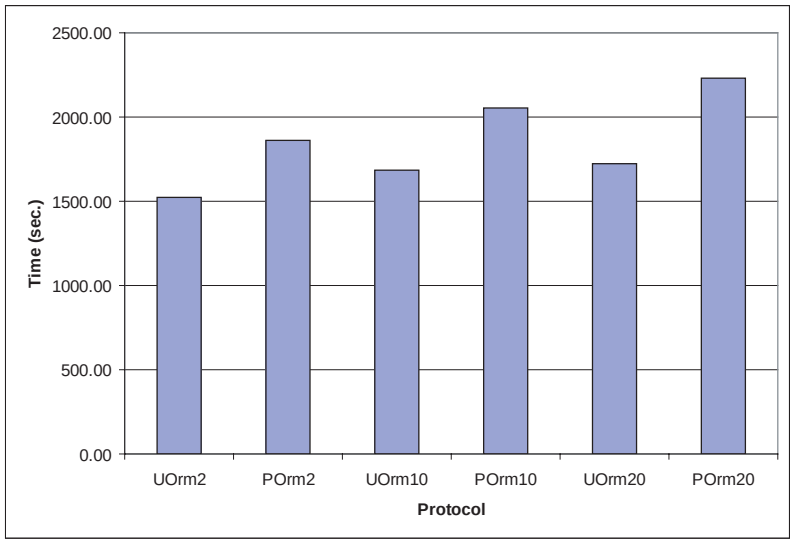

Figure 5.30: Average network lifetime of OLSR for the random movement scenario.

route is selected all nodes supporting the route, next-hop nodes, will be utilized as forwarders for the duration of the communication. This mechanism, as previously mentioned, unfairly expires these supporting nodes as it drains their battery energy. In proactive protocols, particularly in OLSR, periodic exchanges of control messages provide a current topology image of the network. The routing table is based on information found in the topology and neighbor tables [41]. A change in either of these tables will trigger a re-calculation in the routing table. Therefore, in a static scenario, the routing table does not get re-calculated since the topology and neighbor tables stay unchanged. In our proposed power-aware protocol, the re-calculation of the routing table is a function of the percentage of the remaining energy in the sending node, in addition to changes in the topology and neighbor tables. Moreover, routing is done through neighbors with lower reluctance values. Therefore, as nodes start communicating, the residual energy in the intermediate nodes acting as forwarding nodes for a route start depleting at a faster rate than other neighboring nodes in the network. Neighboring nodes are chosen such that their positions are in the path of communicating nodes.

5.3.3.1 Stationary Scenarios

5.3.3.1.1 Node Energy Variation in Low-contention, Limited Energy Scenarios

In this scenario, we observe a slight improvement in NEV in the power-aware protocols over the unmodified protocols. This slight improvement is mainly a result of using alternate nodes as traffic forwarders in a route instead of using only one node as a relay for the life of the

communication. Figure 5.31 shows NEV in a sample of neighboring nodes in DSR. Figure 5.32 shows NEV for a selected set of neighboring nodes in OLSR. Improvement in NEV is not always possible to view in graphs especially in large networks. In large networks, the choice of neighboring nodes increases, therefore, plotting all neighboring nodes, forwarders, on a graph is difficult to discern visually. Therefore, choosing a set of nodes as neighbors in a plot might not clearly show the improvements in NEV obtained by the power-aware protocol. Moreover, since each run of the same scenario might start with a different neighbor to relay packets between two communicating nodes, different results might be obtained. The graphs show some variation in the power-aware protocols, however, both U-DSR and U-OLSR show a monotonic gradual decrease in energy at neighboring nodes. This is due to the fact that in the unmodified versions, nodes transmit at full power. Therefore, it is possible that the sending and receiving nodes can communicate directly without any relay nodes. Figures 5.33 and 5.34 show more close-up graphs for neighboring nodes for DSR and OLSR, respectively. The graphs, in general, plot three different nodes under the power-aware and unmodified protocols. For example Figure 5.33 shows energy variation of nodes 25,26 and 28 in PA-DSR and U-DSR, while Figure 5.34 shows energy variation for nodes 5, 22, and 7 in PA-OLSR, and U-OLSR.

5.3.3.1.2 Node Energy Variation in Low-contention Unlimited Energy Scenarios

In this scenario we ran simulation tests for 3000 seconds. Each node is initialized with 140,000 Joules. The large initial node energy and the limited simulation time we chose did

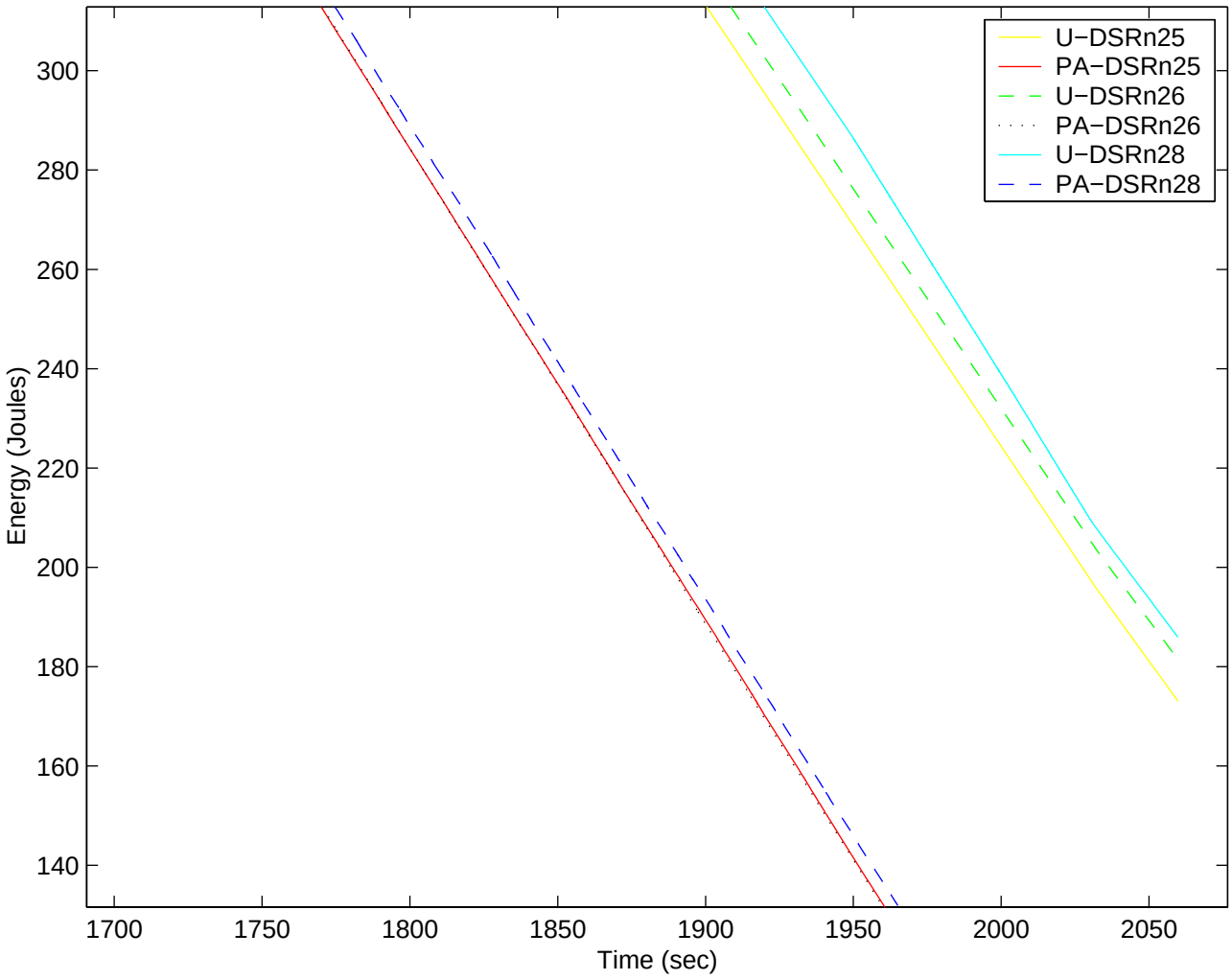

Figure 5.31: Node energy variation for DSR in low-contention limited energy scenario.

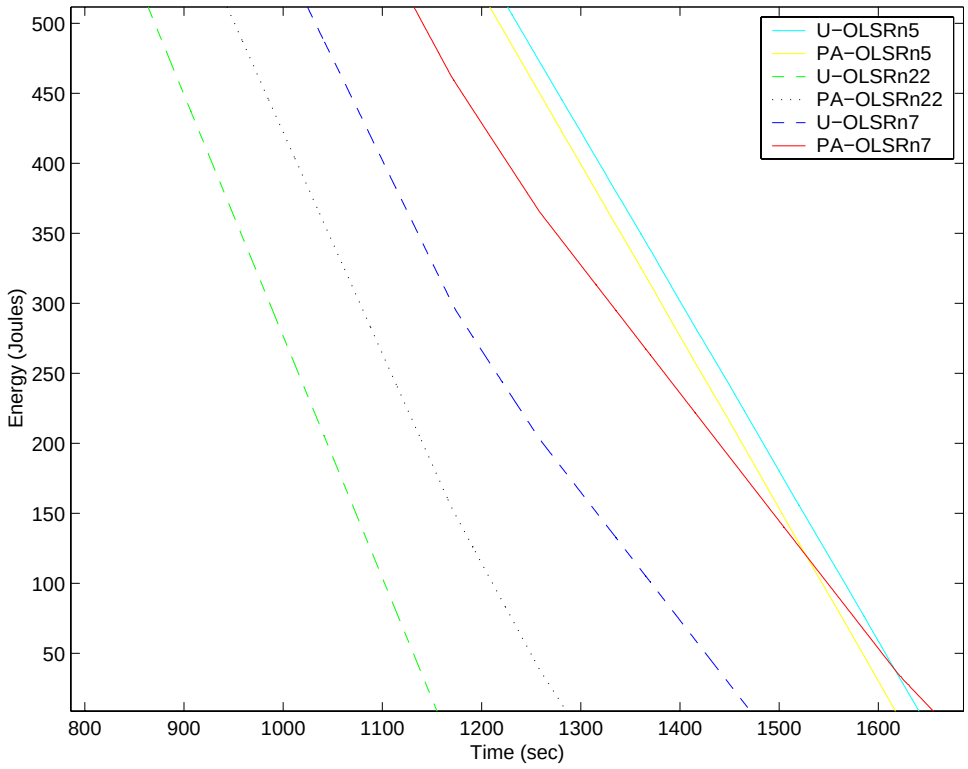

Figure 5.32: Node energy variation for OLSR in low-contention limited energy scenario.

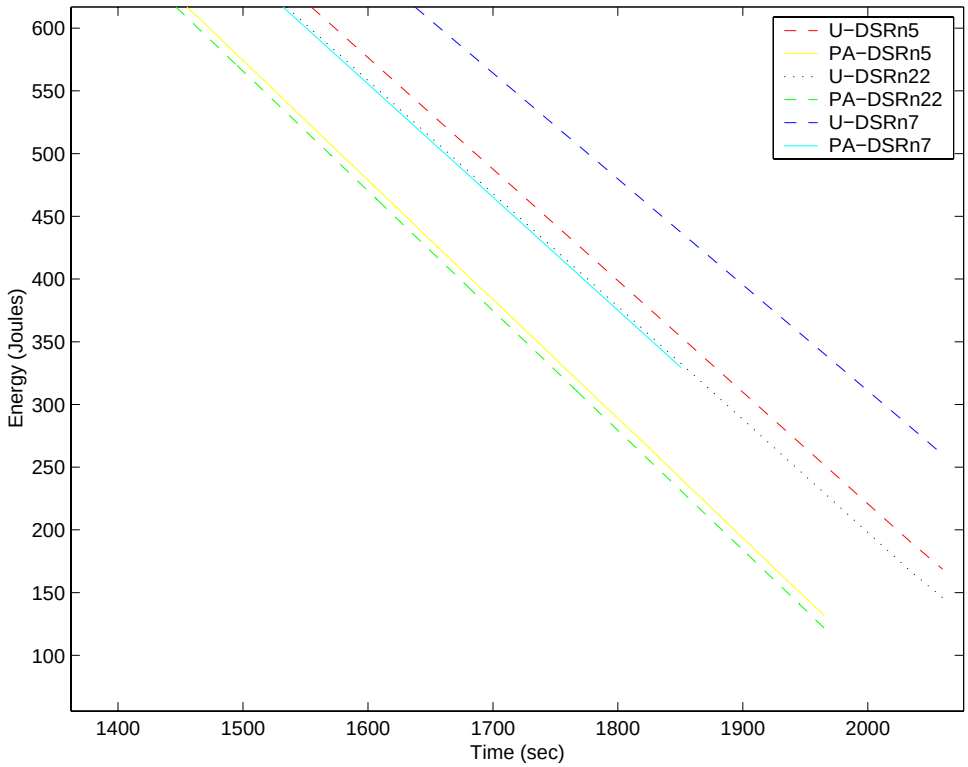

Figure 5.33: Node energy variation for DSR in low-contention limited energy scenario.

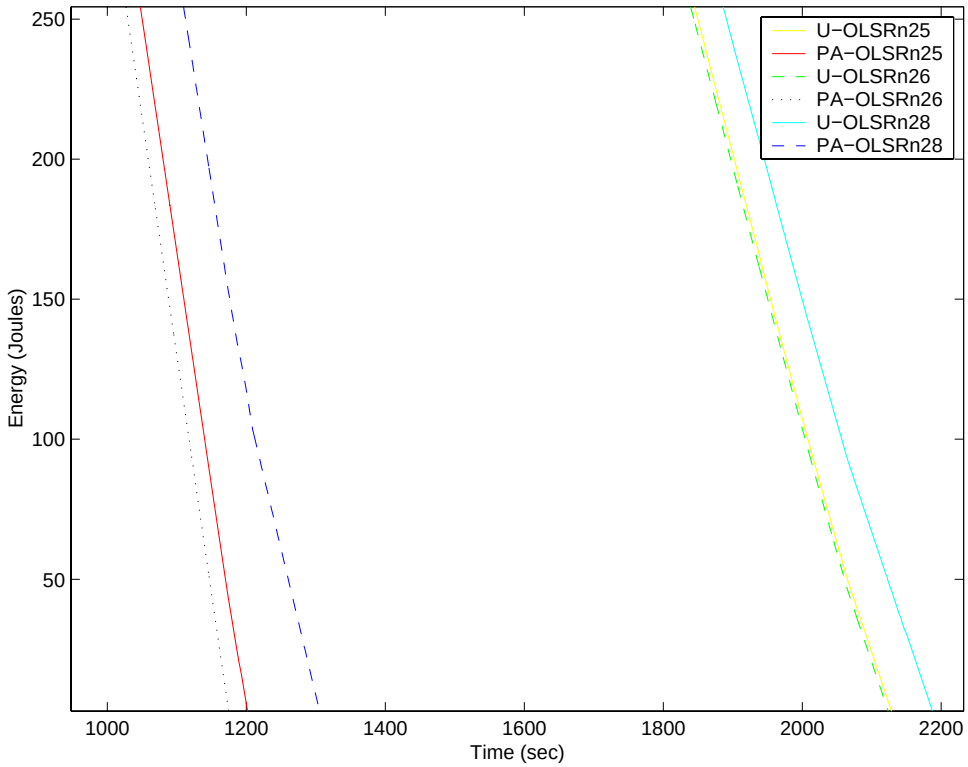

Figure 5.34: Node energy variation for OLSR in low-contention limited energy scenario.

not allow the power-aware protocol to switch routes among neighbors. Therefore, we see no noticeable difference between the power-aware and the unmodified protocols. Figures 5.35 and 5.36 show NEV for three neighboring nodes in both DSR and OLSR, respectively. The figures show no advantage in NEV observed in the power-aware protocols to that of the unmodified protocols due to the reasons mentioned above.

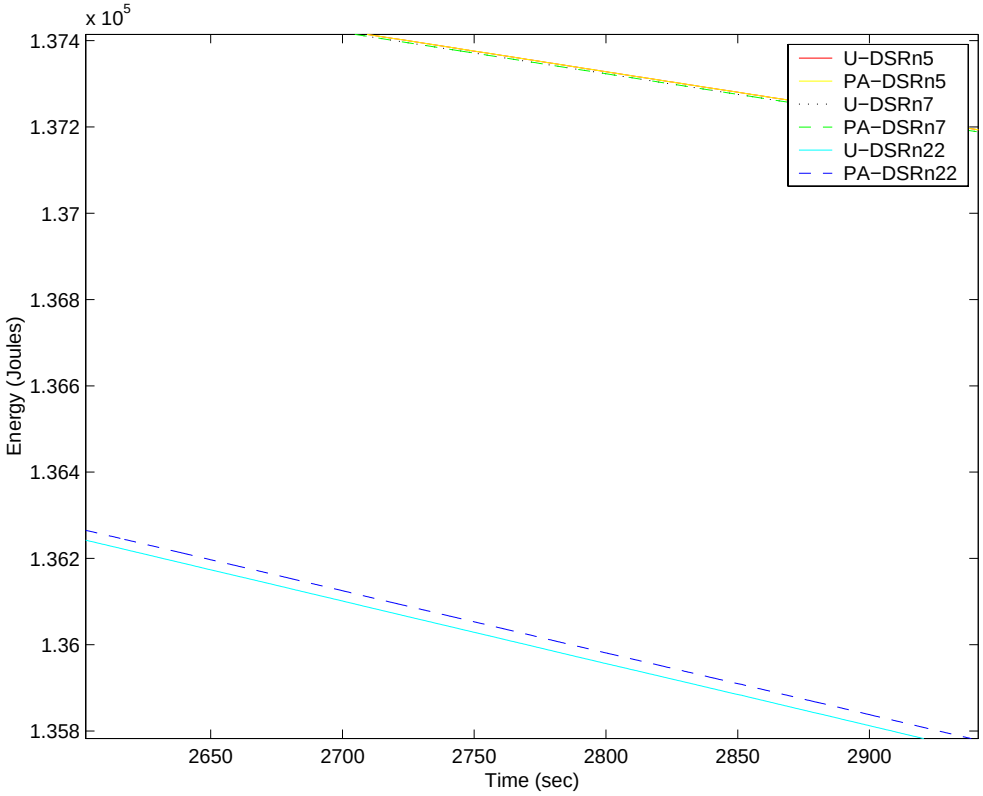

Figure 5.35: Node energy variation for DSR in low-contention unlimited energy scenario.

5.3.3.1.3 Node Energy Variation in High-contention Limited Energy Scenarios

Even though protocol performance goes down under high-contention, NEV for this scenario shows a slight improvement in the power-aware protocol over the unmodified one. Figures

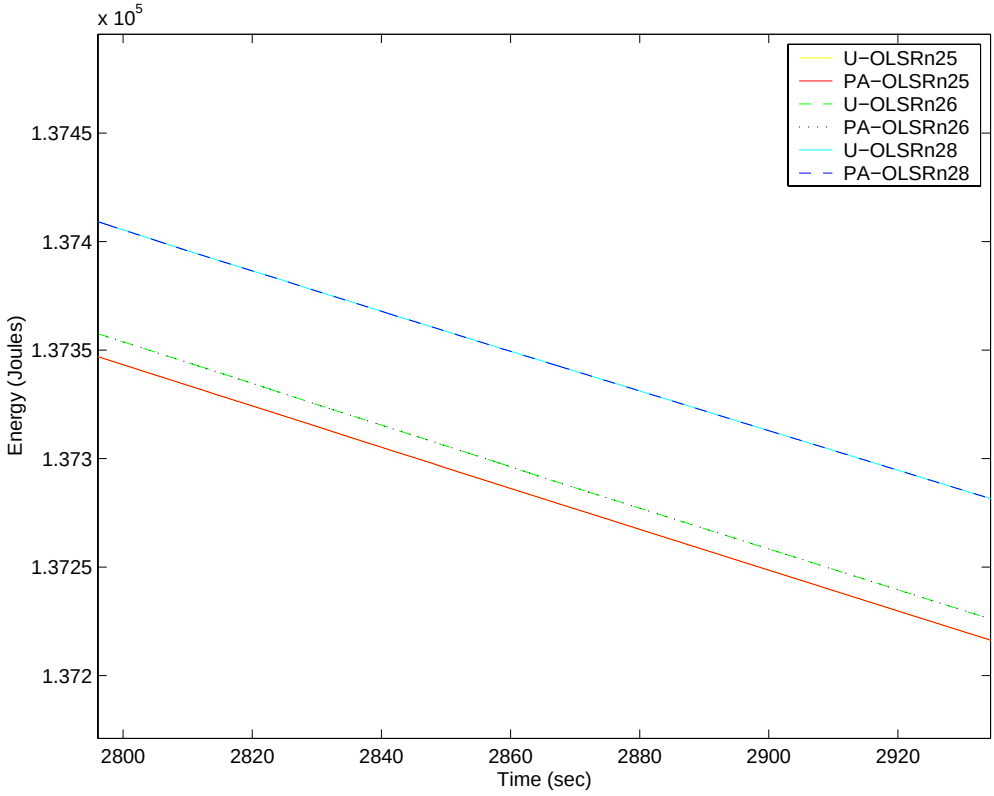

Figure 5.36: Node energy variation for OLSR in low-contention unlimited energy scenario.

5.37 and 5.38 show NEV for neighboring nodes for both protocols DSR and OLSR.

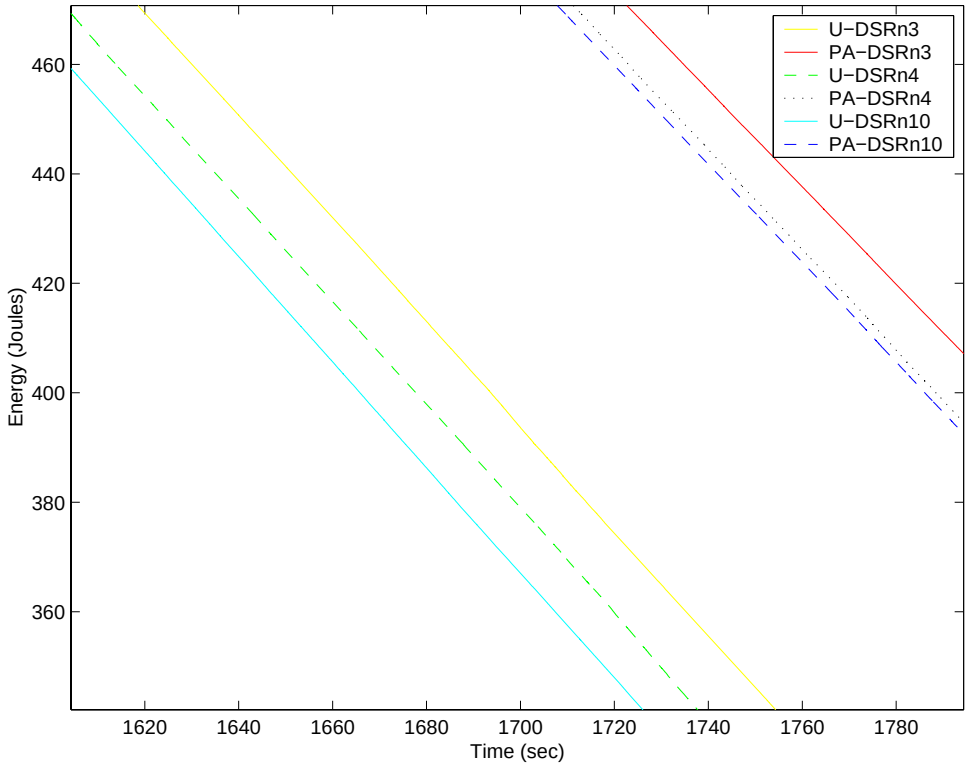

Figure 5.37: Node energy variation for DSR in high-contention limited energy scenario.

5.3.3.1.4 Node Energy Variation in High-contention Unlimited Energy Scenarios

Results in this section are similar to those obtained in the low-contention unlimited energy scenario. The high initial node energy and the limited simulation time prevented the power-aware protocols from switching routes. Results in Figure 5.39 show a slight improvement for some nodes in DSR. Figure 5.40 shows NEV for neighbors in OLSR. In Figure 5.40 the energy variation is lower between nodes 12 and 19 in PA-OLSR than U-OLSR.

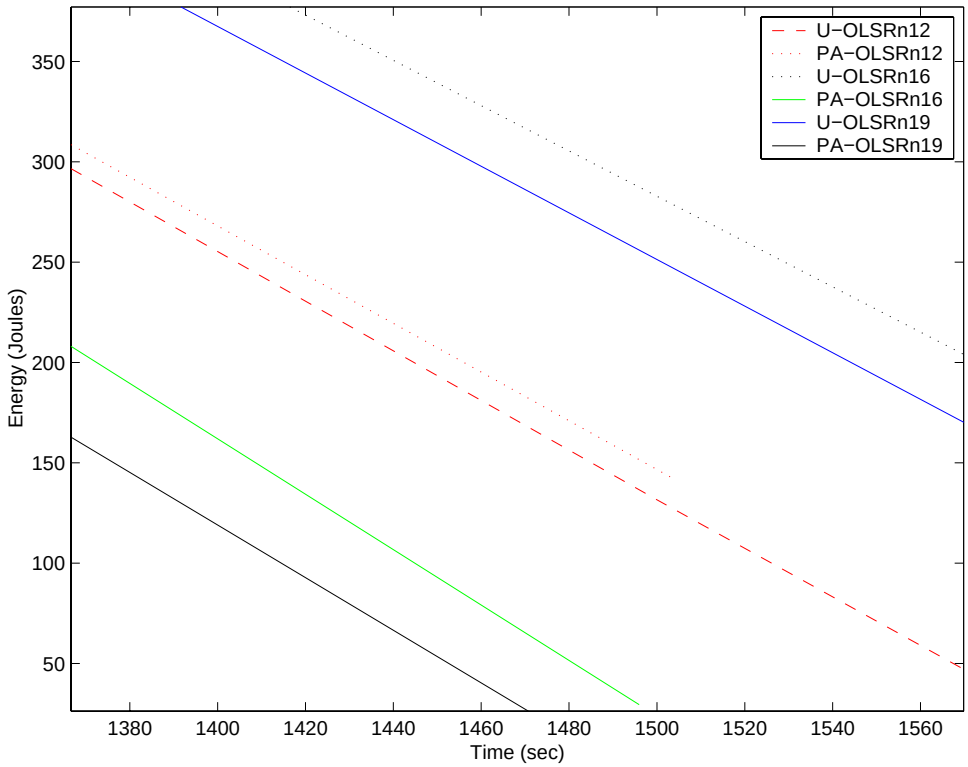

Figure 5.38: Node energy variation for OLSR in high-contention limited energy scenario.

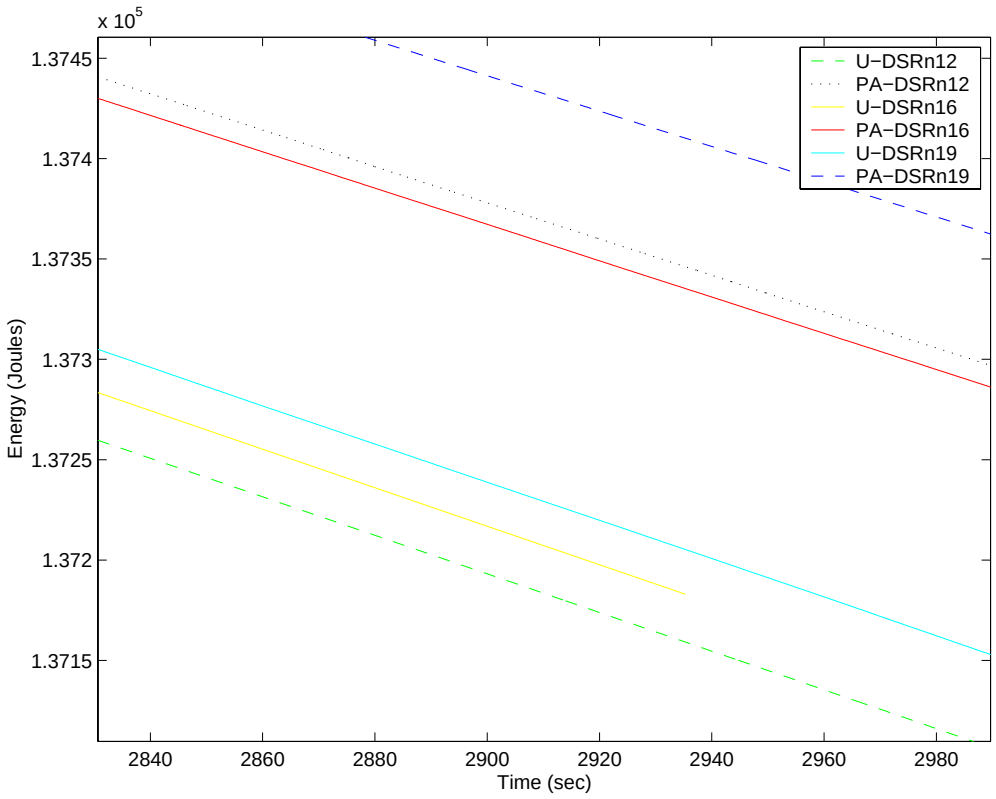

Figure 5.39: Node energy variation for DSR in high-contention unlimited energy scenario.

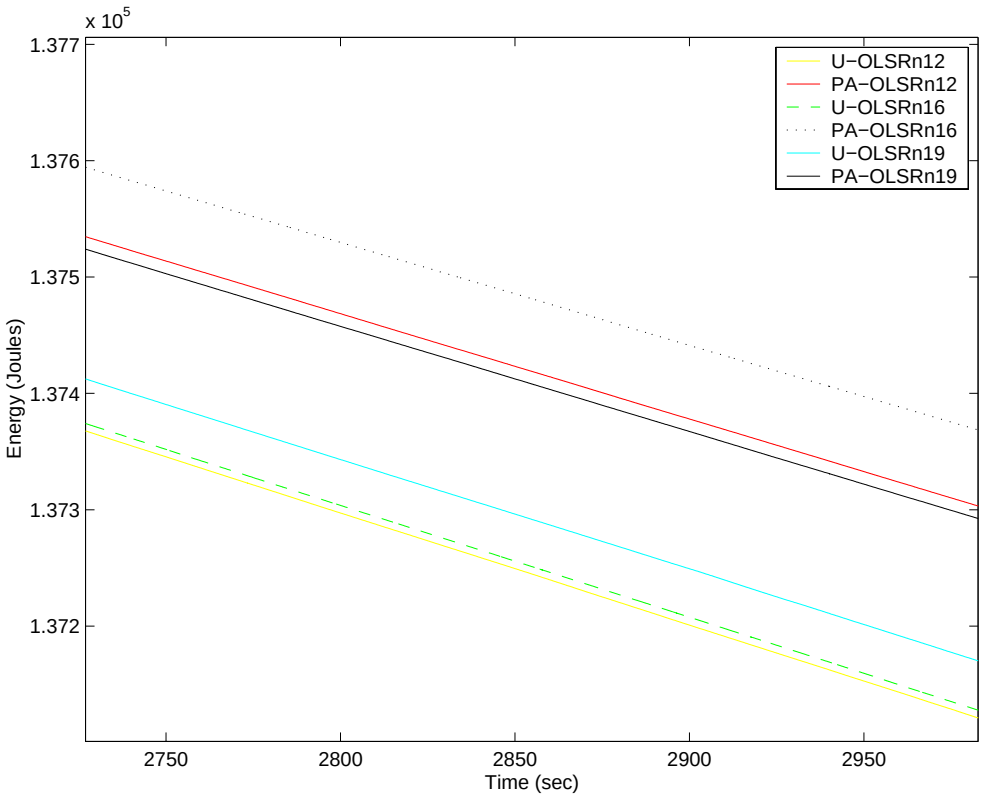

Figure 5.40: Node energy variation for OLSR in high-contention unlimited energy scenario.

5.3.3.2 Mobile Scenarios

5.3.3.2.1 Node Energy Variation in Coordinated Movement In coordinated movement, the sending and receiving nodes travel at comparable speeds and in similar directions. With mobility, intermediate nodes or neighbors tend to change over the period of the simulation. This makes comparing NEV among power-aware and unmodified protocols difficult. At high speeds, routes tend to break at a faster rate than at lower speeds. This is indicated by the low percentage of packets delivered to the destination. Figures 5.41 and 5.42 show NEV for a sample of neighboring nodes for DSR and OLSR at low speeds. Figures 5.43 and 5.44 show NEV for a sample of neighboring nodes for DSR and OLSR at medium speeds, while Figures 5.45 and 5.46 show NEV for a sample of neighboring nodes for DSR and OLSR at high speeds.

5.3.3.2.2 Node Energy Variation in Random Movement In random movement, nodes travel at random speed and direction. Therefore, communicating nodes are placed at random positions and travel at different speeds and directions. Therefore, it is difficult to establish routes except, if possible, during pause time. For this reason most graphs for DSR and OLSR tend to show a slow and gradual decrease in node energy. This is also reflected in the low percentage of packets delivered. Figures 5.47 and 5.48 show NEV for randomly selected nodes moving at random at low speeds. Figures 5.49 and 5.50 show NEV for randomly selected nodes moving randomly at medium speeds. Figures 5.51 and 5.52 show NEV for randomly selected nodes moving randomly at high speeds.

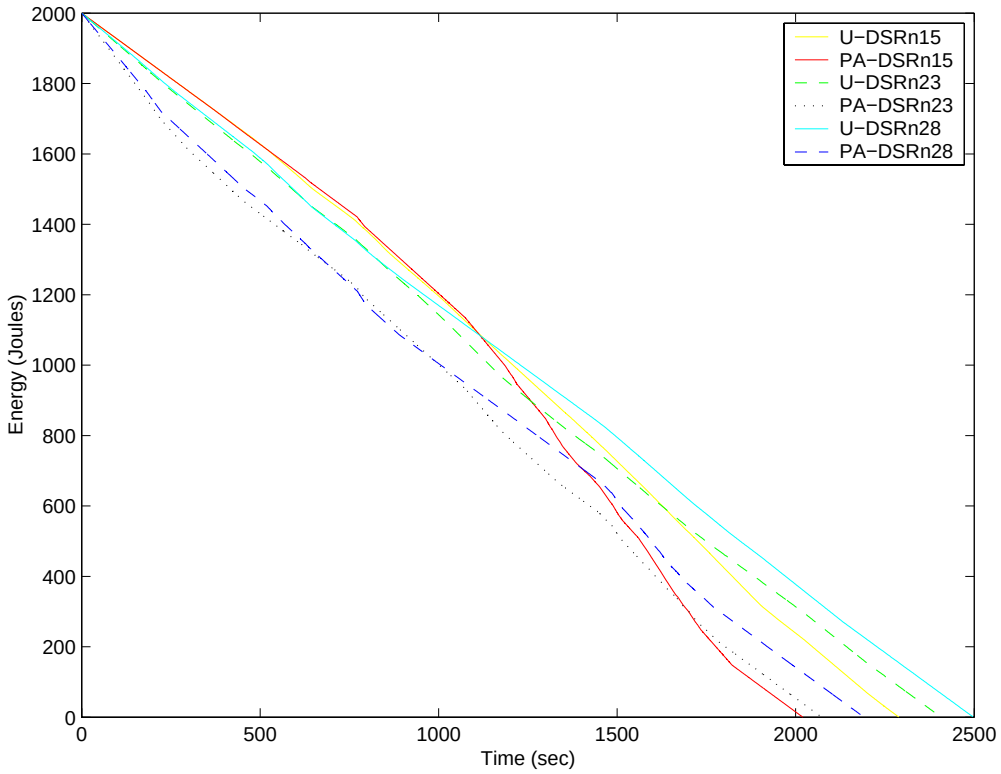

Figure 5.41: Node energy variation for DSR in coordinated movement low-speed scenario.

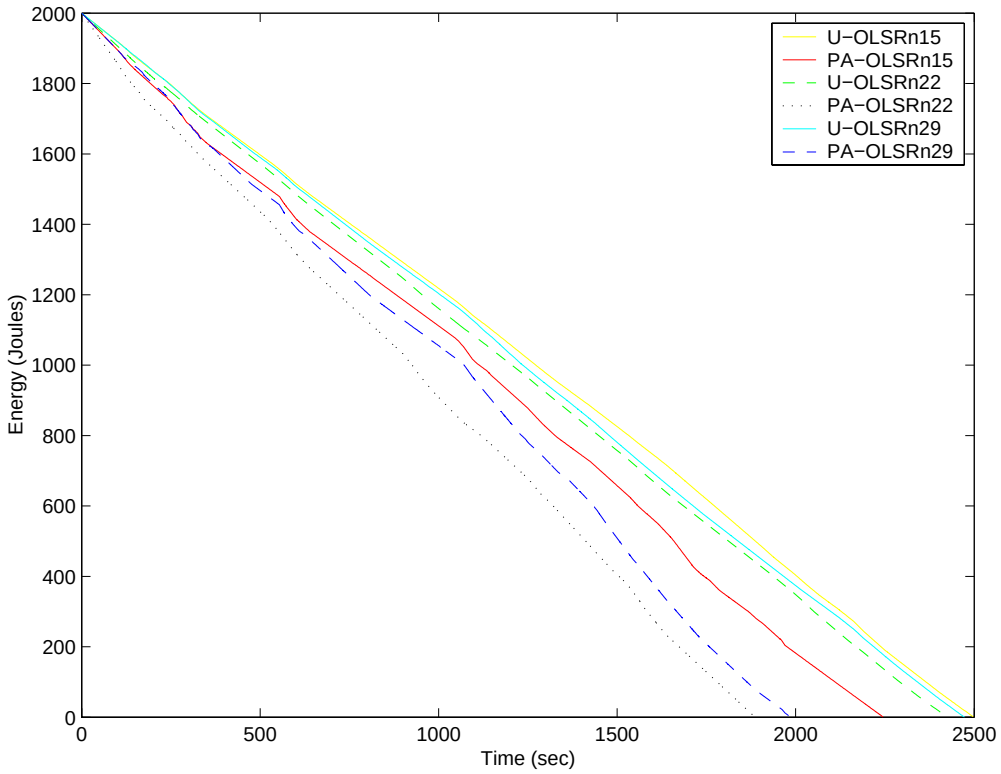

Figure 5.42: Node energy variation for OLSR in coordinated movement low-speed scenario.

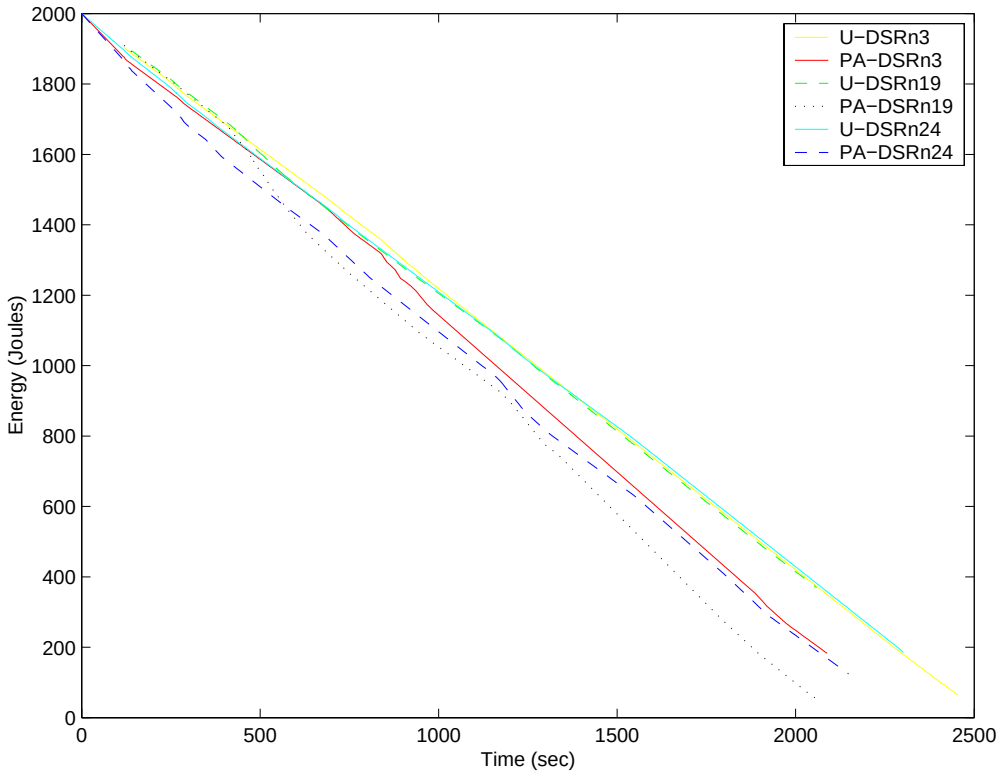

Figure 5.43: Node energy variation for DSR in coordinated movement medium-speed scenario.

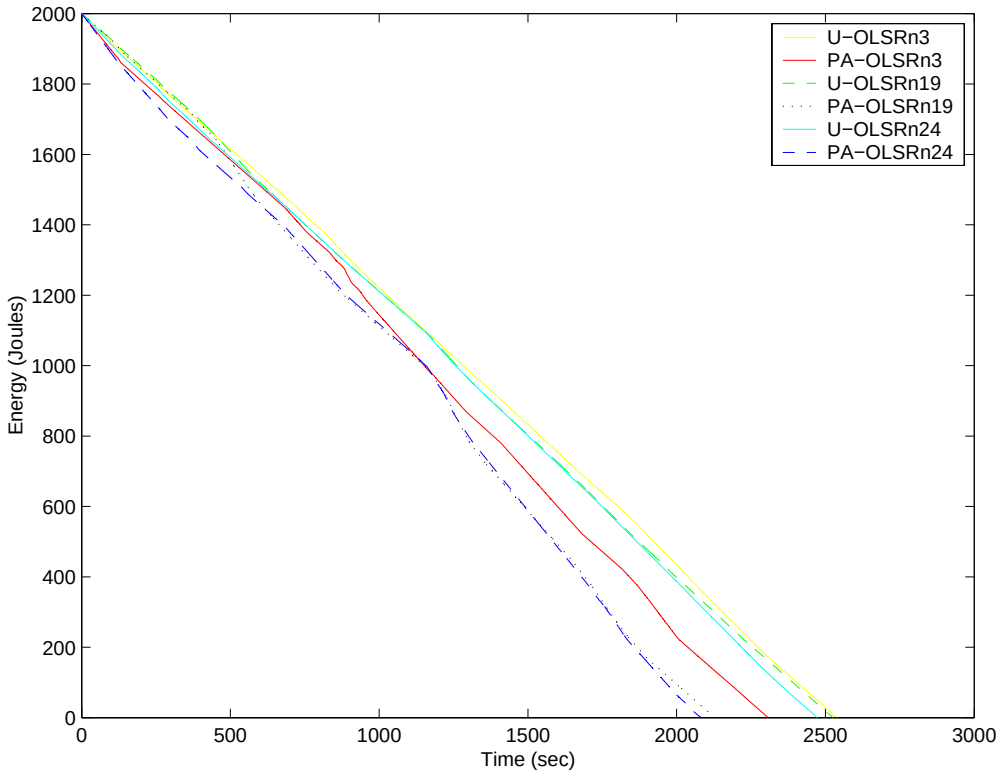

Figure 5.44: Node energy variation for OLSR in coordinated movement medium-speed scenario.

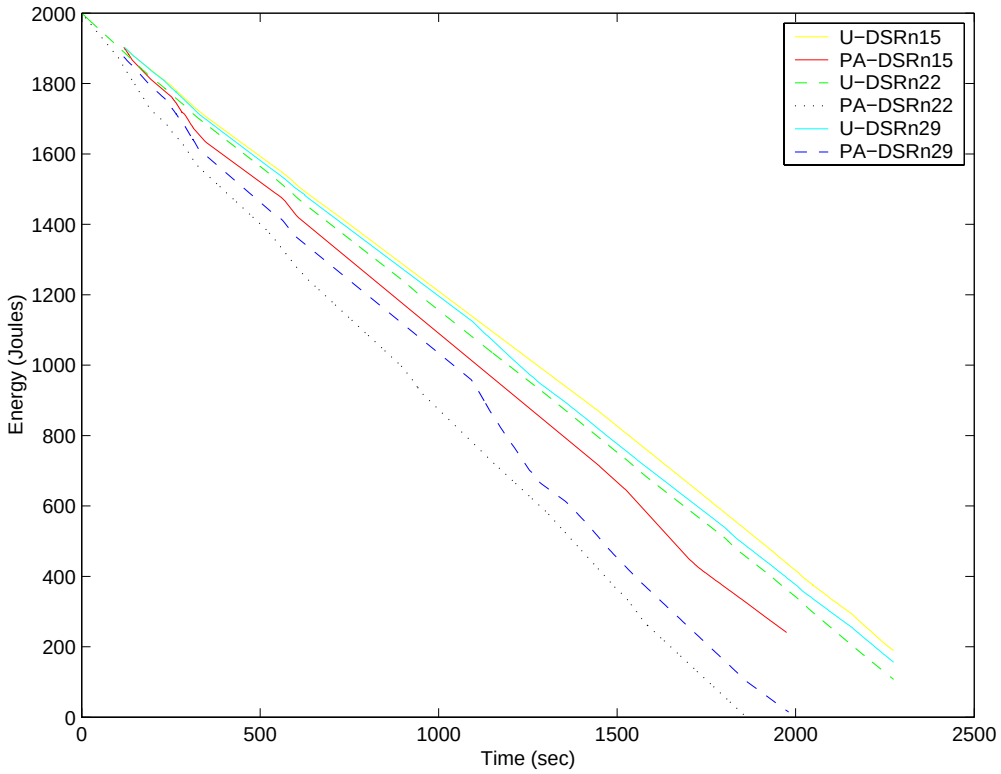

Figure 5.45: Node energy variation for DSR in coordinated movement high-speed scenario.

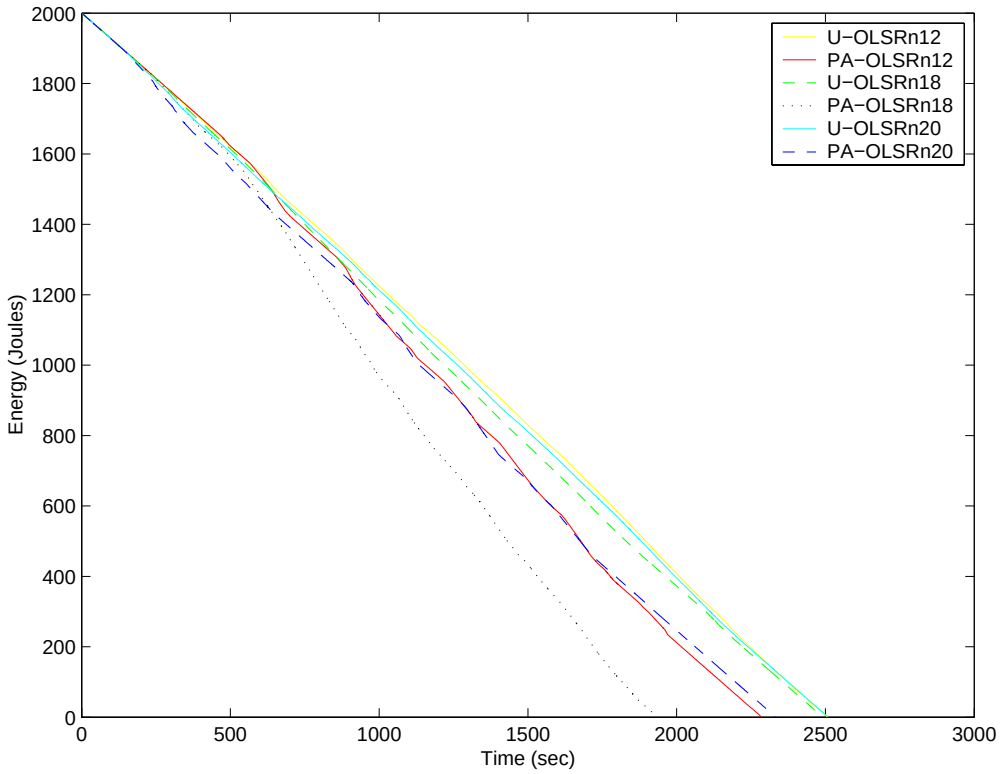

Figure 5.46: Node energy variation for OLSR in coordinated movement high-speed scenario.

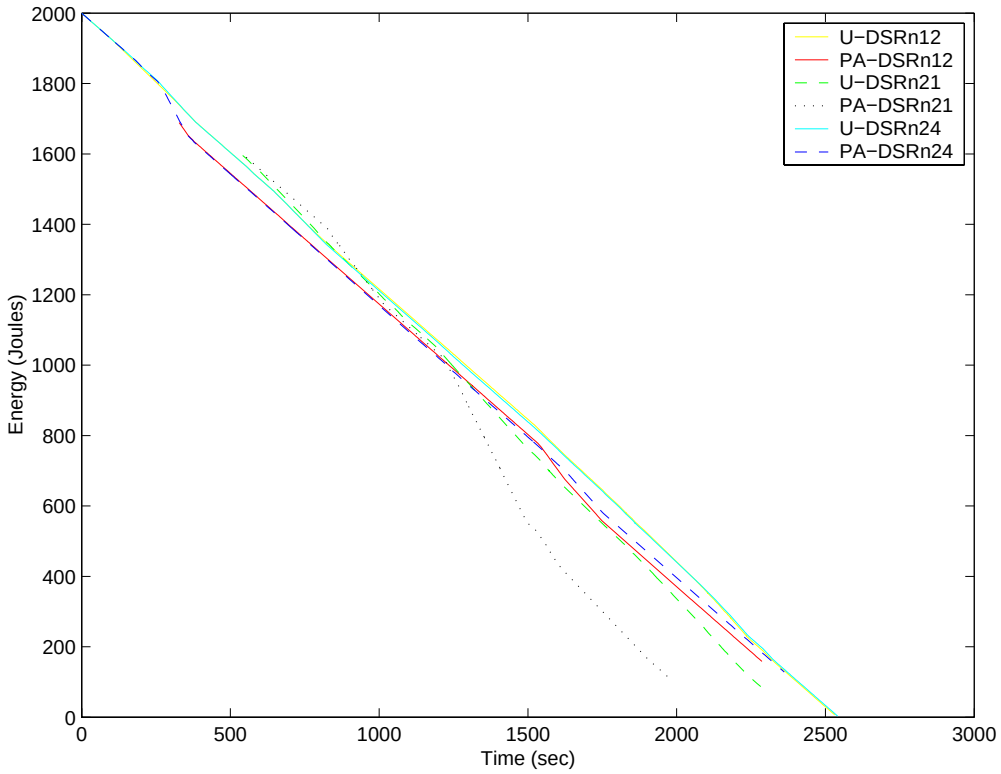

Figure 5.47: Node energy variation for DSR in random movement low-speed scenario.

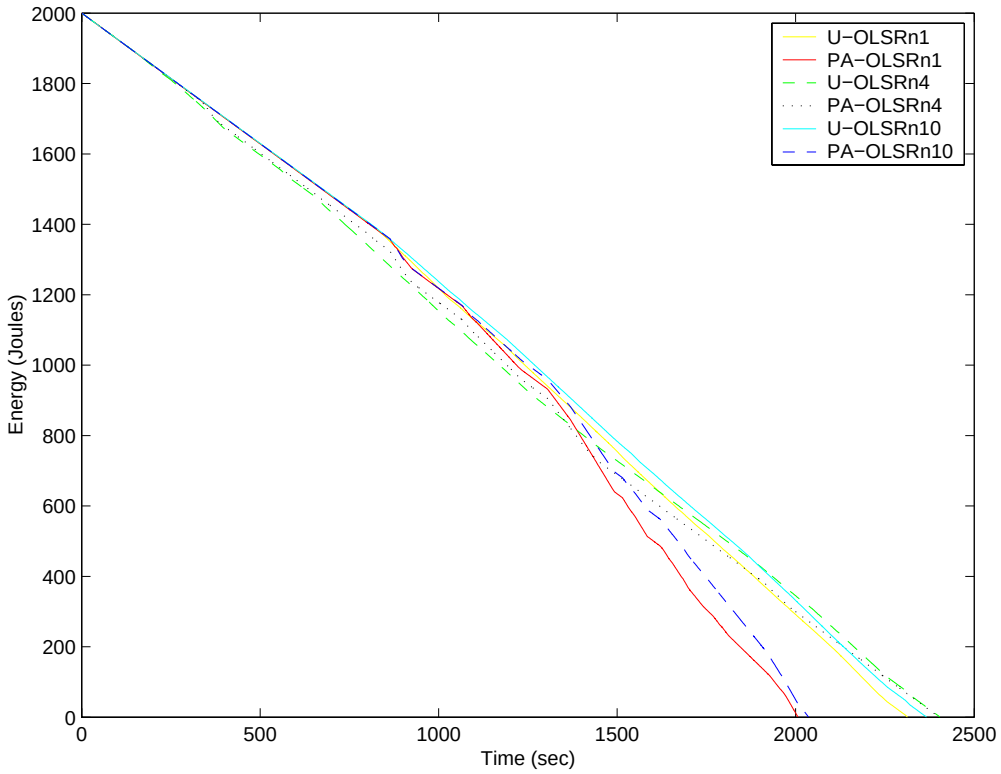

Figure 5.48: Node energy variation for OLSR in random movement low-speed scenario.

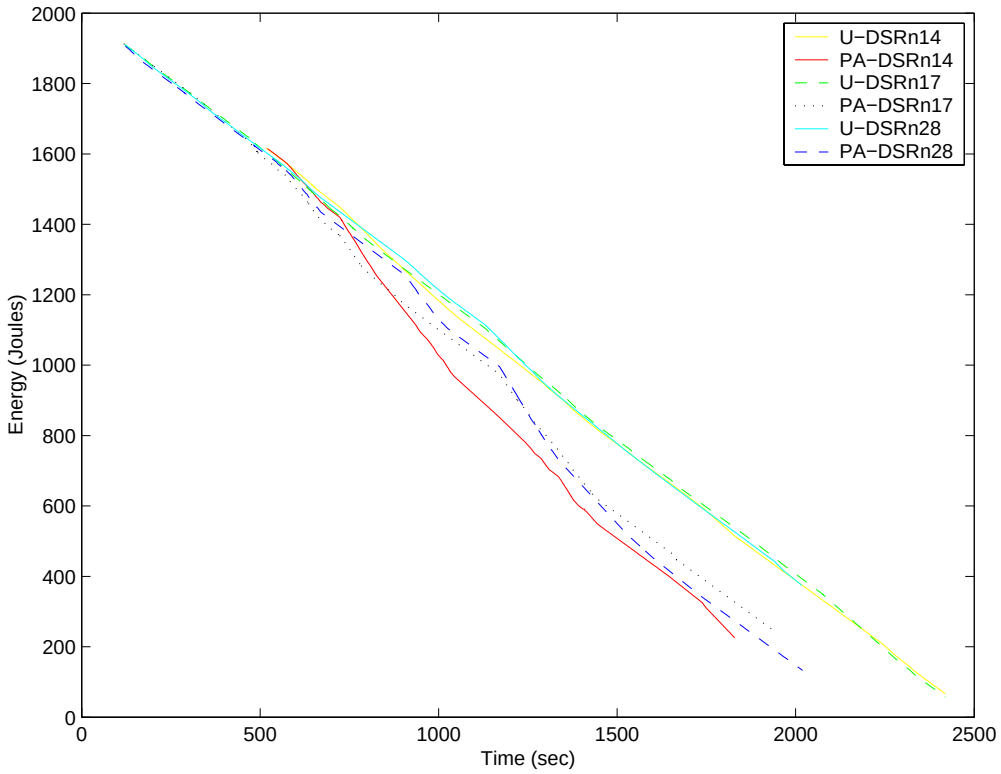

Figure 5.49: Node energy variation for DSR in random movement medium-speed scenario.

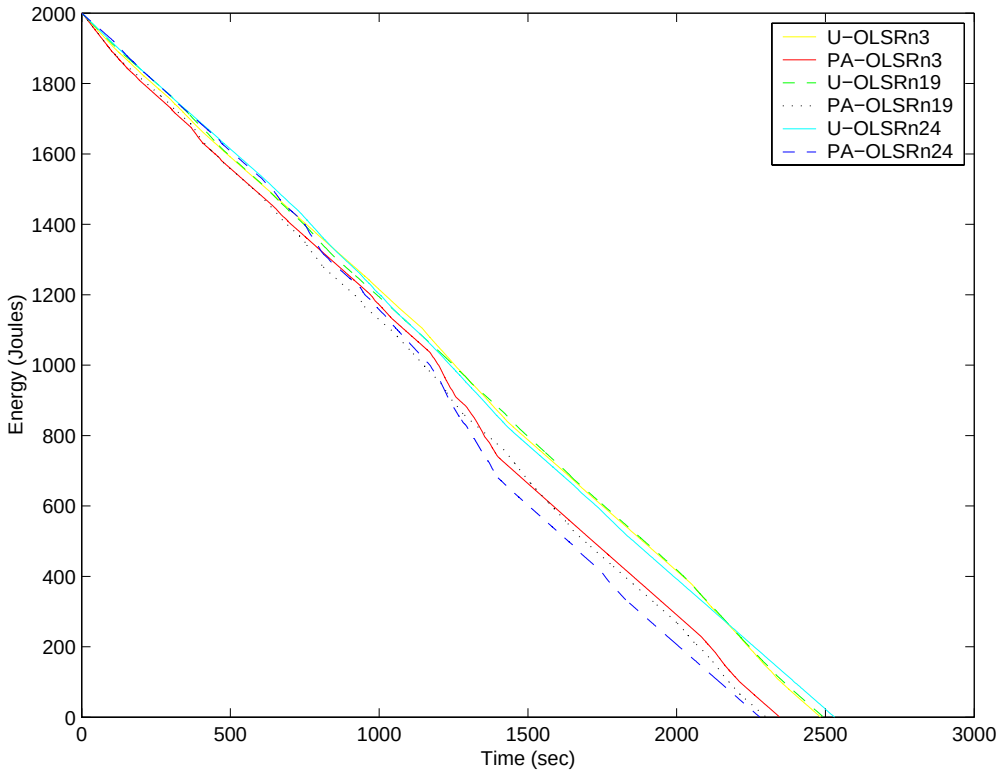

Figure 5.50: Node energy variation for OLSR in random movement medium-speed scenario.

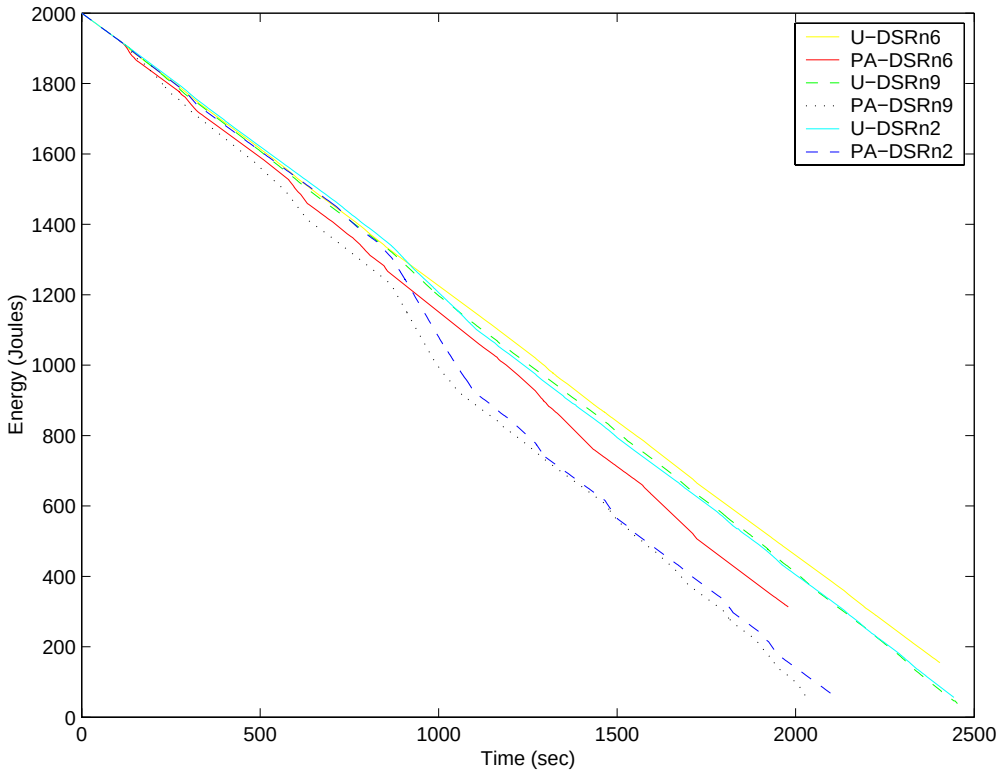

Figure 5.51: Node energy variation for DSR in random movement high-speed scenario.

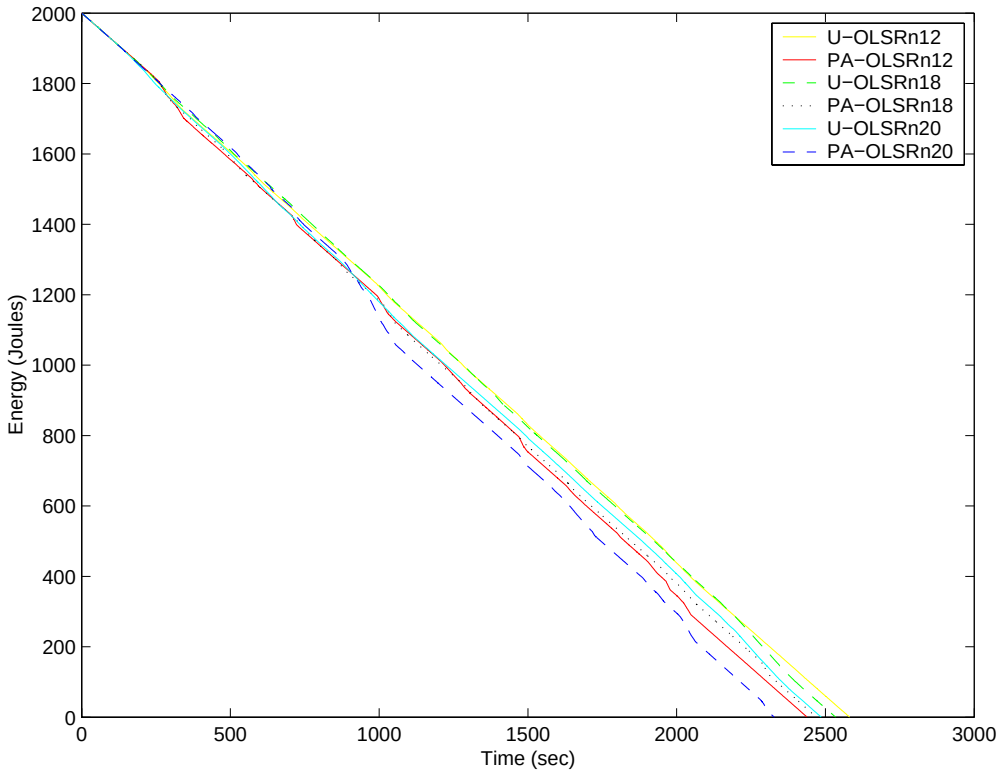

Figure 5.52: Node energy variation for OLSR in random movement high-speed scenario.

5.3.4 Average Change in Energy Analysis

In this section we show improvements in average change in energy over time for neighboring nodes. By taking the average of a set of node energies over time we can see a general trend on how energy is expended. Improvements in average change in energy varies according to protocol and scenario. Figure 5.53 shows an improvement in the average change of energy over time for PA-DSR over U-DSR in the low-contention scenario. The labels PDL and UDL in Figure 5.53 represent PA-DSR and U-DSR in the low-contention scenario, respectively. As time advances, the graph shows average change in energies in the PA-DSR protocol tapers off as the the average change in energy in the U-DSR increases. The reason for the difference in the average change in energy is due to the power-aware protocol. Switching routes among neighbors helps to even out the difference in energy expended. This helps reduce the average change in energy between forwarding nodes. Figure 5.54 shows the average change in energy for the same protocols in a high contention scenario. The labels PDH and UDH in Figure 5.54 represent PA-DSR and U-DSR in the high-contention scenario, respectively. The graph shows similar behavior for the power-aware protocol, however, the average change of energy in U-DSR shows an abrupt increase in the change of energy as time advances. This abrupt increase can be attributed to the fact that as time advances, the number of "dead" nodes increases and the choice of forwarders becomes less. This forces sending nodes to choose a certain neighbor to forward their packets. Having more than one node for which to forward packets, increases the change in energy depletion for the forwarding node.

Figures 5.55 and 5.56 show results for DSR with mobility for slow speed, and for high

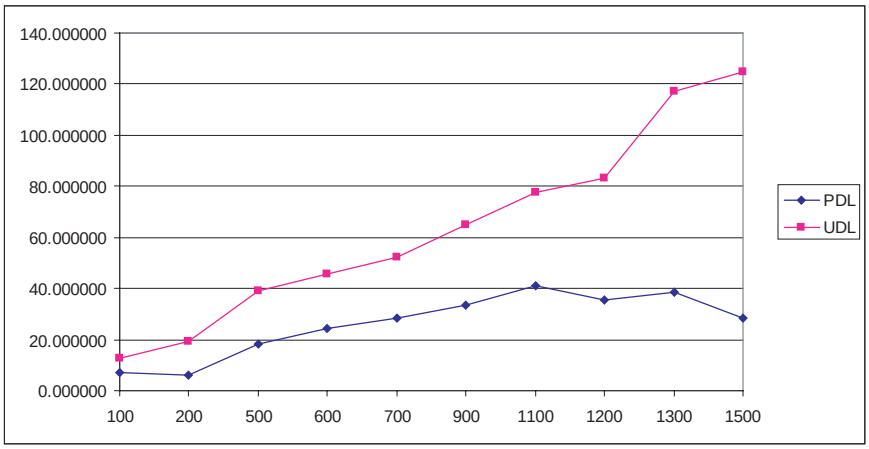

Figure 5.53: Average change in energy for neighboring nodes in DSR low-contention scenario.

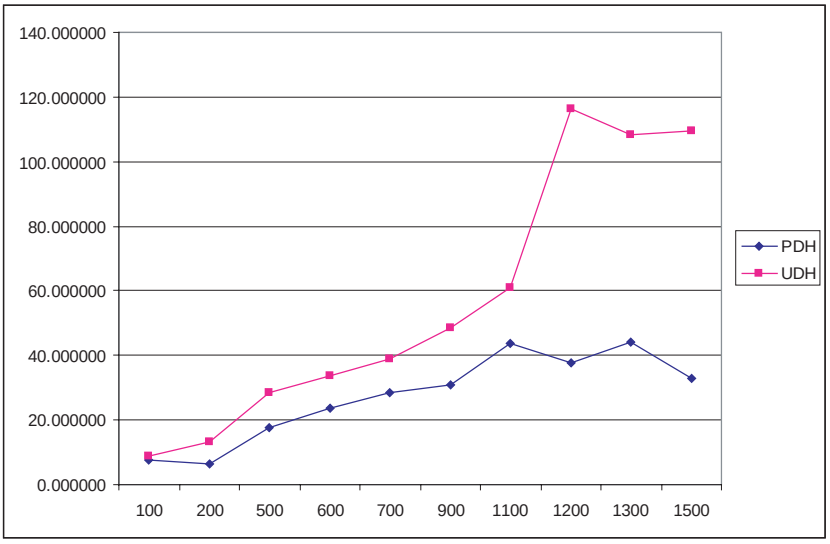

Figure 5.54: Average change in energy for neighboring nodes in DSR high-contention scenario.

speed, respectively. We observe a slight improvement in the average change in energy. This is because nodes are constantly moving. Therefore, the frequency of breaking and establishing routes increases. Re-establishing routes involves new forwarding nodes. A random mobility pattern of neighboring nodes creates an uneven depletion in the battery energy of neighboring nodes in average change in energy. The labels PDcm2 and UDcm2 in Figure 5.55 represent PA-DSR and U-DSR in the low-speed, coordinated movement scenario, respectively. While, the labels PDcm20 and UDcm20 in Figure 5.56 represent PA-DSR and U-DSR in the high-speed, coordinated movement scenario, respectively.

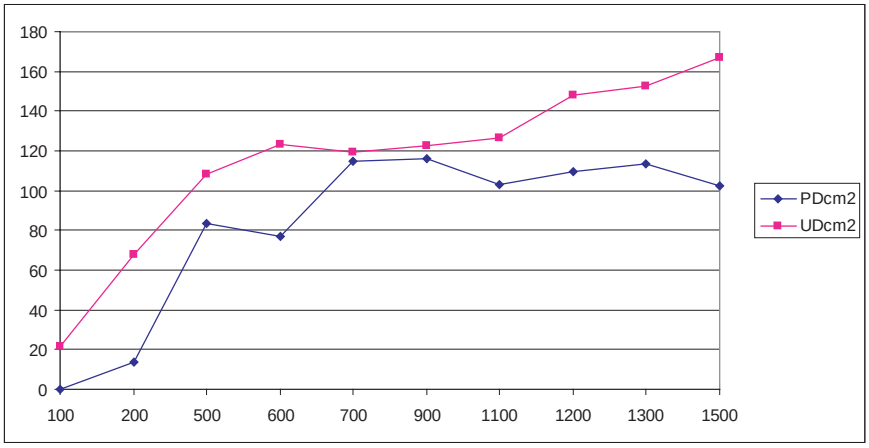

Figure 5.55: Average change in energy for neighboring nodes in DSR low-speed coordinated movement scenario.

The improvement in average change in energy in OLSR is less than that observed in DSR. While we are not trying to make a comparison between DSR and OLSR, we note that in both cases the power-aware protocol improves the average change in energy between neighboring nodes. Figure 5.57 shows the average change in neighboring nodes energy in the OLSR

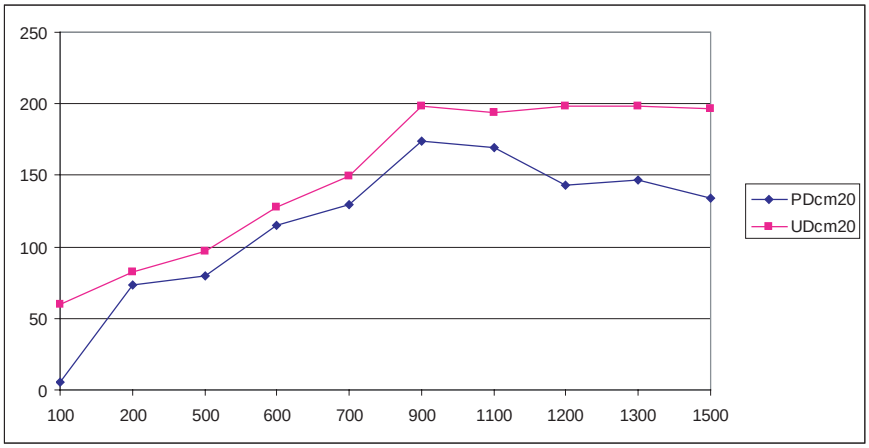

Figure 5.56: Average change in energy for neighboring nodes in DSR high-speed coordinated movement scenario.

low-contention scenario. The labels POL and UOL in Figure 5.57 represent PA-OLSR and U-OLSR in the low-contention scenario, respectively. Figure 5.58 shows average change in neighbor node energies for the OLSR high-contention scenario. The labels POH and UOH in Figure 5.58 represent PA-OLSR and U-OLSR in the high-contention scenario, respectively.

Average change in energy for neighboring nodes in the low-speed coordinated movement in OLSR shows slight improvement. A more obvious improvement is noticeable in the high-speed coordinated movement scenario. This could be due to the fact that at high speeds routes break at a faster rate than at low-speeds, which makes nodes constantly try to establish routes as they break. This energy expenditure by nodes in the network tends to reduce the difference in the average change of energy in the network. Figures 5.59 and 5.60 show the average change in energy for OLSR in the low-speed and high-speed scenarios, respectively. The labels POcm2 and UOcm2 in Figure 5.59 represent PA-OLSR and U-OLSR in the low-

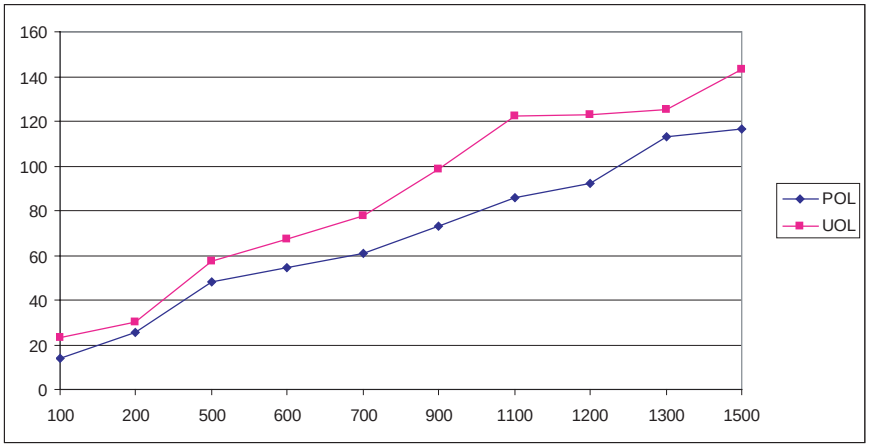

Figure 5.57: Average change in energy for neighboring nodes in OLSR low-contention scenario.

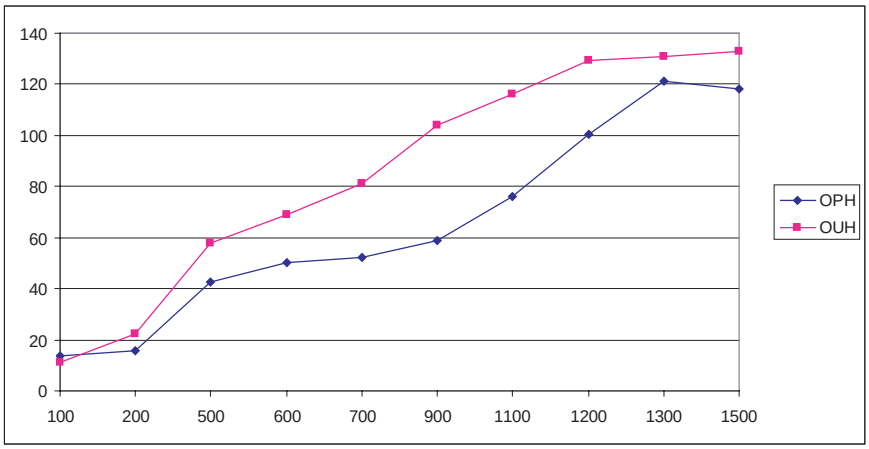

Figure 5.58: Average change in energy for neighboring nodes in OLSR high-contention scenario.

speed, coordinated movement scenario, respectively. While, the labels POcm20 and UOcm20 in Figure 5.60 represent PA-OLSR and U-OLSR in the high-speed, coordinated movement scenario, respectively.

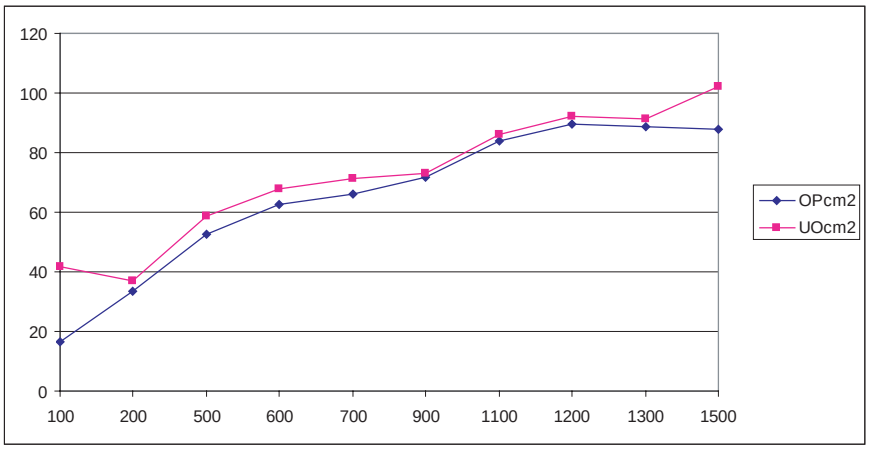

Figure 5.59: Average change in energy for neighboring nodes in OLSR low-speed coordinated movement scenario.

5.3.5 Network Analysis at Simulation End

In this section we look at the average energies for all nodes in the network and the number of "dead" nodes by the time the network "dies" i.e. becomes partitioned. The analysis includes observations for the low-contention, high-contention static network,slow-speed, and fast-speed coordinated movement scenarios for DSR and OLSR.

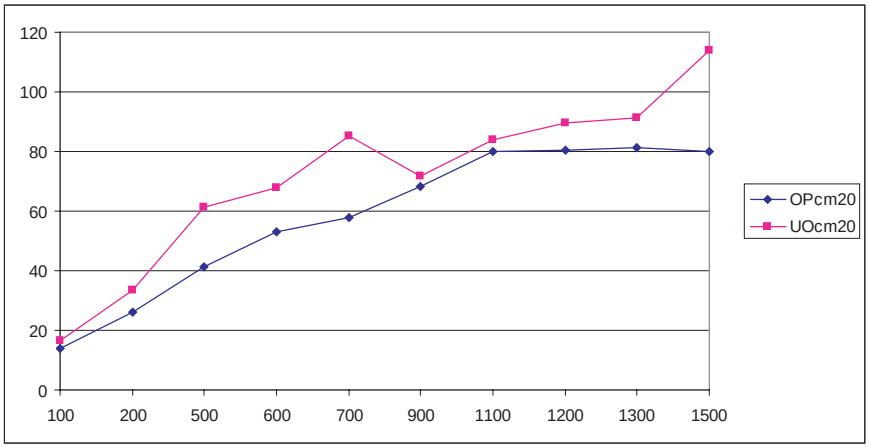

Figure 5.60: Average change in energy for neighboring nodes in OLSR high-speed coordinated movement scenario.

5.3.5.1 Average Final Node Energies Analysis for DSR Scenarios

This section examines the average final node energies for DSR scenarios and the average number of dead nodes in each scenario. Table 5.11 shows the results.

Table 5.11 shows that in general the average energies remained in the nodes in the U-DSR are greater than its power-aware counterpart. Further, the standard deviation for the remaining energy in the nodes are also greater for U-DSR protocol. This implies an uneven distribution of residual node energies by the time the network dies. Therefore, with U-DSR protocol the network dies with some nodes having ample energy and others with low energy. The power-aware protocol, however, shows a lower residual node energy level, along with smaller standard deviation, which implies a more even distribution of energy by the end of the network lifetime. In the high-contention scenario we observe a larger residual node

Table 5.11: Summary of Ending Energies for DSR Scenarios

Protocol	Average Ending Energy (J)	Standard Deviation	Average number of Dead Nodes
U-DSR-HC	42.365	23.636	8
PA-DSR-HC	23.199	6.064	10.5
U-DSR-LC	62.902	4.499	11
PA-DSR-LC	14.504	3.651	12.5
U-DSR-LS	84.968	13.902	8
PA-DSR-LS	58.3718	14.148	8
U-DSR-HS	116.684	30.79	7
PA-DSR-HS	112.04	23.9428	7

energy than in the low-contention. This is because the network lifetime for the low-contention scenario is longer than that of the high-contention scenario. Therefore, more energy is spent in sending and receiving packets. Hence, more energy is expended. The smaller standard deviation for the power-aware protocol signifies that the residual node energies are almost evenly distributed. The larger standard deviation for the unmodified protocol comes from the fact that when U-DSR uses a node for forwarding, it uses it until it dies. This creates a gap in the residual energy among nodes. From the table, we also observe that the residual energies are large in the mobility scenarios. At low-speeds the residual energy is greater for the unmodified protocol. The standard deviation is almost similar for this particular case. At high speeds the residual energies are larger. This is because the nodes are constantly

moving, and the neighbors are also changing quickly. This makes it harder for the power-aware protocol to establish a route connection based on the least reluctance value. Rather, the nodes that stay within range of the sending and receiving nodes will act as forwarders. Therefore, the residual energies of the nodes in the network have some variabilities in them. Moreover, the performance of both protocols under high mobility is poor, therefore, there is no advantage of one protocol over the other under high speeds. The average number of dead nodes is higher in the low-contention stationary scenario and lessens in the high-contention stationary scenario. Again, this is attributed to the fact that in a high-contention network, the sending nodes spend some of their energies trying to route their packets. Therefore, the sending nodes die before other nodes, especially if they forward for other routes. In the mobility scenarios, the number of dead nodes is small due to the fact that the nodes keep changing their positions and routes are being forwarded by different nodes during the network lifetime.

5.3.5.2 Average Final Node Energies Analysis for OLSR Scenarios

This section presents the results obtained for the OLSR protocol. Table 5.12 shows the results obtained.

From the table we observe a similar trend in the results as those obtained in DSR. Power-aware results exhibit less residual energy with a tighter standard deviation. The number of dead nodes in the power-aware are generally higher in the stationary scenario due to higher network lifetime. Under high mobility the results are comparatively similar to those of the

Table 5.12: Summary of Ending Energies for OLSR Scenarios

Protocol	Average Ending Energy (J)	Standard Deviation	Average number of Dead Nodes
U-OLSR-HC	50.799	22.86	11
PA-OLSR-HC	15.301	5.183	10.5
U-OLSR-LC	47.644	6.109	12
PA-OLSR-LC	12.31	4.432	12
U-OLSR-LS	54.025	21.129	7.5
PA-OLSR-LS	25.477	15.316	9.5
U-OLSR-HS	85.249	25.694	6
PA-OLSR-HS	57.169	19.933	6

unmodified power-aware protocol. This is because the performances of both protocols, U-OLSR and PA-OLSR are low in terms of percentage of packets delivered to the application.

5.3.6 Discussion of Results

In general, we observe a modest improvement in the network lifetime with PA-DSR and PA-OLSR in low and high contention scenarios. An increase in the number of packets delivered to the application is also observed. The longer the network lives the more packets can be delivered to the application. Delay times, however, have mixed results. In PA-DSR we see an increase in end-to-end delay times due to power-aware protocol overhead. PA-OLSR on the other hand, shows a decrease in end-to-end delay for reasons mentioned earlier.

In low-speed, coordinated mobility experiments, we observed comparable improvements in the power-aware protocols as in low contention scenarios. At medium speed, because of frequent route breakages, we observed a drop in the percentage of packets delivered to the application. This has slightly affected the network lifetime as nodes do not spend as much energy as when communicating. This reason has also kept end-to-end delay low. At high speed, the rate of dropped packets increases which caused an increase in the network lifetime and a reduction in end-to-end delay.

In random mobility, at all speeds, we observe poor performance in both protocols, power-aware and unmodified. This decline in performance had left no preference of one protocol over the other.

Node energy variation (NEV) showed slight improvements in some of the neighboring nodes in the limited energy stationary scenarios. In the unlimited energy scenarios it was not possible to view the variation in node energy because the initial battery energy was high enough that it prevented the power-aware protocols from switching routes.

In mobile scenarios, random and coordinated, the term neighbor becomes ambiguous since nodes move all the time. Therefore, variations in node energy are difficult to discern visually form NEV graphs in mobile scenarios.

To show the improvements in node energy variation we examine average change in energy over time. From these graphs we see that the average change in node energy is improved in the power-aware protocols over time. Moreover, we were able to see some improvement in

the average change in energy spent by nodes in the power-aware protocol in the coordinated movement scenarios.

Analysis of average final node energies show average residual energies for the unmodified protocols with larger standard deviation, and, generally, fewer dead nodes. This signifies an uneven distribution in the final node energies in the network and that a route when established can unevenly exhaust neighboring node energies since sending nodes transmit at full power. The power-aware protocols, however, show less residual energies and a smaller standard deviation and slightly higher dead nodes. This can imply that by the end of the simulation, the final energies in the nodes by the end of the simulation are more even than those of the unmodified protocols, and since the network lifetime is extended we observe more dead nodes.

5.4 Investigating High Percentage Packet-drop Rate in Low-contention Scenarios

This section investigates the high percentage packet-drop rate observed in the low-contention scenarios. To understand the problem, we setup simulations for low-contention stationary and low-speed coordinated movement networks. In all simulations we limited the energy per node to 2000 Joules and reduced the offered load in the network. By increasing the spacial distance between the flows and reducing the traffic rate in half we managed to obtain,

on average, less than 10% drop rate for the above scenarios. This shows that our initial low-contention scenario might be considered medium-contention instead of low-contention. Tables 5.13 and 5.14 summarizes results obtained for the low-contention stationary and low-speed mobile scenarios, respectively.

In the low-contention stationary scenario we observe an increase in the average number of packets delivered to the application for the power-aware protocols over the unmodified ones. Figure 5.61 shows the average number of packets sent and received for DSR and OLSR in the low-contention scenario. Average end-to-end delay is slightly increased in PA-DSR over U-DSR, and it is slightly decreased in PA-OLSR over U-OLSR. Figure 5.62 shows average end-to-end delay for the protocols in the low-contention scenario. Figure 5.63 shows an increase of 162 seconds in average network lifetime in PA-DSR over U-DSR and an increase of 154 seconds in PA-OLSR over U-OLSR. Figure 5.64 shows average percentage of packets delivered for the protocols. The figure shows an average of 93% of packets delivered for U-DSR and and PA-DSR, while an average percentage of packets delivered of 96% for U-OLSR and PA-OLSR. We believe the increase in the percentage of packets delivered to the application is due to lower traffic rate in the network, and the spacial separation between the flows.

Results for the low-speed, limited-energy coordinated movement scenario show an increase in the number of packets delivered to the application for the power-aware protocols. Figure 5.65 shows the average number of packets sent and delivered for the low-speed, coordinated movement scenario. A slightly higher end-to-end delay is observed in PA-DSR over U-DSR,

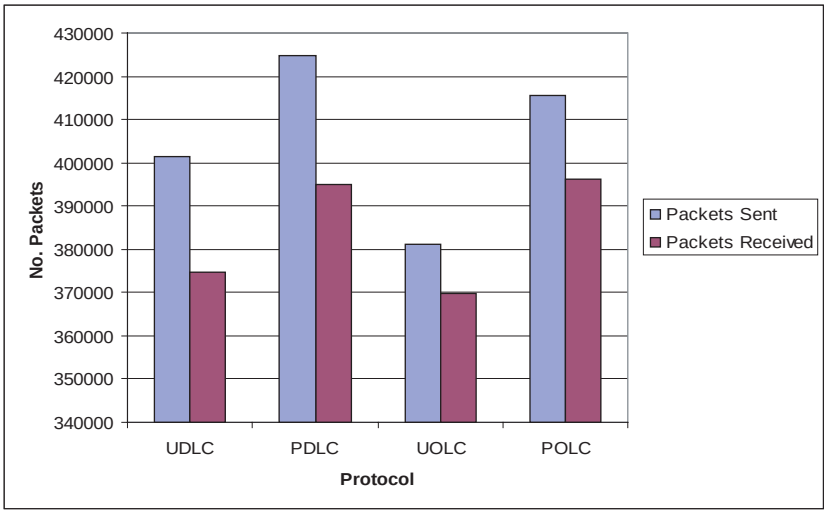

Figure 5.61: Average number of packets sent and delivered in the low-contention, limited-energy scenario.

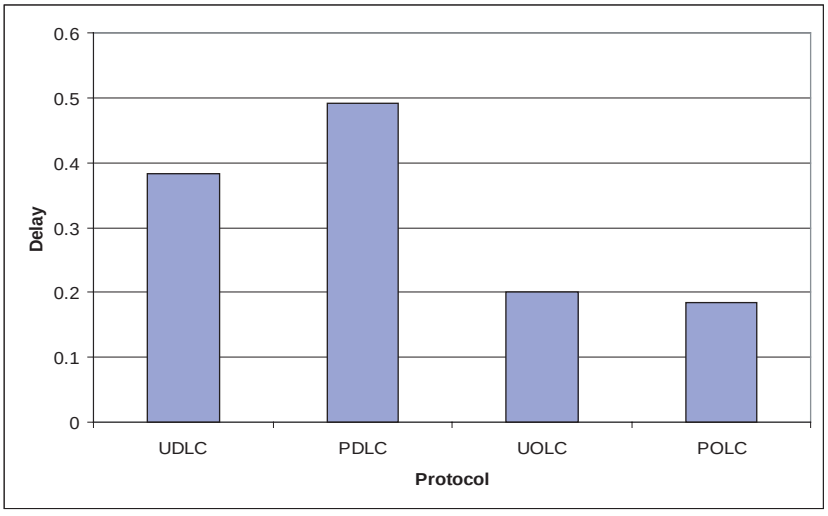

Figure 5.62: Average end-to-end delay in the low-contention, limited-energy scenario.

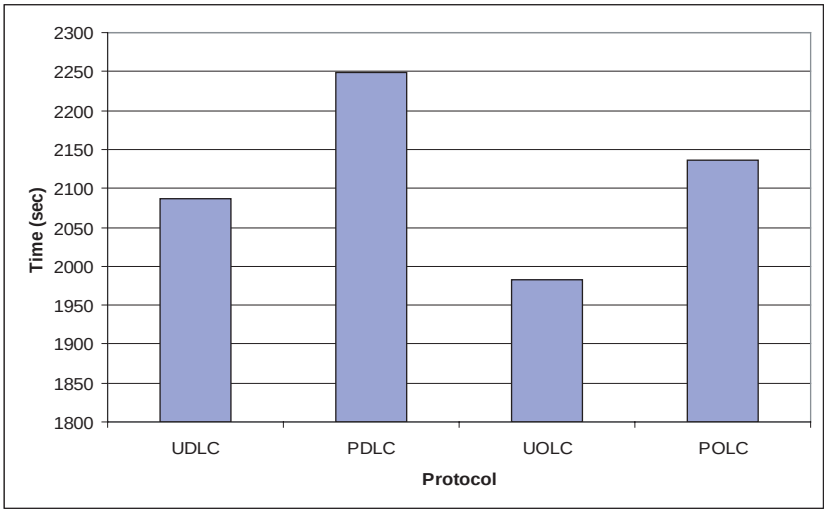

Figure 5.63: Average network lifetime in the low-contention, limited-energy scenario.

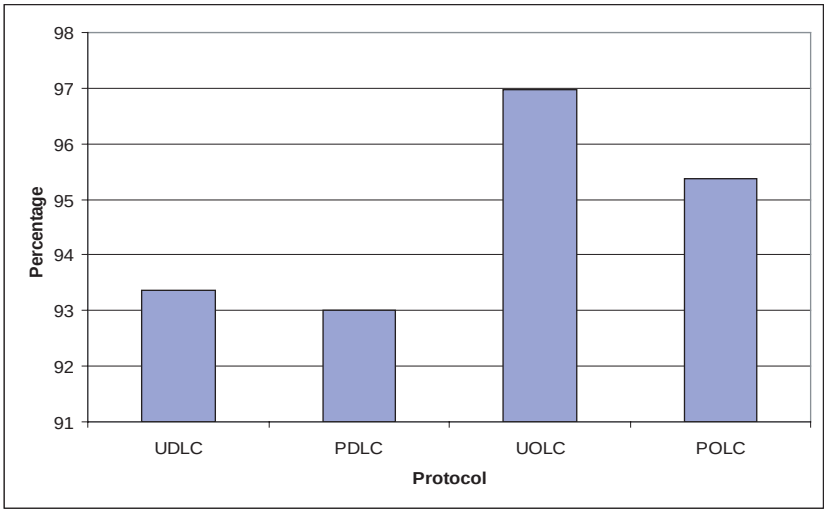

Figure 5.64: Average percentage of packets delivered in the low-contention, limited-energy scenario.

Table 5.13: Summary of Results for, Low-contention Stationary Scenario

	U-DSR	PA-DSR	U-OLSR	PA-OLSR
Average number of packets sent	401426 (±833.98)	424799 (±1097.96)	381293.7 (±719.80)	415492.3 (±419.76)
Average number of packets delivered	374767 (±939.33)	395101.3 (±825.79)	369791.3 (±920.30)	396224 (±632.09)
Average percentage packets delivered	93.35 (±0.937)	93.01 (±0.168)	96.98 (±0.3963)	95.36 (±0.231)
Average end-to-end delay	0.383 (±0.008)	0.492 (±0.0901)	0.200 (±0.0055)	0.184 (±0.0045)
Average network lifetime	2087.46 (±1.84)	2249.38 (±3.12)	1982.553 (±1.863)	2136.61 (±2.80)

while a decrease in the average end-to-end delay is observed for PA-OLSR over U-OLSR. Figure 5.66 shows average end-to-end delay for the power-aware and unmodified protocols. Figure 5.67 shows the average network lifetime for the protocols. An increase in the network lifetime of 124 seconds is observed for PA-DSR over U-DSR, while an increase of 113 seconds is observed for PA-OLSR over U-OLSR. The average percentage of packets delivered for U-DSR and PA-DSR is 89% and 91.31%, respectively. The average percentage of packets delivered for U-OLSR and PA-OLSR is 88% and 91.26%, respectively. Figure 5.68 shows the average percentage of packets delivered to the application for the low-speed coordinated movement scenario. The increase in the percentage of packets delivered to the application is due to the same reasons mentioned in the low-contention stationary scenario.

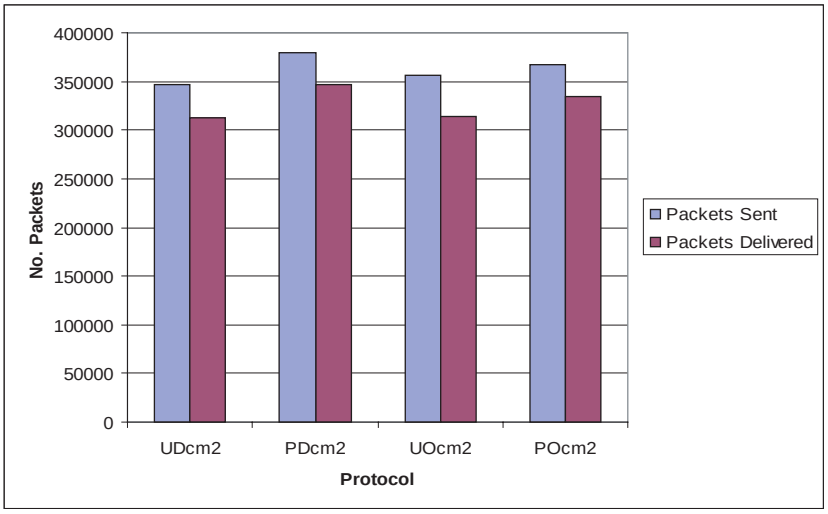

Figure 5.65: Average number of packets sent and delivered in the low-speed, coordinated movement scenario.

Average energy over time analysis for low-contention scenarios show similar behavior as

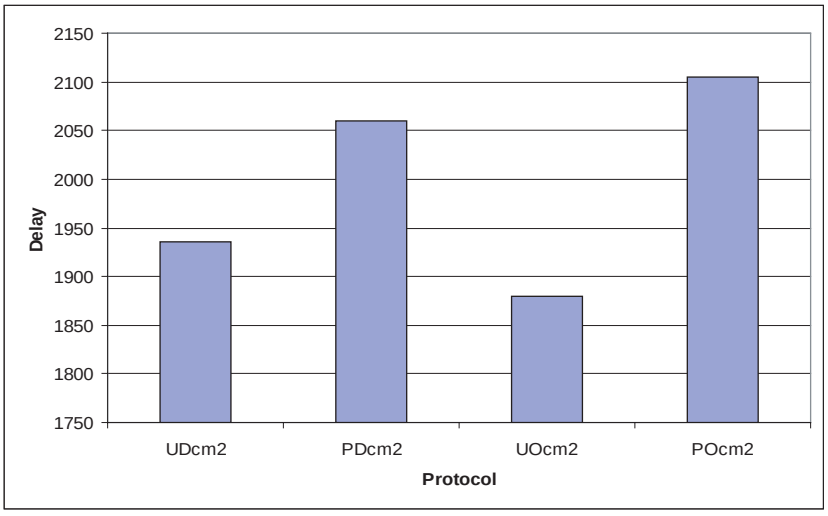

Figure 5.66: Average end-to-end delay in the low-speed, coordinated movement scenario.

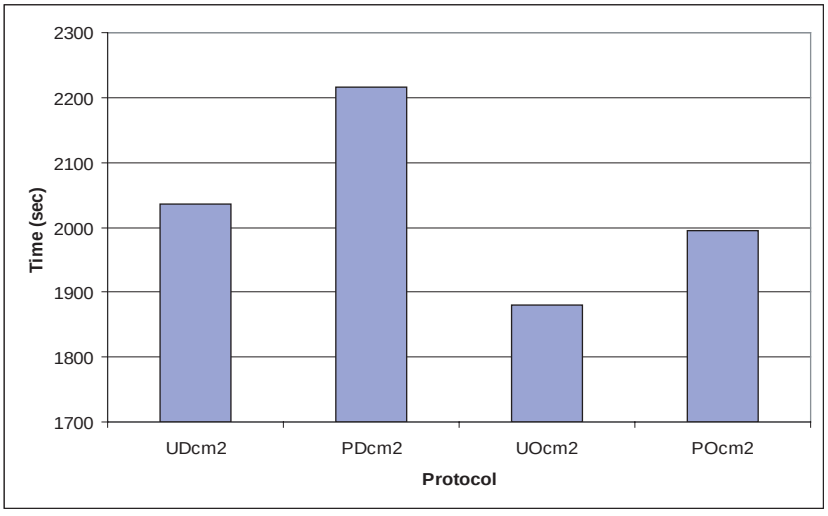

Figure 5.67: Average network lifetime in the low-speed, coordinated movement scenario.

Table 5.14: Summary of Results for, Low-speed Coordinated Movement Scenario

	U-DSR	PA-DSR	U-OLSR	PA-OLSR
Average number of packets sent	346894.3 (±1202.55)	379121.7 (±997.28)	356129 (±1152.86)	366608.3 (±781.8)
Average number of packets delivered	312008 (±1107.85)	346173.7 (±1022.25)	313367.7 (±687.52)	334588.3 (±1073.06)
Average percentage packets delivered	89.94 (±0.075)	91.31 (±0.509)	87.99 (±0.20)	91.26 (±0.171)
Average end-to-end delay	0.572 (±0.01)	0.808 (±0.0118)	0.349 (±0.0088)	0.184 (±0.0052)
Average network lifetime	1935.12 (±8.95)	2059.24 (±7.8)	1880.0 (±3.934)	1993.68 (±6.2)

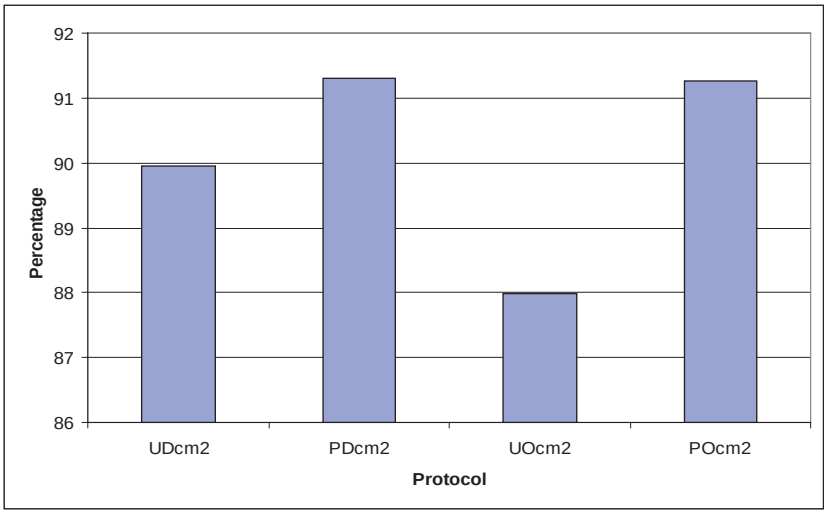

Figure 5.68: Average percentage of packets delivered in the low-speed, coordinated movement scenario.

mentioned in section 5.3.4. In the stationary scenario, we see the average change in energy over time increase with time for U-DSR, while it increases slowly for PA-DSR before it stabilizes. Figure 5.69 shows improvement in the average change in energy over time for PA-DSR and U-DSR protocols. Similar behavior is obtained in the OLSR case. Figure 5.70 shows the average change in energy over time for PA-OLSR and U-OLSR in the low-contention stationary scenario. Results for the low-speed coordinated movement scenarios follow those of the low-contention stationary scenarios. Figures 5.71 and 5.72 show the improvements in PA-DSR and PA-OLSR over U-DSR and U-OLSR in the low-speed coordinated movement scenarios, respectively.

Analysis of average final node energies at simulation end show lower residual node energy for PA-DSR and PA-OLSR over U-DSR and U-OLSR, respectively, for both stationary and

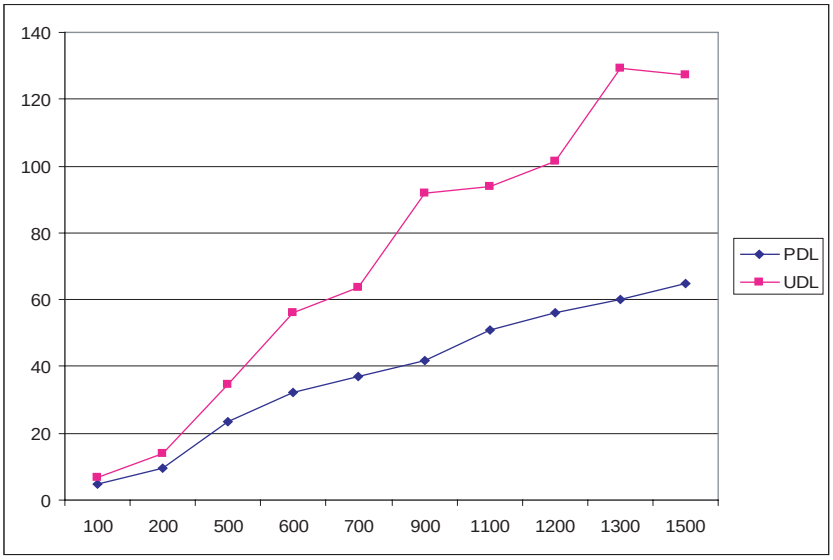

Figure 5.69: Average change in energy for neighboring nodes in DSR low-contention stationary scenario.

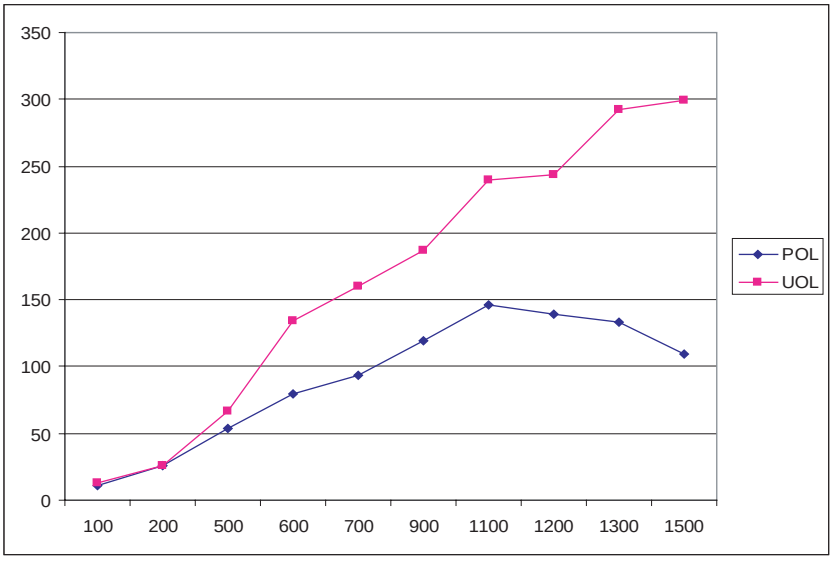

Figure 5.70: Average change in energy for neighboring nodes in OLSR low-contention stationary scenario.

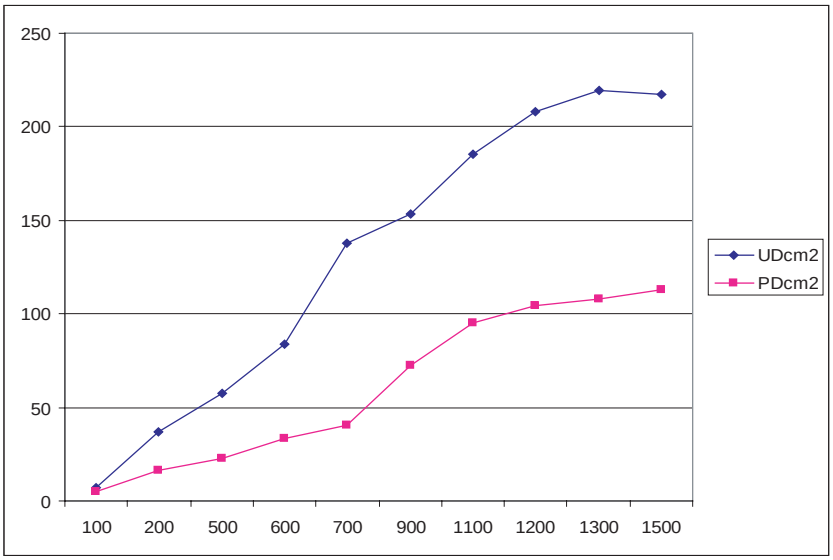

Figure 5.71: Average change in energy for neighboring nodes in DSR low-speed mobile scenario.

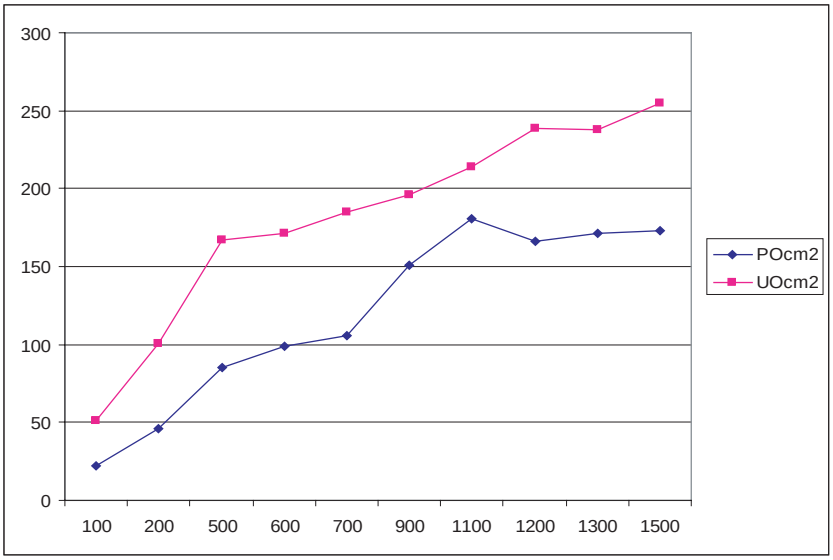

Figure 5.72: Average change in energy for neighboring nodes in OLSR low-speed mobile scenario.

low-speed mobility cases. The standard deviation for the power-aware protocols is similarly lower. This implies even distribution of energy in the nodes for the power-aware protocols. The higher standard deviation implies uneven distribution in node energies in the network for the unmodified protocols. The number of "dead" nodes tend to be higher in the power-aware protocols in the low-contention stationary scenarios. While the number of "dead" nodes in the low-speed mobile scenario tend to be similar on average for both power-aware and unmodified protocols. Table 5.15 show a summary of the average final node energies, the standard deviation, and the number of dead nodes at simulation end.

Table 5.15: Summary of Ending Energies for DSR and OLSR low-contention stationary and low-speed mobile Scenarios

Protocol	Average Ending Energy (J)	Standard Deviation	Average number of Dead Nodes
U-DSR-LC	19.96	14.53	11
PA-DSR-LC	12.58	9.13	14.33
U-OLSR-LC	17.27	20.53	10.33
PA-OLSR-LC	10.7	5.81	12
U-DSR-LS	52.42	26.78	6
PA-DSR-LS	38.66	9.19	7.66
U-OLSR-LS	83.51	22.60	6
PA-OLSR-LS	59.14	9.30	6

5.5 Comparison with other Power-aware Protocols

In this section we compare our proposed protocol with protocols that either use transmit power or residual battery energy to conserve energy. This comparison only considers DSR. The scenario used for the comparison is the same low-contention scenario used in section 5.4. Figure 5.73 shows the average number of packets sent and delivered for U-DSR, PA-DSR, PA-DSRtx, and PA-DSRbt, where PA-DSRtx is DSR protocol that uses transmit power only to conserve energy, and PA-DSRbt is DSR protocol that uses remaining battery energy only to conserve energy. From the figure we observe that our proposed protocol delivers more packets to the destination than PA-DSRtx and PA-DSRbt, followed by PA-DSRbt then PA-DSRtx. End-to-end delay is lower for PA-DSRbt than PA-DSRtx and PA-DSR. Figure 5.74 shows end-to-end delay for the power-aware protocol. Network lifetime is slightly higher for our proposed PA-DSR followed by PA-DSRbt, followed by PA-DSRtx. Figure 5.75 shows network lifetime for the power-aware protocols. Since we are using low-contention scenario, all protocols delivered more than 90% of the packets sent. Figure 5.76 shows the percentage of packets delivered for the power-aware protocols. Table 5.16 summarizes simulation results obtained for the power-aware protocols.

Average energy over time analysis is shown in Figure 5.77. The figure shows our proposed PA-DSR has better energy over time behavior than that of PA-DSRbt and PA-DSRtx. PA-DSRtx shows better average energy over time than PA-DSRbt since PA-DSRbt uses remaining battery energy as its main metric to conserve energy which could lead to greater

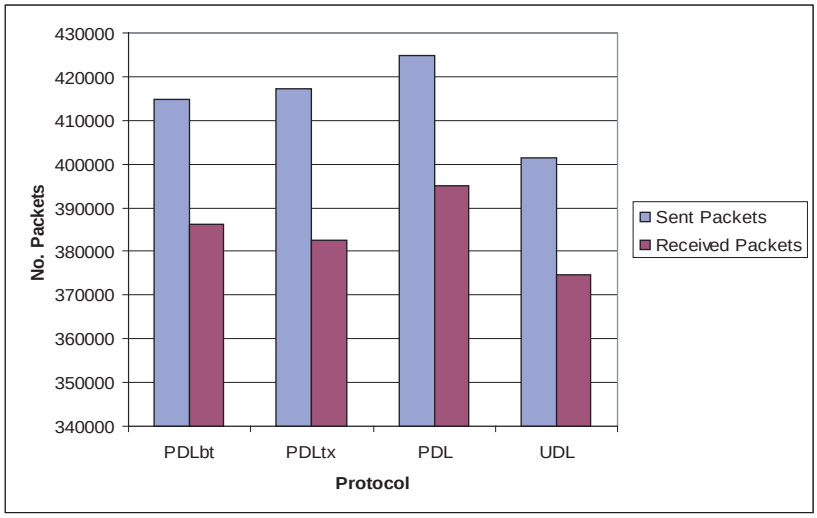

Figure 5.73: Average number of packets sent and delivered in the low-contention, limited-energy scenario.

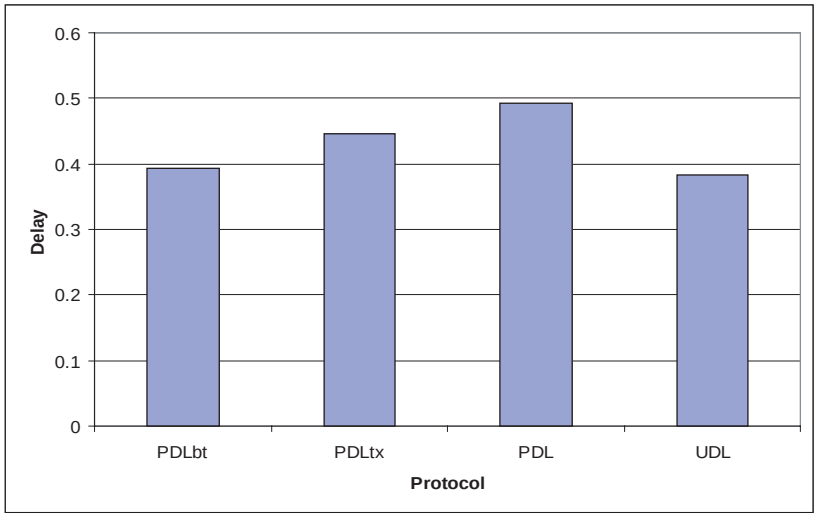

Figure 5.74: Average end-to-end delay in the low-contention, limited-energy scenario.

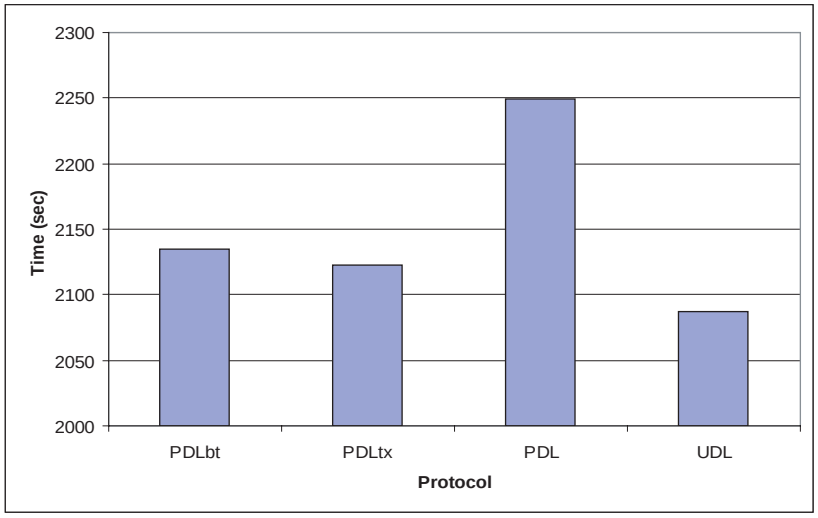

Figure 5.75: Average network lifetime in the low-contention, limited-energy scenario.

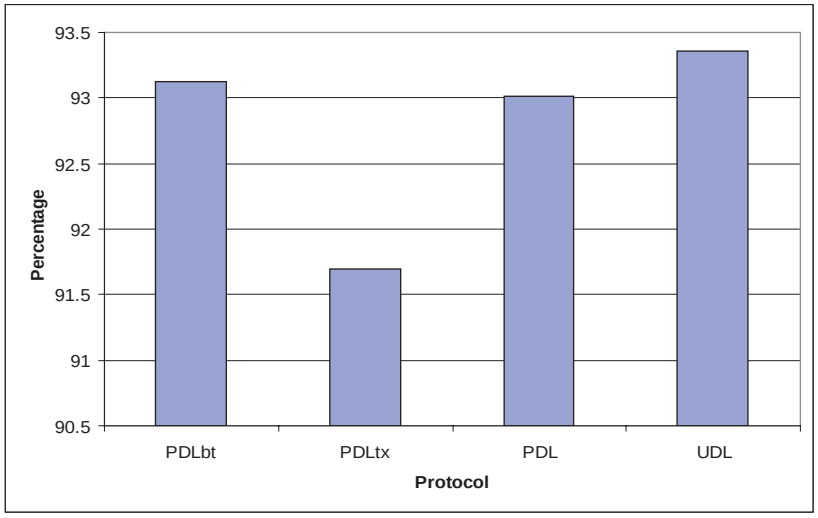

Figure 5.76: Average percentage of packets delivered in the low-contention, limited-energy scenario.

Table 5.16: Summary of Results for, Low-contention Stationary Scenario for Power-aware Protocols

	U-DSR	PA-DSR	PA-DSRbt	PA-DSRtx
Average number of packets sent	401426 (±833.98)	424799 (±1097.96)	414773 (±983.43)	417202.3 (±1157.06)
Average number of packets delivered	374767 (±939.33)	395101.3 (±825.79)	386249 (±1145.84)	382557.3 (±1209.90)
Average percentage packets delivered	93.36 (±0.937)	93.0 (±0.168)	93.12 (±0.29)	91.69 (±0.98)
Average end-to-end delay	0.383 (±0.008)	0.492 (±0.0901)	0.394 (±0.037)	0.446 (±0.11)
Average network lifetime	2087.46 (±1.84)	2249.38 (±3.12)	2134.87 (±4.47)	2122.94 (±6.50)

difference among residual node energy in the network.

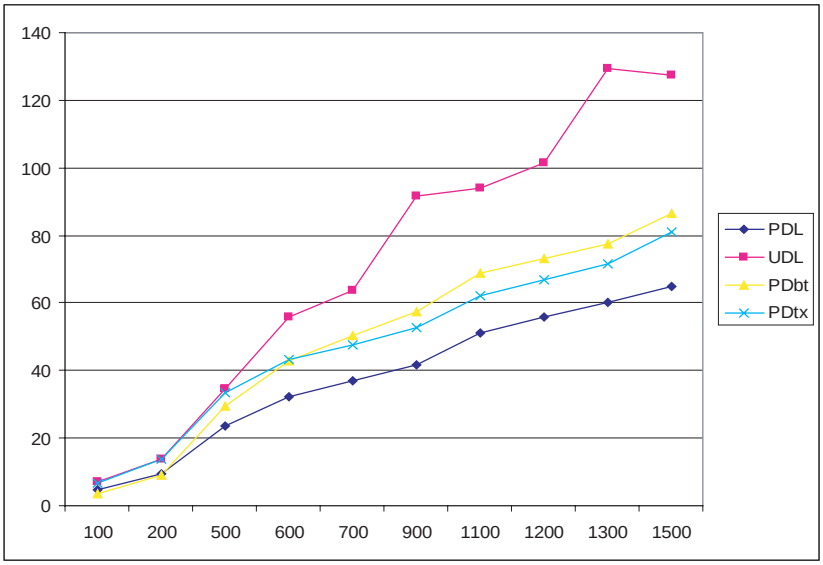

Figure 5.77: Average change in energy for neighboring nodes in DSR low-contention stationary scenario.

Analysis of average final node energies at simulation end show lower residual node energy for PA-DSR over PA-DSRbt and PA-DSRtx. The standard deviation is also slightly lower for PA-DSR than those of PA-DSRtx and PA-DSRbt. PA-DSRtx shows slightly lower standard deviation than PA-DSRbt. This could be due to PA-DSRbt reliance on the most residual battery energy node to route packets in the network. This creates a larger difference among the residual battery energies among the nodes in the network. The number of "dead" nodes is higher for PA-DSR than PA-DSRtx and PA-DSRbt. Table 5.17 summarizes the results of the average final node energies at simulation end analysis.

Table 5.17: Summary of Ending Energies for Power-aware DSR Low-contention Stationary Scenario

Protocol	Average Ending Energy (J)	Standard Deviation	Average number of Dead Nodes
U-DSR-LC	19.96	14.53	11
PA-DSR-LC	12.58	9.13	14.33
PA-DSRbt	14.71	15.80	12.33
PA-DSRtx	17.7	11.94	12

5.6 Summary

In this chapter we presented results observed by running U-DSR, PA-DSR, U-OLSR and PA-OLSR protocols in a 30-node network with 6 flows. Simulation runs spanned multiple scenarios and cases. Simulations were carried out for stationary and mobile networks under different conditions in terms of contention and speeds. The results obtained show slight improvements in network lifetime, and number of packets delivered to the application. It also shows improvements in NEV for the stationary case and coordinated mobility case. Improvements in NEV led to better distribution of energy among nodes in the network. It showed no improvements in the random mobility case. Average change in energy over time showed that the average change in energy increase as time advances for the unmodified protocols, while it shows an increase in the beginning of time, it levels for sometime before it starts to decrease. Average final node energies showed an uneven distribution of final average energies in the unmodified protocols, while it showed a more balanced distribution

of final average node energies in the power-aware protocols. We investigated the high packet drop rate in the low-contention scenario and found that lower-contention scenarios can be achieved by lowering the traffic rate per flow and increasing the spacial distance between flows in order to reduce the packet drop rate. We also compared our proposed power-aware scheme to schemes that use either transmit power or residual battery energy to conserve energy. The simplicity, and versatility i.e. can be implemented on reactive and proactive protocols, of the proposed power-aware scheme, along with the results obtained, make this power-aware scheme worth implementing in current and future power-aware routing protocols.

Chapter 6

Summary and Future Plans

6.1 Summary

We propose a simple power-aware routing technique that takes advantage of the ability of wireless network adapters to dynamically change their transmission power, as well as ability of the wireless devices to ascertain their remaining battery power. This information is used to create a table of what we term reluctance values at each node. Devices share reluctance values and use them to determine how to route packets.

Nodes assign a reluctance value to themselves according to their battery level and according to the transmit power needed to send the packet to the next node in a path. The reluctance value is embedded in the packet header during route discovery for a reactive routing protocol, and along with the hello messages in a proactive protocol so that other nodes

can decide whether or not to use this node in a route. When a node builds its routing table it chooses a route with the smallest total reluctance value.

A survey of the literature reveals that most of the techniques used in power-aware or power-efficient routing protocols rely mainly on either dynamically changing the transmission power as a means to reduce energy expended in the network or route according to battery energy reserve of the nodes and, thus, prolong network life. In multiple-hop networks, exploiting transmission power or battery energy reserve as the sole means to save energy hastens the "death" of relay nodes that forward packets between a sender and a receiver. Such schemes also lead to uneven variation in the energy resources at different nodes. Therefore, it is important to minimize the variation in energy expended to be fair to intermediate nodes in terms of distributing utilization of network energy resources, reduce network failure by not shrinking the network due to node failure, e.g. when an intermediate node serves two different destination nodes, and extend the life of the network by distributing the energy load among different intermediate nodes over time. The proposed scheme combines these two approaches by assigning a reluctance value to a link from the sending or forwarding node to the node in the next hop. Route updates are initiated over time to account for energy depletion and node movements. This results in updating the reluctance values assigned to the links used. This impacts the sending and forwarding nodes' choice of a route that ultimately leads to distributed route selection.

The simplicity of the proposed technique makes it applicable to both reactive and proactive routing protocols. Initially, the technique was applied to a reactive protocol, specifically

the DSR protocol model in NS-2. Simulations were performed on static networks. Initial simulation results showed an improvement in network lifetime for PA-DSR in densely populated networks. PA-DSR shows no advantage or a disadvantage compared to U-DSR in sparse networks since both protocols essentially transmit at full power. Node energy variation, however, is reduced in both densely and sparsely populated networks in PA-DSR, while in U-DSR routes are changed only when an intermediate node dies, so energy varies greatly. Also, initial results show no considerable performance penalty by introducing the scheme to DSR except increased end-to-end delay. The percentage of packets delivered are about the same for U-DSR and PA-DSR. The increase in end-to-end delay for PA-DSR is due to choosing longer routes, with more reserve battery energy, rather than minimum hop routes. Increased overhead for additional route updates also contributes to increased end-to-end delay.

The power-aware protocol was then extended to use dynamic route discovery in DSR. Moreover, the power-aware protocol was added to OLSR as an example of use with a proactive routing protocol. Further, simulations on large stationary and mobile networks under different conditions were carried out. From simulation results, we looked at improvements in network lifetime and node energy variation among neighboring nodes. We also looked at improvements in the average change in node energy over time among a subset of the nodes in the network. Finally, average final node energies were examined for stationary and mobile networks. Under large networks, the power-aware protocol showed some improvements in network lifetime for low- and high-contention stationary networks and low- and medium-

speed coordinated networks. Nodes were able to deliver more packets to the application in those network scenarios. In high-speed coordinated and random movement scenarios, there is a drop in performance for both the unmodified and power-aware protocols. Therefore, our proposed power-aware protocol favors delay unsensitive stationary networks, such as sensor networks, or well behaved node movement where the positions of the nodes are stationary with respect to each other, such as a marching army or vehicles.

6.2 Future Work

This research presented improvements achieved by our proposed power-aware scheme in existing reactive and proactive routing protocols. The power-aware scheme can be further studied and analyzed. Therefore we suggest the following future studies.

- Apply the proposed power-aware scheme to a hybrid protocol and compare and contrast performance to that for reactive and proactive protocols.
- Currently, the power-aware protocol takes its transmit power value from a static table. It would be desirable to let the protocol select its transmit power table from a set of tables based on the environment in which it is deployed. For example, the power-aware scheme uses transmit power table in a static environment that is different from a table used in a mobile environment. Further, a transmit power table in a sparse network different than a table in a dense network.

- Our work considered a simple mobility model, specifically, random waypoint. Considering more complex mobility models can help us understand the limits of our power-aware scheme.

- The power information we use in our proposed power-aware scheme is of the Lucent WaveLan wireless network adaptor card. It would be desirable if we can adapt our proposed power-aware scheme to power information of newer wireless network adaptors. This helps us further understand the performance of our proposed power-aware protocol under current wireless network adaptors.

- This study assumed a linear battery model. Since batteries exhibit non-linear behavior, it is desirable to study the performance of the proposed power-aware protocols under non-linear battery models.

6.3 Contributions

This work has provided the following contributions.

- We have formulated and presented a simple power-aware routing technique that takes advantage of the ability of wireless network adapters to dynamically change the transmission power, as well as the wireless devices' ability to ascertain the remaining battery power to prolong the network life and distribute the load among energy abundant resources in a network.

- We have assessed the impact of the proposed power-aware scheme on the performance of on existing reactive (DSR) and proactive (OLSR) routing protocols, and we were able to extend the network lifetime for PA-DSR and PA-OLSR in stationary and mobile networks with nodes moving in coordination.

- We have assessed the energy distribution in the network. Our power-aware protocol was able to better distribute residual node energies in the nodes and minimized the variation in the residual node energies among nodes in the network.

- We have assessed our proposed power-aware DSR (PA-DSR) and power-aware OLSR (PA-OLSR) routing schemes under different mobility models.

- We have provided simulation results of the proposed power-aware scheme for DSR and OLSR routing protocols.

Bibliography

[1] B. P. E. U.-B. A. El Gamal, C. Nair and S. Zahedi. "Energy-efficient Scheduling of Packet Transmissions over Wireless Networks". *IEEE INFOCOM, IEEE Proceedings of Twenty-First Annual Joint Conference of the IEEE Computer and Communications Societies*, 3(2002):1773–1782, 2002.

[2] B. H. A. Nasipuri, R. Burleson and J. Roberts. "Performance of Hybrid Routing Protocols for Mobile Ad Hoc Networks". *Proceedings of the IEEE International Conference on Computer Communication and Networks (ICCCN2001)*, pages 296–302, 2001.

[3] M. Abolhasan and T. Wysocki. "Displacement-based Route Strategies for Proactive Routing Protocols in Mobile Ad Hoc Networks". *Workshop on the Internet, Telecommunications and Signal Processing(WITSP03)*, 2003.

[4] A. Bakre and B. R. Badrinath. "I-TCP: Indirect TCP for Mobile Hosts". *Proceedings of the 15th International Conference on Distributed Computing Systems*, pages 136–143, 1995.

[5] S. Banerjee and A. Misra. "Adapting Transmission Power for Optimal Energy Reliable Multi-hop Wireless Communication". *Wireless Optimization Workshop (WiOpt'03)*, 2003.

[6] I. Buchmann. "Batteries in a Portable World: A Handbook on Rechargeable Batteries for Non-Engineers". 2001. http://www.buchmann.ca.

[7] B. R. C. Andren, T. Bozych and D. Schultz. "PRISM Power Management Modes", 1997.

[8] P. A. C. E. Jones, K. M. Sivalingam and J.-C. Cheng. "A Survey of Energy Efficient Network Protocols for Wireless Networks". *ACM Wireless Networks*, 7(4):343–358, 2001.

[9] E. M. B.-R. C. E. Perkins and S. R. Das. "Ad Hoc On-demand Distance Vector (AODV) Routing". *Internet draft*, draft-ietf-manet-aodv-12.txt, RFC3561(Mobile Ad Hoc Networking Group), Nov., 2002.

[10] C. P. I. Chalamtac. "Energy-Conserving Selective Repeat ARQ Protocols for Wireless Networks". *Proceedings of the IEEE PIRMC Conference*, 3:836–840, 1998.

[11] P. A. Chen J.-C., K. Sivalingam and S. Kishore. "A Comparison of MAC Protocols for Wireless Local Networks Based on Battery Power Consumption". *IEEE INFOCOM, Seventeenth Annual Joint Conference of the IEEE Computer and Communications Societies. Proceedings IEEE*, 1:150–157, 1998.

[12] I. Corporation. "ACPI-Frequently Asked Questions". http://www.intel.com/technology/iapc/acpi/faq.htm.

[13] D. A. M. D. B. Johnson and Y.-C. Hu. "The Dynamic Source Routing Protocol for Mobile Ad Hoc Networks (DSR)". *draft-ietf-manet-09.txt*, 2003.

[14] S. Doshi and T. Brown. "Minimum Energy Routing Schemes for a Wireless Ad Hoc Network". *IEEE INFOCOM*, 2002.

[15] T. F. L. K. K. S. E. Ayanoglu, S. Paul and R. D. Gitlin. "AIRMAIL: A Link-Layer Protocol for Wireless Networks". *ACM Wireless Networks*, 1(1):47–60, 1995.

[16] ETSI. "Bluetooth Specification Version 1.1". 2001. http://www.bluetooth.org/spec.

[17] E. T. S. I. (ETSI). "High Performance Radio Local Area Network (HIPERLAN) Standard". http://portal.etsi.org.

[18] L. M. Feeney. "An Energy Consumption Model for Performance Analysis of Routing Protocols for Mobile Ad Hoc Networks". *Mobile Networks and Applications*, 6(3):239–249, 2001.

[19] L. M. Feeney and M. Nilsson. "Investigating the Energy Consumption of a Wireless Network Interface in an Ad Hoc Networking Environment". *INFOCOM*, 3(3):1548–1557, 2001.

[20] M. Gerla. "Clustering and Routing in Large Ad Hoc Wireless Nets", 1998. www.ucop.edu/research/micro.

[21] S. S. H. Balakrishnan, V. N. Padmanabhan and R. Katz. "A Comparison of Mechanisms for Improving TCP Performance over Wireless Links". *IEEE/ACM Transactions on Networking*, 5(August 1996):756–769, 1997.

[22] M. S. H. Woesner, J.-P. Ebert and A. Wolisz. "Power-Saving Mechanisms in Emerging Standards for Wireless LANs: the MAC Level Perspective". *IEEE Personal Communication*, 5(June):40–48, 1998.

[23] J. Haartsen and S. Mattisson. "Bluetooth- A new Low-power Radio Interference Providing Short-range Connectivity". 88(10):1651–1661, 2000.

[24] M. Handy and D. Timmermann. "Simulation Of Mobile Wireless Networks with Accurate Modelling of Non-Linear Battery Effects". *Proceedings of International Conference on Applied Simulation and Modeling*, 2003.

[25] C. P. I. Chalmtac and J.Redi. "Energy-Conserving Selective Repeat ARQ Protocols for Wireless Data Networks". *IEEE 9th Symposium on Personal, Indoors, and Mobile Radio Communications, PIMRC*, 2:836–840, 1998.

[26] IEEE. "IEEE 802.15 Working Group for WPAN". http://grouper.ieee.org/groups/802/15/.

[27] IEEE. "Wireless LAN Medium Access Control (MAC) and Physical Layer (PHY) Specifications,IEEE 802.11b Standard". 2001.

[28] I. A. Inc. "PRISM II 11Mbps Wireless Local Area Network PC Card", 2001.

[29] E. W. J.-P. Ebert, B. Stremmel and A. Woliz. "An Energy-efficient Power Control Approach for WLANs". *Journal of Communications and Networks (JCN)*, 2(3):197–206, 2000.

[30] S. S. J. Stepanek and C. Raghavendra. "Power-Aware Broadcasting in Mobile Ad Hoc Networks". *Proceedings of IEEE PIMRC*, 1999.

[31] G. D. N. J. Wieselthier and A. Ephremides. "On the Construction of Energy-Efficient Broadcast and Multicast Trees". *IEEE Conference on Computer Communications INFOCOM*, pages 585–594, 2000.

[32] G. N. J. Wieselthier and A. Ephremides. "Energy-Limited Wireless Networking with Directional Antennas: the Case of Session Based Multicasting". *IEEE Conference on Computer Communications INFOCOM*, 2002.

[33] T. L. K. Kar, M. Kodialam and L. Tassiulas. "Routing for Network Capacity Maximization in Energy-constrained Ad-hoc Networks". *INFOCOM 2003, Twenty-Second Annual Joint Conference of the IEEE Computer and Communications Societies.*, 1:673–681, 2003.

[34] A. R. K. Lahiri and S. Dey. "Communication Architecture Based Power Management for Battery Efficient System Design". *Annual ACM IEEE Design Automation Conference, Proceedings of the 39th Conference on Design Automation, New Orleans, Louisiana*, pages 691–696, 2002.

[35] P. A. K. M. Sivalingam, J.-C. Chen and M. Srivastava. "Design and Analysis of Low-Power Access Protocols for Wireless and Mobile ATM Networks". *ACM Wireless Networks*, pages 73–87, 2000.

[36] L. Y. C. Z. K. Mandke, H. Nam and T. Rappaport. "The Evolution of Ultra Wide Band Radio for Wireless Personal Area Networks", Sept. 2003. http://highfrequencyelectronics.com/Archives/Sep03/HFE0903$_T$*chReport.pdf*.

[37] H. B. K. Pentikousis, V. Tsaoussidis and X. Ge. "Energy / Throughput Tradeoffs of TCP Error Control Strategies". *Proceedings of the 5th IEEESymposium on Computers and Communications (ISCC)*, 2000.

[38] P. Karn. "MACA - A New Channel Access Method for Packet Radio". *ARRL/CRRL Amature radio 9th Computer networking conference*, pages 134–140, 1990.

[39] P. Krishnan and R. Kravets. "Application-driven Power Management for Mobile Communication". *ACM Wireless Networks*, 6:263–277, 2000.

[40] T. J. Kwon and M. Gerla. "Clustering with Power Control". 2:1424–1428, 1999.

[41] P. C. T. L. A. Q. L. Jacquet, P. Muhlethaler and A. Viennot. "Optimized Link State Routing Protocol for Ad Hoc Networks". *IEEE INMIC 2001, Proceedings*, (INSPEC Accession Number 7425407):62–68, 2001.

[42] J. Monks. "*Transmission Power Control For Enhancing The Performance Of Wireless Packet Data Networks"*. PhD thesis, University of Illinois at Urbana-Champaign, 2001.

[43] J. S. P. Agrawal, B. Narendran and S. Yajnik. "An Adaptive Power Control and Coding Scheme for Mobile Radio Systems". *Proceedings of IEEE Personal Communications Conference*, pages 283–288, 1996.

[44] A. G. G. M. P. Bergamo, D. Maniezzo and M. Zorzi. "Distributed Power Control for Power-aware Energy-efficient Routing in Ad Hoc Networks". *ACM Wireless Networks*, pages 29–42, 2004.

[45] P. M. P. Jacquet and A. Qayyam. "Optimized Link State Routing Protocol,draft-ietf-manet-olsr-06.txt". *IETF MANET Internet draft,RFC3626*, 2002. http://www.ietf.org.

[46] V. K. P. Kumar, S. Narayanaswamy and R. Sreenivas. "Power Control in Ad-hoc Networks: Theory, Architecture, Algorithm and Implementation of the COMPOW Protocol". *European Wireless Conference*, 2002.

[47] C. F. P. Lettieri and M. B. Srivastava. "Low Power Error Control for Wireless Links". *International Conference on Mobile Computing and Networking, Proceedings of the 3rd annual ACM IEEE International Conference on Mobile Computing and Networking*, pages 139–150, 1997.

[48] P. C. P. Sholander, A. Yankopolus and S. S. Tabrizi. "Experimental Comparison Of Hybrid and Proactive MANET Routing Protocols". *MILCOM*, 2002.

[49] R. Pearlman and Z. J. Hass. "Zone Routing Protocol for Ad Hoc Networks". *Internet Draft, draft-ietf-manet-zrp-02.txt*, 1999. http://www.ietf.org.

[50] C. Perkins. "*Ad hoc Networking*". Addison-Wesley, 2001.

[51] H. B. R. Katz and S. Seshan. "Improving Reliable Transport and Handoff Performance in Cellular Wireless Networks". *ACM Wireless Networks*, 1(4):469–481, 1995.

[52] P. B. R. Wattenhofer, L. Li and Y.-M. Wang. "Distributed Topology Control for Power Efficient Operation in Multihop Wireless Ad Hoc Networks". *IEEE INFOCOM 2001*, pages 1388–1397, 2001.

[53] C. Raghavendra and S. Singh. "PAMAS- Power Aware Multi-access Protocol with Signaling for Ad Hoc Networks". *ACM SIGCOMM Computer Communication Review*, pages 5–26, 1999.

[54] R. Ramanathan and R. Rosales-Hain. "Topology Control of Multihop Wireless Networks Using Transmit Power Adjustment". *INFOCOM, Proceedings of the Nineteenth Annual Joint Conference of the IEEE Computer and Communications Societies*, 2:404–413, 2000.

[55] R. R. Rao and M. Zorzi. "Error Control and Energy Consumption in Communications for Nomadic Computing". *IEEE Transactions on Computers*, 46(3):279–289, 1997.

[56] W. Rosch. "Batteries: History, Present, and Future of Battery Technology". 2001. http://www.extremetech.com.

[57] K. Ross and J. Kurose. "*Computer Networking*". Addison Wesley Longman Inc, 2001.

[58] J. H. Ryu and D. H. Cho. "A New Routing Scheme Concerning Power-Saving in Mobile Ad Hoc Networks". *Proceedings of the IEEE International Conference on Communications*, 3:1719–1722, 2000.

[59] M. W. S. Singh and C. S. Raghavendra. "Power-Aware Routing in Mobile Ad Hoc Networks". *International Conference on Mobile Computing and Networking, Proceedings of the 4th Annual ACM/IEEE International Conference on Mobile Computing and Networking*, pages 181–190, 1998.

[60] J. Schiller. "*Moblie Communications"*. Addison-Wesley, 2001.

[61] A. Singer. "802.15 aims to Secure Wireless PANs". *Network World*, 2002. http://www.nwfusion.com.

[62] A. Spyropoulos and C. S. Raghavendra. "Energy Efficient Communications in Ad Hoc Networks using Directional Antennas". *The IEEE Conference on Computer Communications INFOCOM*, pages 220–228, 2002.

[63] C. Systems. "Cisco Aironet 350 Series Client Adapters data sheet". 2003, 2003.

[64] L. Tassiulas and J. H. Chang. "Energy Conserving Routing in Wireless Ad-Hoc Networks". *The IEEE Conference on Computer Communications INFOCOM*, pages 22–31, 2000.

[65] E. Thompson. "Smart Batteries to the Rescue". 2003. http://www.mcc-us.com/techsrc.htm.

[66] L. Tudose. "The Effect of Beaconing on the Battery Lifetime". 2001.

[67] U. UC Berkeley, LBL and X. PARC. "The Network Simulator (NS-2)". (version 2.9b1a).

[68] K. Varadhan and K. Fall. "The NS manual". 2002.

[69] D. E. W. Ye and J. Heidemann. "An Energy-efficient MAC Protocol for Wireless Sensor Networks". *INFOCOM 2002 IEEE Proceedings of Twenty-First Annual Joint Conference of the IEEE Computer and Communications Societies*, 3, 2002.

[70] S.-C. Woo. "*Routing in Ad Hoc Networks"*. PhD thesis, University of South Carolina, 1999.

[71] L. Xu and I. Stojmenovic. "Power-Aware Localized Routing in Wireless Networks". *IEEE Transactions on Parallel and Distributed Systems*, 12(11):1122–1133, 2000.